Petrographic characterization of sandstones in borehole E-BA1, Block 9, Bredasdorp Basin, Off-Shore South Africa

By

Chantell Berenice Van Bloemenstein

A mini-thesis submitted in partial fulfillment of the requirements for the degree of Magister Scientiae in the Department of Earth Sciences, University of the Western Cape

SUPERVISOR: ***Paul Carey PhD (Queens, Belfast)***

Lecturer in Petroleum Geology

Department of Earth Sciences,

University of the Western Cape

CO-SUPERVISOR: ***Reginald Domoney***

Lecturer in Regional Geology

Department of Earth Sciences,

University of the Western Cape

December 2006

Petrographic characterization of sandstones in borehole E-BA1, Block 9, Bredasdorp Basin, Off-shore South Africa

Chantell Berenice Van Bloemenstein

KEYWORDS

Bredasdorp Basin

Petrography

Thin Sections

XRD

SEM

Clays

Reservoir quality

Porosity

Permeability

Matrix Acidization

ABSTRACT

Petrographic characterization of sandstones in borehole E-BA1, Block 9, Bredasdorp Basin, Off-shore South Africa

Chantell Berenice Van Bloemenstein

Magister Scientiae Mini-thesis, Department of Earth Sciences, University of the Western Cape

The reservoir quality (RQ) of well E-BA1 was characterized using thin sections and core samples in a petrographic study. Well E-BA1 is situated in the Bredasdorp Basin, which forms part of the Outeniqua Basin situated in the Southern African offshore region. Rifting as a result of the break up of Gondwanaland formed the Outeniqua Basin. The Bredasdorp Basin is characterized by half-graben structures comprised of Upper Jurassic, Lower Cretaceous, Cretaceous and Cenozoic rift to drift strata.

The RQ analysis included the identification of mineralogical, textural and fluid flow properties. The mineralogical properties that were taken into account included rock composition divided into categories of framework, ductile and authigenic minerals. The textural aspects included the identification of grain sizes, sorting and grain shapes. The fluid flow properties involved the porosity and permeability of the rock and took into account the packing and support of grains. Clay minerals, both detrital and authigenic were studied in detail to determine the restrictions in the reservoir to fluid flow. These clays have also provided the means for a solution to increase fluid flow and production into the borehole.

The diagenetic history, constructed from the results of the RQ study, revealed that there were several stages in the total diagenetic process involved. It illustrated several phases of cementation with quartz, carbonate and dolomite with dissolution of feldspar. The paragenesis of the rock could then be formulated.

A potentially good reservoir interval was identified from the data and was characterized by several heterogeneous zones. Identifying such zones is highly beneficial when devising recovery techniques for production of hydrocarbons. Secondary recovery methods have thus been devised to enhance well performance.

December, 2006

DECLARATION

I declare that *Petrographic characterization of sandstones in borehole E-BA1, Block 9, Bredasdorp Basin, Off-Shore South Africa* is my own work, that it has not been submitted before for any degree or examination in any other university, and that all the sources I have used or quoted have been indicated and acknowledged as complete references.

Chantell Berenice Van Bloemenstein

December 2006-11-15

Signed:……

ACKNOWLEDGEMENTS

The author wishes to thank the contributors of this study, Petroleum Agency SA, for the availability of the thin sections, core samples and reports on well E-BA1 for analyses; iThemba Laboratory, for their assistance in the XRD analysis, and University of Cape Town Physics Department, for their assistance in the SEM analysis. I thank my lecturers Professor P. Carey, Professor C. Okujeni and Mr. R. Domoney for their assistance throughout the study, their efforts, advice and support is greatly appreciated. A special thanks to all my fellow student colleagues for their support and assistance throughout the project.

List of Figures

List of tables

CHAPTER ONE:

INTRODUCTION

The E-BA1 borehole is situated in the Bredasdorp Basin having coordinates of 21.4747605 latitude and -35.7583581 longitude. This basin is a product of rift and drift activity during the Gondwanaland break up. It is thus a rift basin containing rift-to drift-sediments bounded by two arches [Brown et. al., 1995]. The main structures being half-grabens are characterized by thick sedimentary rock sequences namely massive sandstones and shales.

The aim of this study is to determine the general reservoir characteristics of a well representing an area in the Bredasdorp basin, by performing a ‘three step analyses, namely a petrographic analysis of thin sections, X-ray diffraction of several samples from selected depths and scanning electron microscopy analysis. The thin sections were obtained from two cores as well as rock cuttings recovered from the E-BA1 Borehole. A full petrographic characterization of each thin section was done, with respect to mineralogical aspects, textural aspects and fluid flow determinations. These aspects of porosity, grain-size, mineralogy and cement types constitute important geological factors in describing a reservoir [Hussain et al., (2006)]. The nature of the thin sections thus led to the investigation of sedimentary rocks observed under a microscope, as this is the basis of the study.

The characteristics revealed in the thin sections, led to the investigation of selected samples using x-ray diffraction methods. This analysis was used to discover the types of clays present in the samples which in effect has an impact on the reservoir. The final step involved a scanning electron microscopy analysis which was performed on selected samples. The basis of this analysis was to discover the structures of the clays which in turn would help describe the reservoir quality on the basis of porosity and permeability.

History of hydrocarbon exploration of South African Off-shore

The birth of hydrocarbon exploration in South Africa began in the 1940s by the Geological Survey of South Africa [Petroleum Agency SA, 2004/5]. Soekor (Pty) was established in 1965, by the government, for onshore exploration of the Karoo, Algoa and Zululand Basins [Petroleum Agency SA, 2004/5]. The first offshore well was drilled in 1969 after the new Mining Rights were passed for offshore exploration in 1967. With these new rights came international interest and many international companies began exploration of the offshore area. The first gas and condensate discovery was by international company Superior, which was situated in the Pletmos Basin. However this was not adequate to hold the international companies' interests and during 1970 they started to withdraw. Soekor thus became the sole operator for the South African offshore area [Petroleum Agency SA, 2004/5].

Exploration activity between 1981 and 1991 led to 181 exploration wells being drilled, with the Bredasdorp Basin being of primary focus resulting in several oil and gas discoveries [Petroleum Agency SA, 2004/5].

Petroleum Agency SA was established in 1999 [Petroleum Agency SA, 2004/5], with the responsibility of managing exploration in South Africa by soliciting bids for offshore acreage. In 2001 Soekor (Pty) merged with Mossgas to form PetroSA [Petroleum Agency SA, 2004/5].

To date, the South African offshore area has been probed by more than 300 exploration wells, this includes appraisal and production wells [Petroleum Agency SA, 2004/5]. The Sable Field to date is expected to produce 30 000 bbl per day, which would replace 7% of the total crude oil imports of South Africa [Petroleum Agency SA, 2004/5].

During recent years, international oil and gas exploration companies showed renewed interest and this could implicate larger resources being discovered and produced commercially [Roux, J., 2005].

1.1 Literature Review

Submarine fan development and deep marine conditions

On the report of Shanmugan and Moiola (1985), submarine fans constitute major hydrocarbon reservoirs on a world-wide scale. There are three major controls on the nature of submarine fans, viz. sediment types and their supply, tectonic settings and sea-level changes [Stow et al., (1985) and Stow (1985]. These controls aid in determining the potential of a reservoir.

The most common sediment is terrigenous material [Stow et al., 1985]. Grain sizes of sediments and distance of transport affects the geometry of the deposit, these along with the volume and the rate at which sediments reach the area for deposition also plays key roles [Stow et al., 1985]. The number of entry points of sediment supply determines whether single, multiple or overlapping fans will develop. Source rock types determine the composition, particle sizes, erodibility of sediments and end products of submarine fans. The climate and vegetation in the source area determines the weathering processes and mode of transportation [Stow et al., 1985]. Relief and tectonic activity would influence the rate of sediment transport, for instance sediments travelling down a submarine canyon would be faster than sediments travelling over a plain. Marine conditions would affect the biogenic and organic carbon supply depending on currents, Coriolis force, water temperature and upwelling [Stow et al., 1985]. Coriolis force is the deflection of a water body towards the left (in the southern hemisphere) affected by the Earth's rotation [Kearey, 1996: 69].

Deepwater fans can develop as a result of major tectonic activity such as the rifting of margins [Stow et al., 1985]. These activities affect uplift and denudation rates, drainage patterns, sediment supply and relative sea-level changes. The rate of tectonic uplift and subsidence are secondary factors controlling submarine fan development. The nature and frequency of tectonic activity in the source and transitional areas determines the rate and volume of transport by gravity flows deeper into the basin. Sediment gravity flows will thus be greater in volume (in an area marked by less

frequent but high magnitude tectonic events) than an area which experiences more frequent activity at a lesser magnitude [Stow e. al., 1985].

As in the case of the Bredasdorp Basin, having greater magnitude of earthquakes during rifting (due to stress release), larger slumps (during failure) developed large debris flows and turbidity currents. Physical experiments [Amy et al., 2005] have shown that turbidite bed geometries are spatially extensive deposits with tapered margins. These high-density (built up over a long period of time) turbidity currents have gradual particle settling out of 'turbulent suspension' [Amy et al., 2005]. Some turbidites may even contain debris flow deposits in large proportions, which often occur in conjunction with forced removal [Amy et al., 2005] from the transition zone during tectonic activity.

Changes in sea-level have effects on nearshore areas as well as deep-sea regions with regard to sedimentation. Submarine fans are "mostly active during periods of low sea-level" [Stow et al. 1985]. This is a result of the direct access of rivers (as a result of low sea-level exposure) which feed deeper areas.

These controlling factors merely contribute to the development of reservoirs in deep-marine conditions. Basic requisites for the accumulation of hydrocarbons in nearshore and deep-marine conditions are relatively similar [Wilde et al. 1985]. Source rocks should have an abundance of organic carbon suitable for petroleum generation. These rocks should be brought to suitable thermal maturation levels for generation and be 'connected' to reservoir beds [Wilde et al., 1985]. The reservoir rocks require adequate porosity and permeability, in the form of a network [Karmakar et al., 2003], for petroleum migration. Matthews and Ridgway (1996) eloquently state that the void space within a porous solid can be regarded as a network of void volumes (pores) connected by a network of smaller void channels (throats). Main controls on reservoir quality for sandstones, as studied by Hamel and Thom (2001), would be porosity and permeability. Adequate trapping mechanisms are required for petroleum accumulation. Two types of traps are recognised: structural traps and stratigraphic

traps. The Bredasdorp Basin has a structural trap characteristic mirroring fault planes which trap hydrocarbons and seal them in. The sealing of accumulated hydrocarbons is vital in determining the extent of the reserves which also determines its commercial viability [Wilde et al., 1985].

Diagenesis

The process of hydrocarbon generation to maturation occurs in conjunction with a vital process of sediment evolution known as diagenesis. Diagenesis involves all low temperature, low pressure changes to sediments including lithification and de-lithification [Press et al. 2004, Kearey 1996: 85]. These processes aid in transforming sediments into sedimentary rocks [Karmakar et al., 2003].

Temperature and pressure realms of diagenesis are between near surface weathering conditions and metamorphism [Boggs, 2001]. Taylor et al. (2004) stated that diagenetic processes are controlled by and dependant on spatial and temporal patterns of sedimentary successions. Thus stages of diagenesis exists which occur at different levels of depth and time. These stages are shallow burial (Eodiagenesis), deep burial (Mesodiagenesis) and late-stage diagenesis (Telodiagenesis) [Boggs, 2001].

Shallow burial is characterised by bioturbation, compaction with grain repacking and mineralogical evolution [Boggs, 2001]. Compaction of sediments is minor, at this stage, due to the shallow burial depth. Compaction is a mechanical process causing volume reduction and promoting pore fluid expulsion thus decreasing the pore volume of the rock [Kearey, 1996: 63]. Mineralogical changes are minerals precipitated out of solution (pore fluids at this stage) [Boggs, 2001]. In reducing conditions, particularly in marine environments, the precipitation of pyrite occurs at this stage as a cement or replacive mineral through pyritization [Kearey, 1996: 250]. Many other minerals and cements are formed such as clays, carbonate cements, quartz and feldspar overgrowths and glauconite. Glauconite forms at the sediment-water interface [Rasmussen 2005, Pasquini et. al. 2004], ideally under conditions of slow sedimentation [Pasquini et. al. 2004, Weaver and Pollard 1975], agitated saline

water with reducing conditions [Weaver and Pollard, 1975] thus forms quite early during burial. Glauconite occurs in two forms, as mineral pellets containing iron-rich clays and as the authigenic recrystallized form [Weaver and Pollard 1975, Pasquini et. al. 2004].

Most cements are allogenic (precipitated during or shortly after deposition) at this stage. Quartz, carbonates, and calcites are precipitated during burial. The presence of clays would inhibit quartz cementation [Storvoll et al., 2002] and enhance the dissolution of quartz [Renard et al., 1997], when in contact with each other. Clay is precipitated from solutions containing potassium and silicates sourced from K-feldspar. Chlorite, kaolinite and smectite precipitate at relatively low temperatures (25°C) and thus form early in the diagenetic process. Illite requires a higher temperature (100°C) threshold for precipitation [McHardy et al., 1982].

Deep burial involves mechanical and chemical compaction. Mechanical compaction is the physical aspect whereby the weight of the overlying deposited sediments causes load pressure forcing grains to become more tightly packed together. This would reduce the primary porosity of that layer. As grain boundaries move closer together, their contacts become soluble [Boggs, 2001]. Grains then become partially dissolved at the contacts by a process known as pressure solution [Kearey 1996: 245, Boggs 2001] or chemical compaction. This process further reduces porosity [Boggs, 2001] and forms sutured contacts between grains with the principle stress being perpendicular to the length of the sutured grain [Kuntcheva et al., 2006]. Dissolution of minerals such as feldspar during pressure solution is as a result of contact with undersaturated pore fluid [Wilkinson et al., 2001]. The sites of feldspar and carbonate dissolution are economically important as they generate secondary porosity [Gier and Johns, 2005].

On the other hand, as more elements are dissolved from framework grains, inevitably precipitation would form authigenic minerals by cementation. The cementation, in turn, reduces the porosity available for hydrocarbon migration and accumulation

[Haszeldine et al., 2003]. This “cycle’ of dissolution and precipitation is aided by heat from brine solutions which flow into the basin [Lee et al., 2005] and fill up the pores. Thus diagenesis forms the restructuring of pore networks by these processes [Karmakar et al., 2003]. These secondary pore networks can either remain intact to become a “net contribution to total rock porosity” [Wilkinson et al., 2001] or they could by filled by authigenic clays and other cementing materials. As the sandstone becomes more deeply buried, the illitization of shallow authigenic and detrital clays becomes prominent [Matthews and Ridgway, 1996]. These clays fill pores and aid in reducing porosity.

Late-stage diagenesis begins once deeply buried rocks experiences uplift [Boggs, 2001]. The rocks thus experience lower temperatures and pressures along with oxygen-rich meteoric water having low salinities. Thus the mineralogical framework is altered by continued dissolution of cements and framework minerals. Grain replacement reactions of feldspar by clays prevail. In certain cases kaolinite could replace feldspar after dissolution [Gier and Johns, 2005]. Precipitation of new cements occurs. These processes continue along with chemical weathering due to uplift [Boggs, 2001].

1.2 The Regional Setting of Southern African offshore basins

The Karoo plume centred in Mozambique is the cause of the break up of Gondwana, specifically the splitting of Africa from Antarctica [Thomson, 1999]. There are three tectonostratigraphic zones [Petroleum Agency SA, 2004/5] within the basins found off South Africa’s shores. In the west coast and its offshore region, which comprises 45% of the total area of all basins, the area spans about 191600km^2 [Petroleum Agency SA, 2004/5]. This basinal area is a ‘broad passive margin’ [Petroleum Agency SA, 2004/5], which was formed in the Early Cretaceous during the opening of the South Atlantic, illustrated by Figure 1 [Petroleum Agency SA, 2004/5]. This basin is known as the Orange Basin [Petroleum Agency SA, 2004/5].

The eastern offshore section being a ‘narrow passive margin’ [Petroleum Agency SA, 2004/5], formed in the Jurassic during the Africa, Madagascar and Antarctica break up (seen in Figure 1), is characterised by limited sediment deposition with considerable amounts only in the Durban and Zululand Basins [Petroleum Agency SA, 2004/5]. These basins contribute 25% of the total basin area of the South African offshore and span about 107 000km^2 [Petroleum Agency SA, 2004/5].

Figure 1 Map of Southern African Offshore basins.

Source: Petroleum Agency SA, 2003.

The Outeniqua Basin, located in the southern offshore area, seen in Figure 1, comprises of a chain of 'en echelon sub-basins' [Petroleum Agency SA, 2004/5] namely the Algoa Basin (furthest to the east) followed by the Gamtoos Basin, the Pletmos Basin and the Bredasdorp Basin (furthest to the west). Each basin is characterised by half-graben structures formed by rifting that is overlain by variably thick sediments of the drifting stage [Petroleum Agency SA, 2004/5]. This drift stage marked occurrences of cyclic sedimentation and accumulation as the basin was formed. The Bredasdorp, Pletmos and Gamtoos Basins extend towards the deep marine and converge into the Southern Outeniqua Basinal area. The entire basin contributes 30% of the total basinal area and spans about 124 000km^2 [Petroleum Agency SA, 2004/5]. The Outeniqua Basin has a history of strike-slip movement, which occurred during the Gondwanaland break-up [Petroleum Agency SA, 2004/5].

It is thus clear that the break up of Gondwanaland played a vital role in the formation of basins off the Southern African offshore area and that rifting was the key element in shaping these basins (illustrated in Figure 1).

1.3 Regional Chronostratigraphy of Southern African offshore basins

The Upper Palaeozoic in this region was characterised by subduction during the Late Carboniferous to Early Permian along the southwest margin of Gondwana [Petroleum Agency SA, 2004/5]. This changed an old passive margin into a foreland basin known as the Great Karoo Basin [Petroleum Agency SA, 2004/5]. Sediments were fed into this basin from the south. The Cape Fold Belt formed during the Permo-Triassic by the formation of an arc which thrusted the Cape Supergroup (shown by Figure 2), which spans over four continents [Petroleum Agency SA, 2004/5].

The Mesozoic is characterised by volcanism in the Early to Middle Jurassic, which marked the end of erosion and peneplanation. This occurred in South Africa, the Falklands and Antarctica, which is evident of the Gondwana break up [Petroleum Agency SA, 2004/5]. The eastern margin of Africa started to break away with

Madagascar and Antarctica pulling away. This caused the formation of the Durban and Zululand Basins [Petroleum Agency SA, 2004/5].

Figure 2 Evolution of Cape Fold Belt.

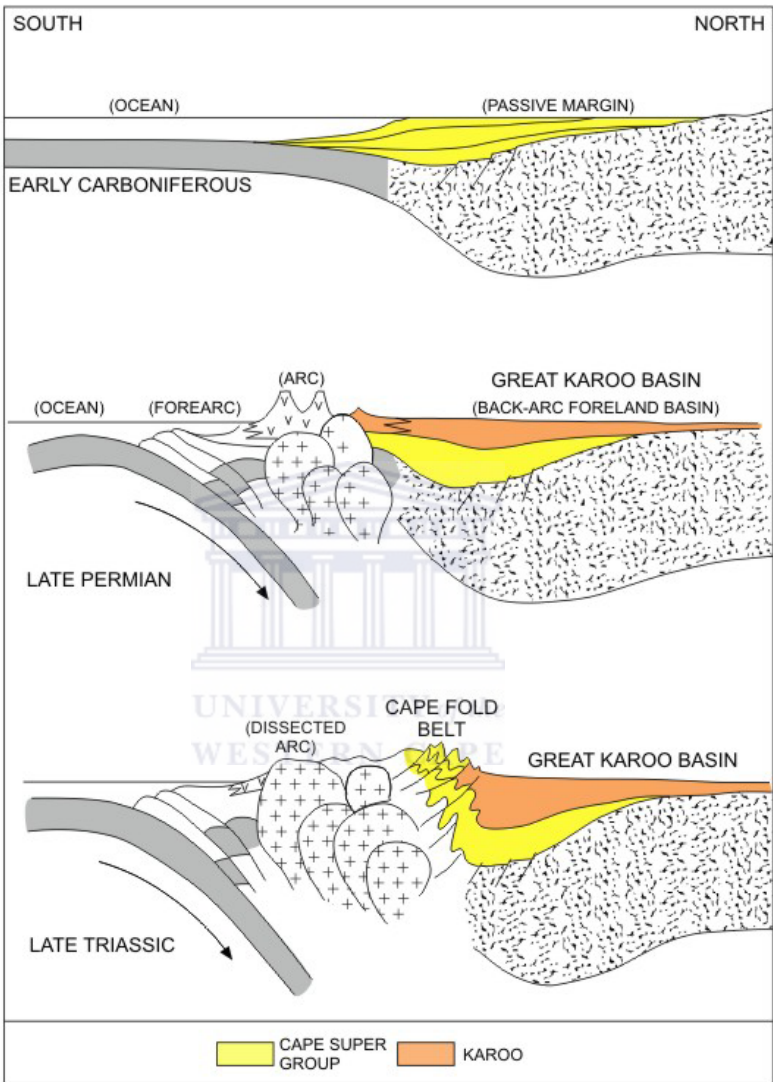

Source: Petroleum Agency SA, 2003.

The movement of microplates past southern Africa caused shearing between plates. The Falkland Plateau, in particular, during the Early to Middle- Cretaceous moved towards the south west past the south coast of Africa which resulted in dextral shearing between the plates [Petroleum Agency SA, 2004/5]. This movement marked the formation of the sub-basins of the Outeniqua Basin as failed rifting created half-grabens, which started in the east and progressed towards the west. Thus the Algoa

Basin was first formed and followed in sequence by the Gamtoos Basin, then the Pletmos Basin and lastly the youngest Bredasdorp Basin [Petroleum Agency SA, 2004/5].

During the Early Cretaceous, in the lower Valanginian, the onset of the drift was marked by an unconformity 1At1 [Petroleum Agency SA, 2004/5, Turner et al., 2000], the letter given by the sequence overlying it (A) and the number before it marks the order of occurrence and the 't1' marking the nature of the sequence (type 1). Most sequences are third and higher order sequences [Petroleum Agency SA, 2004/5]. The drift-onset stage continued with dextral shearing which ended only in the Mid-Albian, which is marked by unconformity 14At1. Within this period the Falkland Plateau made its final separation from Southern Africa. This is known as the transitional rift-drift Phase that is part of the development of a passive margin [Petroleum Agency SA, 2004/5; Davis et al. 1996]. These three phases (rift, transitional rift-drift, and drift) are shown in Figure 4.

The break up of Gondwanaland marked the connection between activities onshore and its relationship to the activities offshore. The link between the tectonic nature of moving microplates as adjacent 'potential continents' sheared passed each other, marked the tectonic activities now evident in the stratigraphic sequencing of respective layers within the basins offshore Southern Africa.

CHAPTER TWO:

2.1 The structure of the Bredasdorp Basin

The field of study requires a background into the formation of the Bredasdorp Basin. The following is a brief introduction into the formation of the Bredasdorp Basin on a local scale and how it is linked to the regional geology that has been discussed.

The Bredasdorp Basin is located beneath the Indian Ocean on the southern South African Coast. It covers about 18, 000km^2 (200km long and 80km wide) [McMillan et al., 1997] comprising Upper Jurassic, Lower Cretaceous (synrift continental and marine strata) and Cretaceous and Cenozoic (post-rift divergent margin strata) [Brown et al. (1995), Turner et al. (2000)]. The basin is bounded by two arches, the Agulhas Arch (west and southwest) and the Infanta Arch (northeast). Figure 3.1 below illustrates this.

Figure 3.1 Location map of The Bredasdorp Basin.

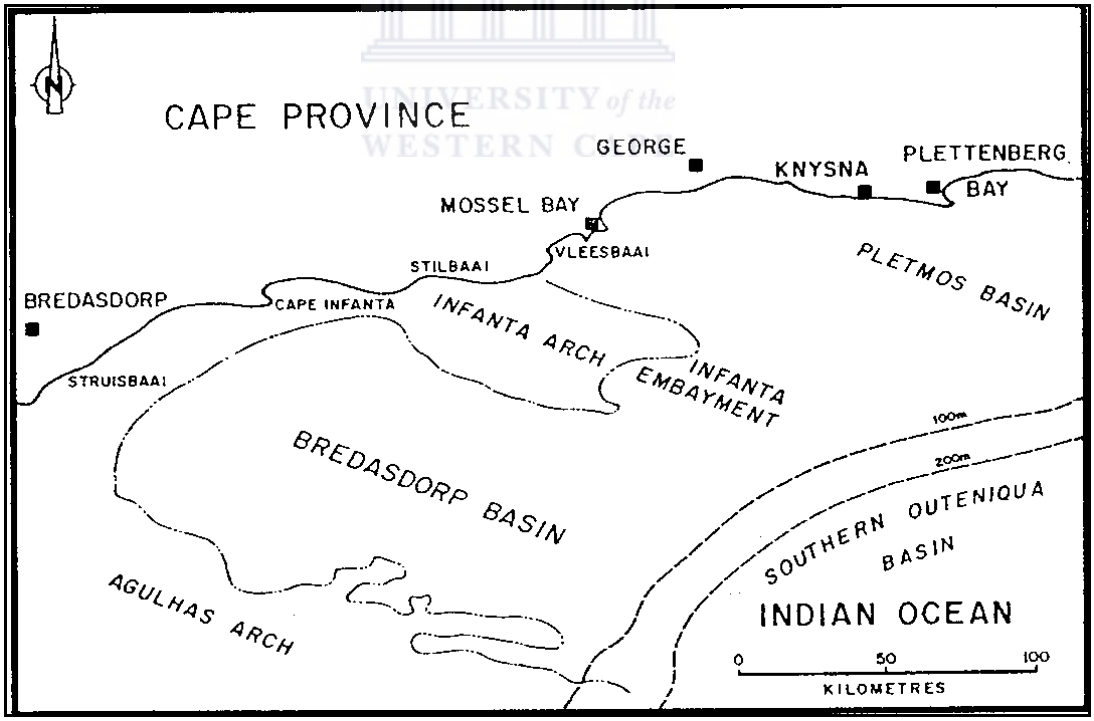

Source: De Wit and Ransome, 1992

Rift faults are found along the Agulhas Arch margin with minor faults along the Infanta Arch margin (northeast) [Brown et. al., 1995]. An opening in the southeast

area of the basin allows it to link up to the adjacent Southern Outeniqua Basin. A structural cross section of the Bredasdorp Basin is shown in Figure 3.2 below.

Figure 3.2 Rift faulting in The Bredasdorp Basin

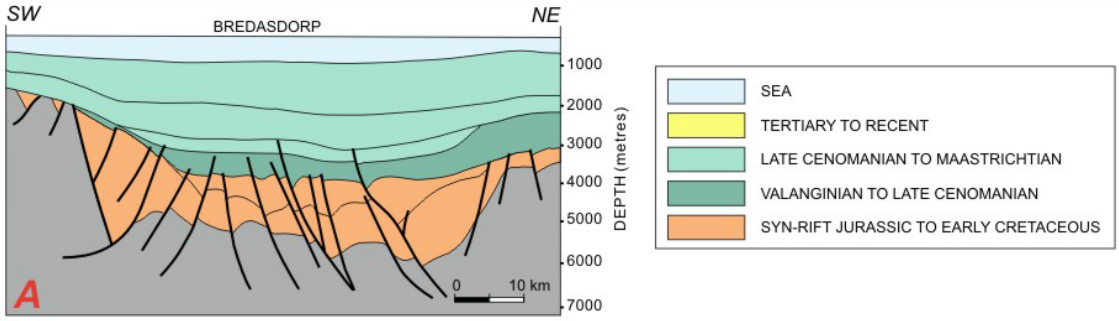

Source: Petroleum Agency SA, 2003.

2.2 The Tectonic Setting of the Bredasdorp Basin

Break up in the east caused dextral transtensional stresses [McMillan et al., 1997], which gave rise to normal faulting in the northern Agulhas-Falkland Fracture Zone. Faulting in the synrift stage, between the Agulhas Arch and Infanta Arch, trends northwest to southeast. This normal faulting resulted in graben and half-graben basins [Brown et al., 1995, McMillan et al., 1997]. Sedimentation continued from horizon D to 1At1 (Figure 4) until about ~126Ma from continental and marine sources. During this period rift faulting ceased and post-rift activity (tectonics, erosion, and deposition) commenced [Brown et al., 1995]. Evidence of differential subsidence is apparent in the sedimentation as horst structures contain condensed units and grabens contain expanded units from horizon D to 1At1 (Figure 4) [McMillan et al. 1997]. During the rift phase, the sediment supply into the Bredasdorp Basin was sourced from provenances in the north and northeast comprising of orthoquartzites and slates from the Cape Supergroup as well as sandstones and shales from the Karoo Supergroup [McMillan et al. 1997].

The 1At1 unconformity was triggered by upliftment of the arches and horst blocks [Brown et al., 1995] and terminated the active rift sedimentation [McMillan et al.,

1997]. Sequences 1At1 to 13At1 were formed by thermal subsidence, reactivated normal faulting and continued deposition of post-rift onlap-fill sequences [McMillan et al., 1997]. This cycle occurred predominantly in the central Bredasdorp Basin between 126-117.5Ma [Brown et al., 1995], which coincided with late synrift activity of subsiding basins by rift faulting. This subsidence was rapid initially (1At1 times), but started diminishing towards the end of the supercycle (1At1 to 5At1) [Brown et. al., 1995, McMillan et al., 1997]. Erosion occurred during this time which carved submarine valleys and canyons into pre-1At1 units, these then provided channels for sediment supply into the deeper basin area from the northwest, west and southwest [McMillan et al., 1997]. The onset of unconformity 6At1 was triggered by uplift [Brown et. al., 1995]. Turbidity currents dominated the sediment flow into the Central region of the basin from 5At1 to 13At1. This area lacked adequate water circulation and oxygen [McMillan et al., 1997].

The second supercycle of the post-rift stage gave cycles 6-12 (third-order). This occurred between 117.5-112Ma [Brown et al., 1995]. Regional subsidence at high rates produced sequence 6A [Brown et al., 1995]. As subsidence rates and faulting slowed down (115.5-112Ma) the deposition of system tracts 8-12 occurred with sequence 7 removed by 8At1 erosion during 116-115Ma [Brown et al., 1995].

During the Early Aptian (112Ma) to mid-Albian (103Ma) the sea level dropped which caused material to be eroded from highstand shelf sandstones that were transported into the centre of the basin by turbidity currents from west to southwest [Turner et al., 2000]. These sediments formed “stacked and amalgamated channels and lobes” [Turner et al., 2000], which include fan lobes of a coarsening-upward nature with reservoirs consisting of channel deposits characterised by fining-upwards [Turner et al., 2000]. The Channels dominate the western to south-western area where as the fan lobes are dominant in the eastern parts of the basin [Turner et al., 2000]. Source rocks of Aptian age can be found in the south of the basin (this being due to the formation of a 5km wide and 50km long submarine channel with tributaries updip serving as conduits of deeper sedimentation) [McMillan et al., 1997] and the organic

material is predominantly type II having a type-I component [Van Der Spuy, 2000]. The channel of 13A forms the site of oil accumulations according to McMillan et al. The 14A sequence contains basin floor-fan sandstones in the centre of the basin which contain some oil bearing reservoirs [McMillan et al., 1997].

The late Cenomanian (Figure 4) shows erosion, marked by 15At1, with minor warping and some uplift [McMillan et al., 1997]. Erosion was at a maximum in the most eastern part of the basin. A shale found immediately above 15At1 (Figure 4) contains a rich content of plankton and other organic materials, which has a source rock potential mostly in the south and absent in the north [McMillan et al., 1997]. Its viability is unfortunately a factor as the rock is too immature with little prospect of a source in the southern region. Progradation occurred between Turonian and mid-Coniacian time. A domal structure was formed in the south eastern region of the Bredasdorp Basin around the latest Cretaceous period (Figure 4), which forms one of few late structures forming in the basin [McMillan et al., 1997].

During the Tertiary to present day sedimentation of highstand shelf deposits comprising of glauconitic clays, biogenic clays with minor sands occurred. These sediments were obtained from the erosion of the Agulhas Arch flanks by uplift of the Late Cretaceous deposits [McMillan et al., 1997]. Early Miocene marks the end of uplift of the arch and biogenic clay deposition over the southerly parts of the basin. Unconformities in Holocene and late Pleistocene are found overlying the Miocene rocks. [McMillan et al., 1997]

These features can be seen in the chronostratigraphic log in Figure 4 which marks several Type-1 sequence boundaries as unconformities designated to their respective sequences. It displays two synrift phases, the first from the Early Jurassic (157.1Ma) to the Lower Cretaceous (121Ma) and the second considerably shorter synrift phase within the Hauterivian (part of the Lower Cretaceous), which was separated by the first Type-1 inconformity (1At1).

Figure 4 Chronostratigraphy of The Bredasdorp Basin

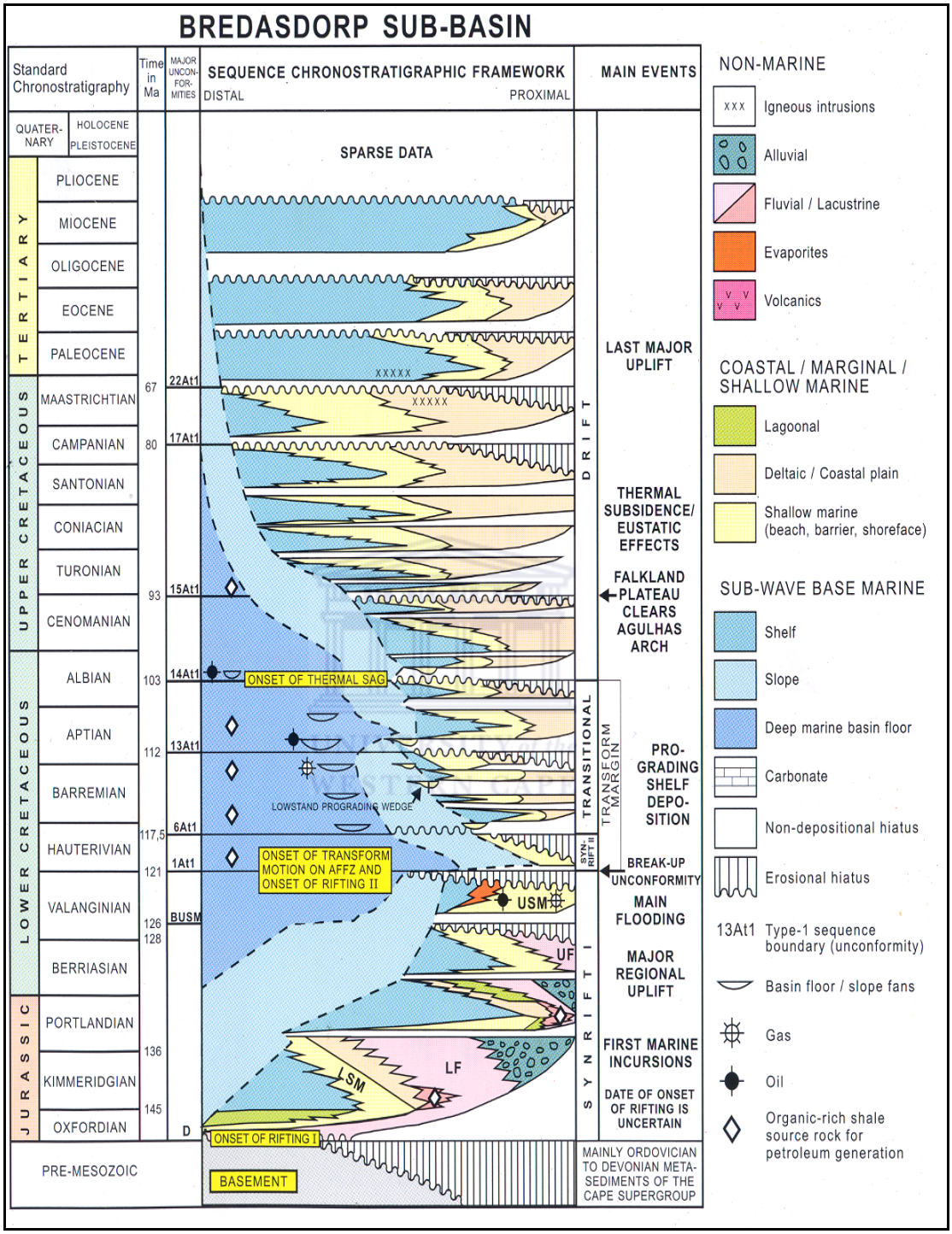

Source: Petroleum Agency SA, 2003.

The transitional phase marks the development of a lowstand prograding wedge due to shelf deposition and basin floor and slope fans towards the distal part is evident

(Figure 4). It is apparent that the main organic-rich shale, which is a good possible source rock for petroleum generation, occurs predominantly in the distal part within the transitional phase. The onset of the drift phase is marked by the unconformity 14At1 as well as the onset of thermally induced sag.

2.3 Thermal Gradient history of the Bredasdorp Basin

The Bredasdorp Basin has a present thermal gradient of 35-49°C.km-1 [Davies, 1997], with a moderately high heat flow. Late Cretaceous saw a reduced temperature gradient due to reduced heat flow and subsidence after rifting. The migration of Africa over a mantle plume during the late Cretaceous to early Tertiary saw regional uplift which increased heat flow in the Basin. Burial rates, on the other hand, were low compared to post-rift subsidence. Until ~80Ma [Davies, 1997], temperatures in the basin increased at a rate >3°C/Ma. From ~80Ma to ~55Ma, sedimentation rates decreased, and thus the temperature increase rate dropped to <0.3°C/Ma on average during the Early Tertiary and increasing again during the Miocene to Pliocene. Turonian source rocks for oil generation increased in temperature by <10°C during ~80Ma to ~55Ma [Davies, 1997]. Migration of formation waters from the Southern Outeniqua Basin into the Bredasdorp Basin post-Aptian sequences saw temperatures increase by ~20°C this was evident by the change in maturation upon burial.

Maturation of the Aptian and older formations were affected by early burial, hotspot transit and a hydrothermal event [Davies, 1997]. The burial history of the Bredasdorp Basin is characterised by an unusual thermal history due to variable heat flow rates throughout the formation of the basin.

2.4 The Area of interest within the Bredasdorp Basin

Well E-BA1 is situated 125km south-southwest of Mossel Bay, 8km northwest of borehole E-AR1 and southeast of borehole E-Z1 [Ludik (1990), Ranoszek and Labuschagne (1990)] in Block 9. Two cores were drilled back to back within the 9At1 to 13At1 sequences and interpreted by Ludik (1990). The depths of the two cores were 2828 to 2834 mbKB for core #1 and 2834 to 2848 mbKB for core #2

respectively [Ludik, 1990]. Thin sections were prepared from depth intervals 2412 to 2435 mbKB and 2793 to 2868 mbKB. A total of 32 slides were selected for analysis from both Cores #1 and #2 as well as from rock cuttings outside the depths of the cores. Samples (8) for X-ray Diffraction were also selected from core #1 and #2. A further study of Scanning Electron Microscopy was performed using 4 samples from selected depths also obtained from the cores.

Core #1, according to Ludik (1990), is composed of two facies types. Facies A is sandstone and Facies B is a claystone. The sandstone Facies (A) is described by Ludik (1990) as a massive proximal deep marine channel fill sandstone of fine to medium grain, which is well sorted. There is a minor component of glauconite and detrital carbonaceous grains [Ludik, 1990]. A claystone of deep marine pelagic clays and turbidites [Ludik, 1990] was described for Facies B, with horizontal laminations in cm scale. It is dark to greyish black (high carbonaceous content). Sandstone and siltstone intercalated laminae are present [Ludik, 1990]. Core #2 is a continuation of the sandstone unit with an underlying conglomerate.

CHAPTER THREE:
METHODOLOGY

3.1 Thin section analytical methods

A petrographic microscope was used to perform the analysis.

Quartz, feldspar, lithic fragments, accessory minerals, ductile minerals and authegenic minerals were identified in PPL and XPL. The grain size, grain shape and level of alteration were observed. The percentage of each mineral was determined. In XPL, the extinctions of these minerals, the contacts between minerals were observed.

Quartz, feldspar and lithic fragments were observed by using a set format.

1. Grains were identified using PPL and XPL.
2. Grain shape and boundaries were noted.
3. Extinctions on grains were noted via XPL. This could be seen by rotating the stage and watching certain minerals go completely black. These extinctions could be plane (whole grain extinct) or undulose (a sweep of extinction across the grain).
4. Inclusions or vacuoles were also noted this was better done under PPL. These are little 'bubbles' found inside the minerals. They can either be gas, water or oil.
5. Twinning features were noted (under XPL).
6. Mineral alteration and deformation of ductile minerals were identified.

When a feature of interest was spotted, the magnification could be adjusted to 'zoom' into the feature for a closer view. This was used when looking at clays. The type of clays may not have been identified but it could distinguish between grain rimming and pore filling clays. Finer material could also be identified such as the content of rock fragments. By using a higher magnification it was possible to identify what mineral types were in the lithic fragment and if the fragment was purely grains or if a matrix was present between the grains, such as clays.

The textural aspects of the slide were observed as an overall representation of the slide. The main aspects looked at:

1. Grain size. An average value was determined by visual comparison.
2. The sorting. It was graded using a 'poor-moderate-well' system using visual comparison charts.
3. Grain Shape. Its range includes: round, subround, subangular to angular using visual American/Canadian Stratigraphic comparison charts.
4. Sphericity. This has a range from low to high with low sphericity being more oblong in shape and a high sphericity being more like a sphere.
5. Compaction. Well compacted- tightly packed
   Moderate compaction- moderately packed
   Poor compaction- poorly packed
6 Contacts. These could either be identified as long, tangential, concavo-convex or sutured.
7 Lithification aspects. This could either be matrix- supported or grain supported.
8 Porosity. The volume of pore spaces were identified visually and classified into a range- excellent, good, average, poor or very poor.
9 Connectivity. These are the pores which are connected by pore-throats. Pore-throats are restricted openings which connect adjacent pores [Kearey, 1996]. These too were classified into range- excellent, good, average, poor or very poor. The classification was possible by the introduction of blue epoxy fluids which illustrated connectivity. The blue epoxy fluid was thus unable to penetrate the isolated pores but could easily penetrate the connected pores thus making it possible to determine the level of connectivity using visual comparison charts for each thin section.

Once all of these aspects were identified a paragenetic history was devised. This was done by using the diagenetic minerals' relationship to the framework grains. The

quality of the thin sections received was also taken into account during the analysis process and is noted as being of quality that is not up to standard for an accurate detailed description. In all honesty, some identifications are made complicated by the quality of the slides. The slides were not correctly polished and were received with no glass cover slip on top of each slide. This is however, not an attack directed at the contributors of the slides as the nature of quality control during the production of these slides is not clearly known. It is understood that the slides have been produced fifteen years ago and wear and tear could have resulted in the poor quality at present. This is merely a noted problem that should be taken into account when looking at the results.

Once the analysis was completed, photographs were taken which are representative of each thin section. At least two photographs were taken, one in PPL and another in XPL. This was done by using a specialized digital camera (model 100NIKON) which was mounted to the petrographic microscope. These photographs are included in the results.

The results of the analysis were then put into a database which characterizes each aspect in a particular order. These results are displayed in the subchapter: Results of the detailed petrographic analysis.

3.2 X-ray diffractometry (XRD) methods

Clays were observed within the thin section samples. The types of clays are important in the quality of the reservoir and for this reason a XRD analysis was performed to determine the types of clays present, as the thin section analysis was not sufficient. A powder diffraction analysis was conducted using a multipurpose powder diffractometer known as the D8 Advance by Bruker. The machine houses a detector called a Vantec1 which is a sensitive detector with a multi-channel position. Samples were crushed to a powder and mounted in the sample holder. Lock coupled Theta-

Theta scans were conducted. The D8 Advance was used as an experimental trial conducted in Germany (By iThemba Labs), which proved less time-consuming reducing analysis time from hours to minutes. The data was analyzed using the Bruker DiffracPlus Evaluation program along with the powder diffraction database. The results are illustrated in Chapter 4.3.

3.3 Scanning electron microscopy (SEM) methodology

In order to gain knowledge of the structures of the clays in the samples, it was necessary to perform a scanning electron microscopy (SEM) study of numerous samples.

Samples were selected at various depths from cores 1 and 2. These samples were pieces of >5mm in length and >2mm in width. Each sample was coated in Gold Palladium for about 30minutes. This is done to make sure that the sample is conductive. Once coated, each sample is put on a palette-like stand where it is placed under an electron beam. The machine used to do the analysis is a LEO Stereoscan 440 which is a high vacuum microscope.

The stereoscan workstation is connected to a computer which enables the operator to view images taken by the electron microscope. The magnification can be adjusted to the choice of view, these can be seen in the results. Images were taken by freezing the view and taking a ‘snapshot’ of the desired image.

CHAPTER FOUR:
RESULTS

4.1 Results of the Detailed Petrographic Analysis

Sample: SWC I 40 **Depth: 2412.00m**

Composition: Framework minerals:	***Percentages***
Quartz	50%
Feldspar	20%
Lithic Fragments	10%
Minor Glauconite	3%

Quartz: Monocrystalline and polycrystalline (Figure A2- XPL).
Undulose and planar extinctions.
Grain to grain contacts.
Sutured, long and tangential grain boundaries and contacts.
Dark borders around boundaries.
Inclusions in grains.

Feldspar: Cracked with no distinct grain shape.
No visible twinning.
Vacuoles in grains.

Lithic Fragments: Fine quarts grains in clay matrix

Glauconite: Green in PPL, Green in XPL. (Figures A1- PPL and A2-XPL)

Ductile Minerals:	***Percentages***
Clays	5%
Micas	2%

Clays: Clasts and matrix.
Rimming framework grains and filling pores.
Micro pores within clays.

Micas: Clear in PPL, brilliant colours in XPL.
Deformed flakes.
Muscovite and biotite

Authigenic Minerals:	***Percentages***
Quartz cement	7%
Carbonate Cement	3%

Quartz Cement: Overgrowths on detrital grains

Carbonate Cement: Found between grains and in pores.
Shows patchwork cleavage.

***Porosity*:** Average
Pore sizes vary
Intergranular and intragranular pores.
Isolated pores within grains, connected pores between grains.

Primary and secondary porosity.
Poor connectivity (lack of blue epoxy dye Figure A1-PPL)
Some pores contain muddy material.

***Texture*:** Fine-grained (0.1mm average) [x4 magnification]
Angular shape grains.
Low sphericity.
Moderately sorted.
Tightly packed grains
Long, Tangential and sutured contacts.
Matrix and grain supported.

Name: SubArkose (Sandstone)

Comments: The overall slide is scratched by poor quality preparation. The porosity and permeability of the slide is average and the grains are fairly tightly compacted.

Two figures of a section representing the slide at depth 2412m are shown.

FIGURES A. Sample: SWC I 40 Depth: 2412.00m

Figure A-1- PPL

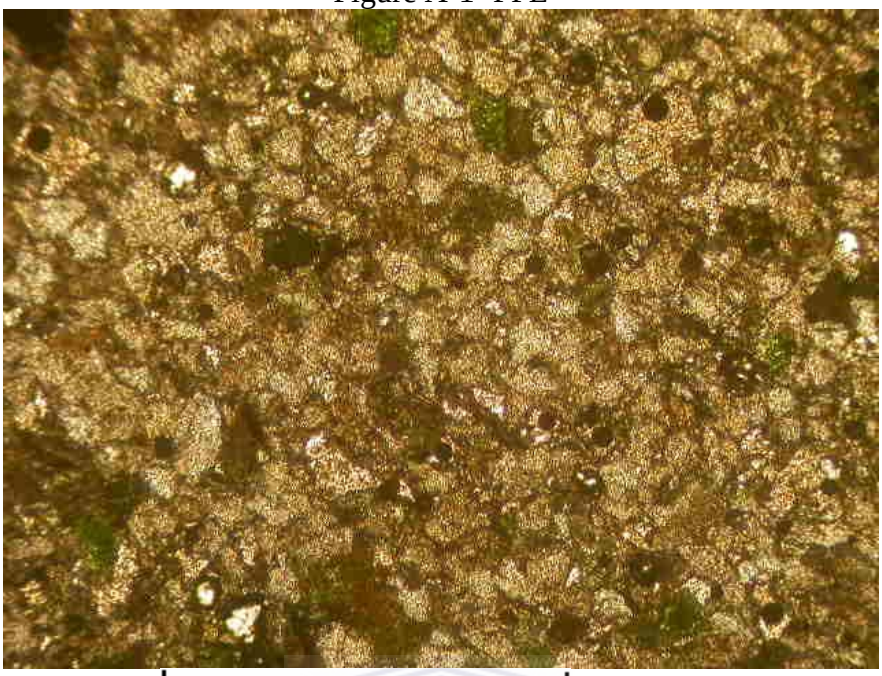

Scale (Magnification x5)

Figure A-2- XPL

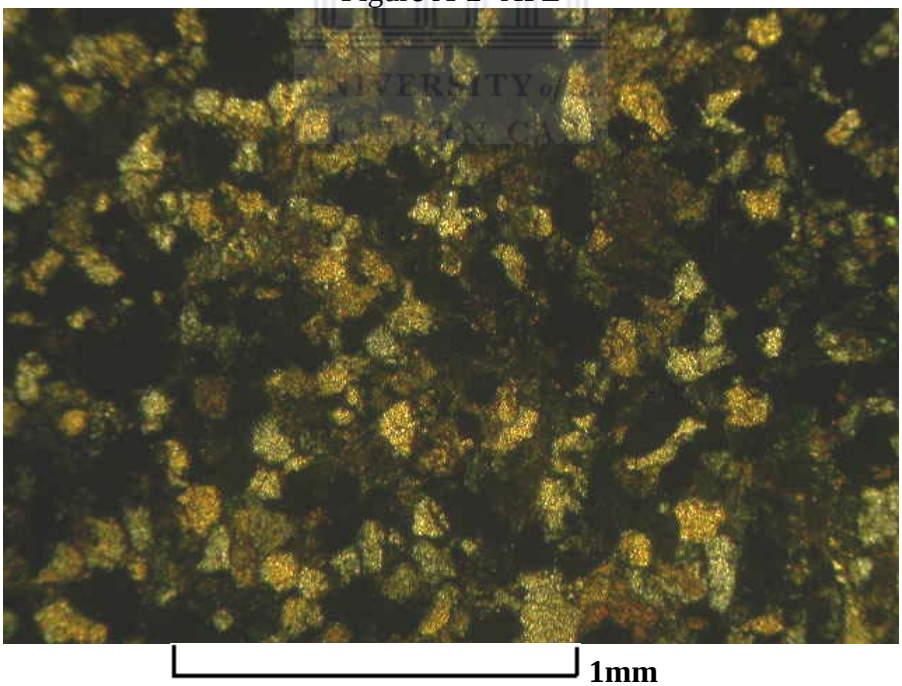

Scale (Magnification x5)

Sample: SWC I 39 **Depth: 2413.50m**

Composition: Framework minerals: ***Percentages***

Quartz	55%
Feldspar	15%
Lithic Fragments	10%
Glauconite	3%

Quartz: Monocrystalline and polycrystalline
Undulose extinctions
Grain to grain contacts
Sutured grains

Feldspar: Cracked
Twinning- mocrocline and orthoclase
Vacuoles within grains or bubbles in the resin
Partially dissolved grains

Lithic Fragments: Fine quartz grains in clay matrix

Glauconite: Green grains in PPL and XPL. (Figures B1-PPL and B2-XPL)
No distinct shape, mostly pellets

Ductile Minerals: ***Percentages***

Clays	3%
Muds	2%
Micas	1%

Clays: Grain rimming and as matrix (claystone)
Calcite grains in clays
Appears as dark dusty material between grains in XPL (Figure B2)

Muds: Brown material found between some grains

Micas: Very few grains
Appear as flakes that are deformed
Clear in PPL and Brilliant Colours in XPL
Muscovite and Biotite

Authigenic Minerals: ***Percentages***

Quartz Cements	5%
Carbonate Cements	5%

Quartz Cement: Appear as overgrowths on detrital grains

Carbonate Cement: Found between grains
Patchwork Cleavage
Pastel colours in XPL, clear in PPL

***Porosity*:** Good porosity
Large pores
Intergranular and intragranular porosity
Primary and secondary porosity
Poor connectivity

***Texture*:**	Fine-grained (0.5 average) [x4 magnification] Moderately sorted Subangular grain shapes Moderate compaction Matrix and grain supported Long, tangential and sutured contacts
Name:	Subarkose (Sandstone)
Comments:	The overall sample displays poor connectivity seen by the lack of blue pores penetrated by the dye (Figure B1). Some isolated pores are seen in Figure B1 which appear black in XPL (Figure B2). There are many air bubbles in the thin section that was formed when the slide was made. Black material in pores is mud formed by alteration of less resistant grains such as feldspars.

FIGURES B. Sample: SWC I 39 Depth: 2413.50m

Figure B-1- PPL

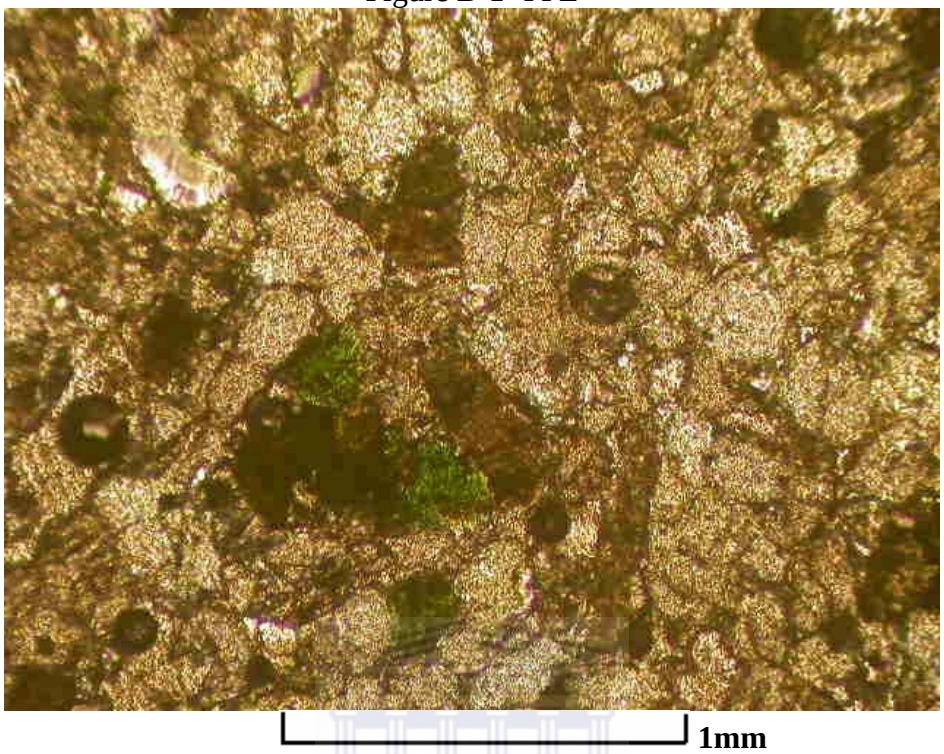

Scale (Magnification x5)

Figure B-2- XPL

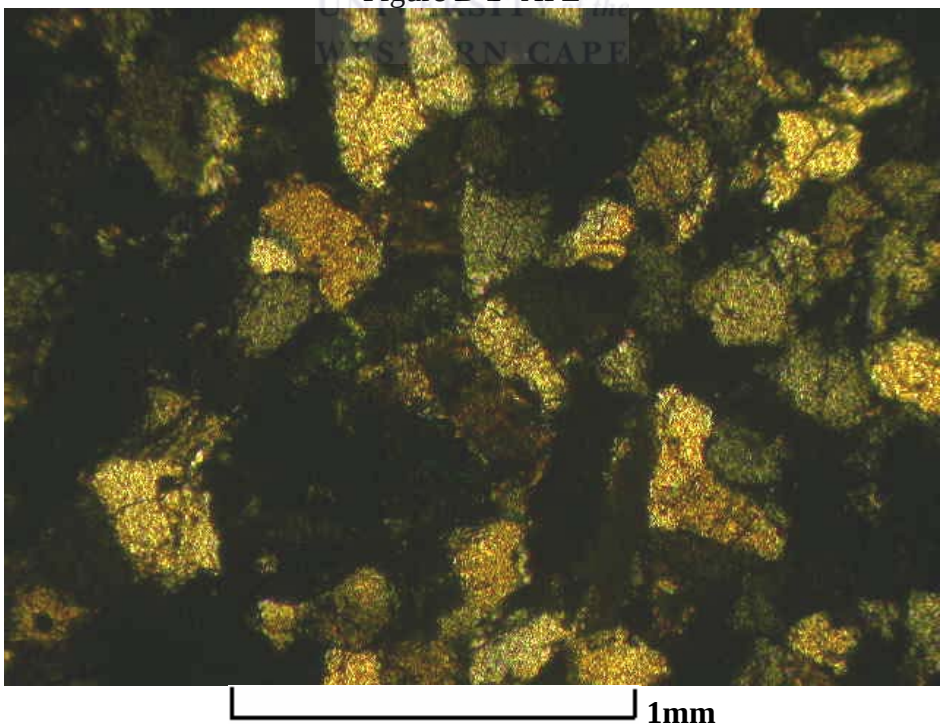

Scale (Magnification x5)

Sample: SWC I 38 **Depth: 2418.50m**

Composition: Framework minerals:	***Percentages***
Quartz	60%
Feldspar	15%
Lithic fragments	5%
Glauconite	5%

Quartz:	Monocrystalline and polycrystalline Grain to grain contacts Undulose extinction
Feldspar:	Cracked No visible twinning (orthoclase) Contain overgrowths
Lithic Fragments:	Fine quartz grains in clay matrix
Glauconite:	As Pellets between grains and in pores.

Ductile Minerals:	***Percentages***
Clays	5%
Muds	4%
Micas	1%

Clays:	Matrix (Claystone) containing tiny fragments of micas and calcite are found between grains
Muds:	Dusty material found between grains and pore spaces
Micas:	Flakes which are clear in PPL and Brilliant colours in XPL

Authigenic Minerals:	***Percentages***
Quartz Cement	3%
Carbonate Cement	2%

Quartz cement:	Overgrowths on detrital grains. Clear overgrowths on feldspar grains
Carbonate cement:	Found between grain Fills pores

***Porosity*:** Moderate porosity (few pores)
Poor connectivity (no blue dye) seen in figure C-1

***Texture*:** Fine grained (0.5mm average) [x4 magnification]
Sorting is moderate
Grain shape is angular
Sphericity is low (mostly oblong)
Grain packing moderately tight
Grains are supported by the matrix
Grain contacts are long

Name: Subarkose (Sandstone)

Comments: The section is tightly compacted with low porosity and permeability. There are gas bubbles in the pores which are as a result of the mounting medium which has started to lift from the thin section. Primary and secondary porosity is not prominent. These features can be seen in Figures C (PPL and XPL).

There appears to be a ‘streak’ running across a few grains which is quartz cement (Figure C-2).

There are traces of red material in the thin section which was identified as an unknown. These were observed in some pores but could be a red dye that was applied, but the nature of this material is unknown.

FIGURES C. Sample: SWC I 38 Depth: 2418.50m

Figure C-1- PPL

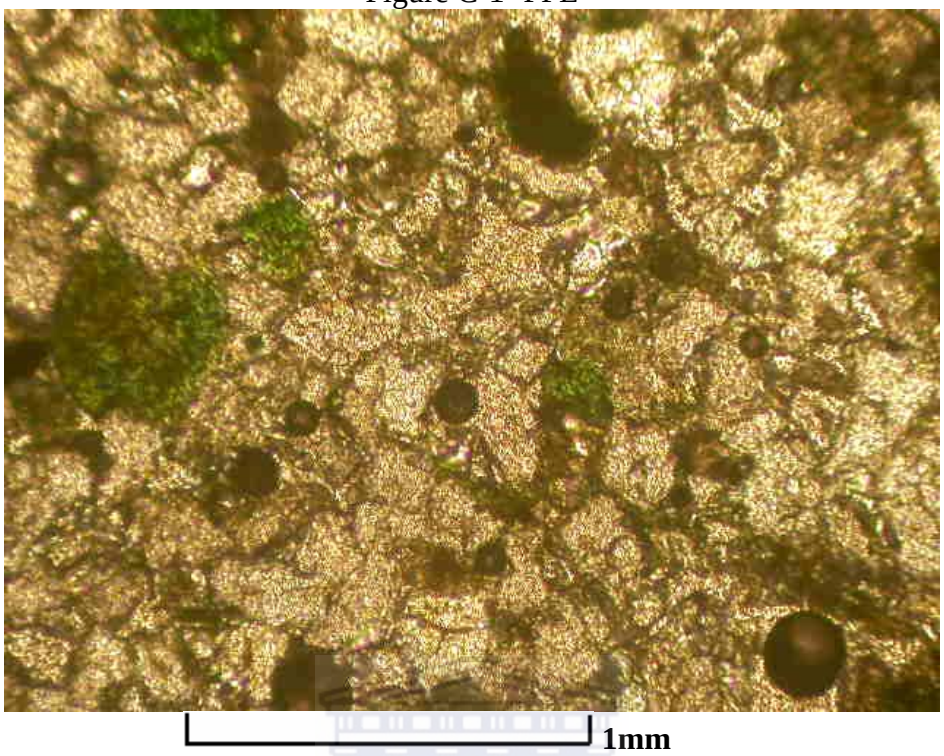

Scale (Magnification x5)

Figure C-2- XPL

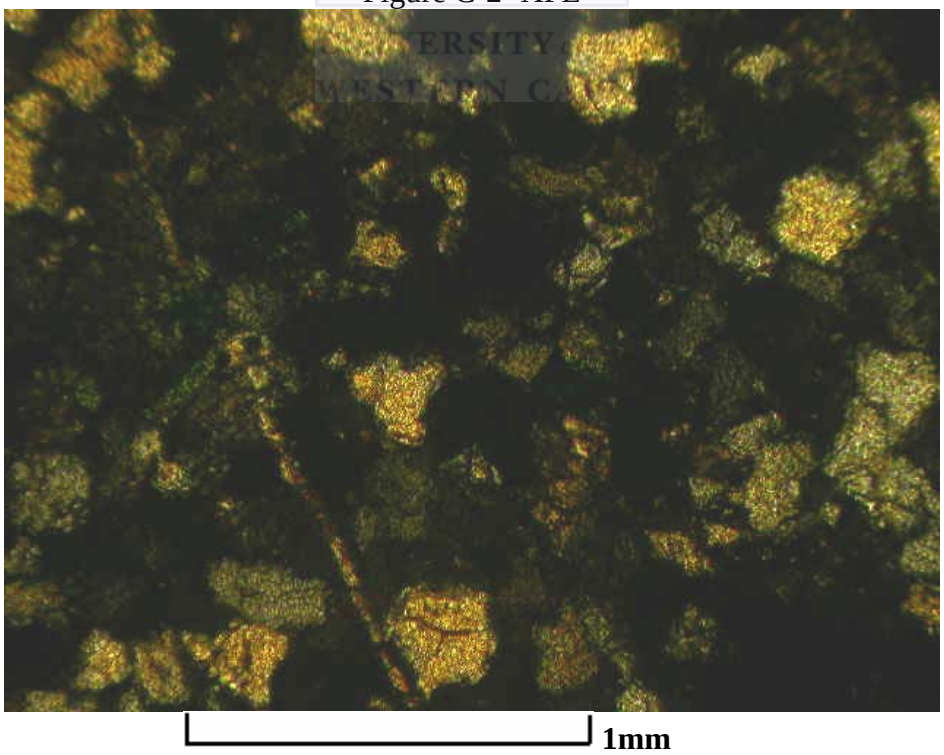

Scale (Magnification x5)

Sample: SWC I 37 **Depth: 2435.00m**

Composition: Framework minerals:	***Percentages***
Quartz	55%
Feldspar	15%
Lithic fragments	5%
Glauconite	5%

Quartz:	Polycrystalline
	Yellow coating on grains
	Planar and undulose extinction
	Cracked grains
Feldspar:	Cracked
	Twinning not prominent
	Orthoclase or microcline altered to kaolinite
Lithic Fragments:	Fine quartz grains in claystone matrix
Glauconite:	Pellets is oblong in shape

Ductile Minerals:	***Percentages***
Clays	5%
Muds	3%
Micas	<1%

Clays:	Grain rimming and pore filling
Muds:	Clasts found between grains
Micas:	Type not distinguished
	As flakes and tiny fragments in clays

Authigenic Minerals:	***Percentages***
Quartz cement	6%
Carbonate cement	5%

Quartz cement:	Overgrowths on detrital grains
Carbonate cement:	Between grains and fills up pores

***Porosity*:** Very few pores visible
Primary and secondary porosity very poor
Poor connectivity
Pores filled with cements, clays and muds

***Texture*:** Fine grained (0.5mm average) [x4 magnification]
Sorting is moderate but some sections are poorly sorted
Grain shapes are mostly sub angular
Most grains are oblong with low sphericity
The packing of the rocks are tight
The grains are mostly supported by matrix but there are some grain supports
The contacts are mostly long due to the grains oblong shape.

Name: Subarkose (Sandstone)

Comments: Porosity and permeability are poor due to the very tightly packed grains and the pore filling muds, clays, cements and the presence of stylolites formed by pressure solution. The reservoir quality can clearly be seen in Figures D-1 and D-2.
Gas bubbles are seen in the slide as a result of the mounting medium and this should not be mistaken for natural porosity.

FIGURES D. Sample: SWC I 37 Depth: 2435.00m

Figure D-1- PPL

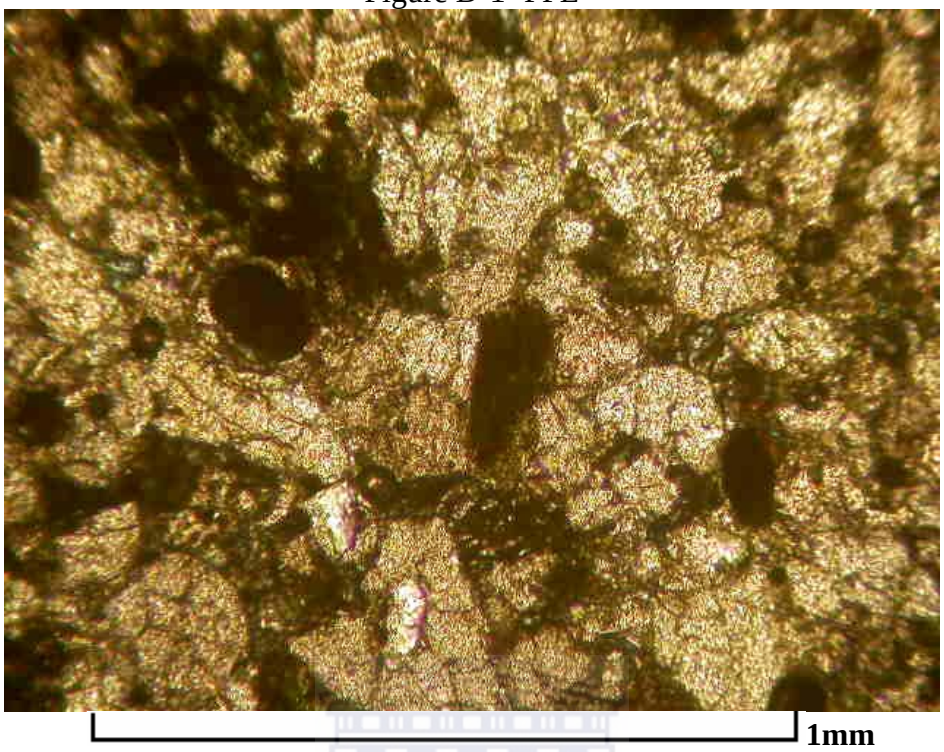

Scale (magnification x10)

Figure D-2- XPL

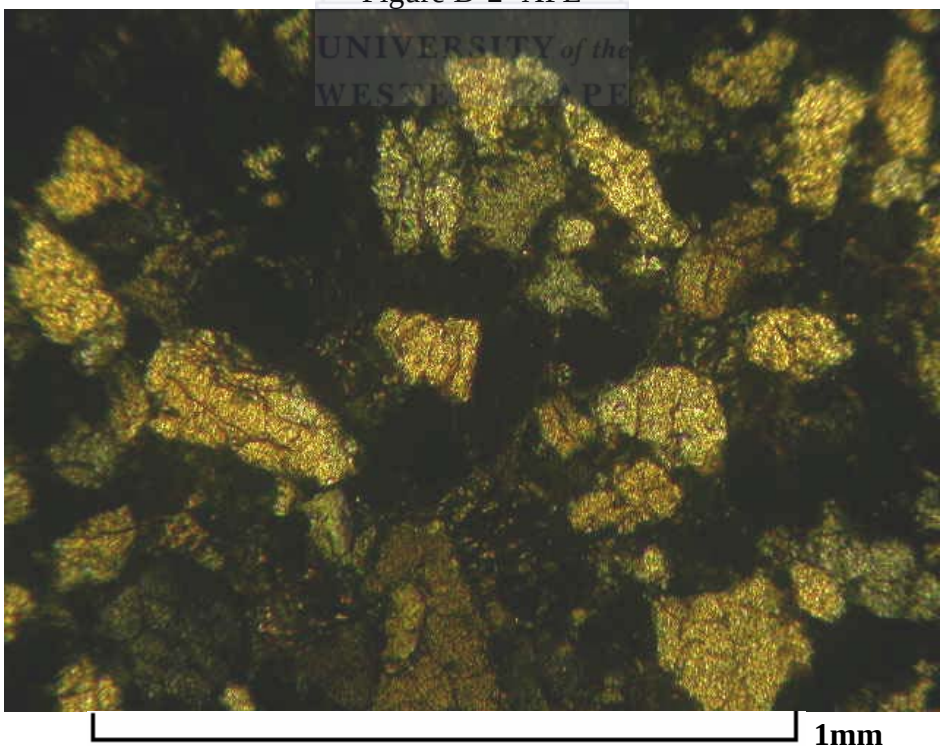

Scale (Magnification x10)

Sample: SWC I 23 **Depth: 2793.00m**

Composition: Framework minerals:	***Percentages***
Quartz	65%
Feldspar	10%
Lithic Fragments	7%
Glauconite	5%

Quartz: Fine to very fine grains
Mostly polycrystalline grains
Grains are sutured together (Figure E-2)
Undulose extinction

Feldspar: Cracked grains
Type of feldspar not distinguishable due to a lack of twinning features
Dissolution of grains

Lithic fragments: Fine material (indistinguishable) but in clay matrix

Glauconite: Pellets are partially overgrown by cement (Quartz) Figure E-1 shows overgrowths of quartz.

Ductile Minerals:	***Percentages***
Clays	5%
Muds	3%
Micas	<1%

Clays: Mainly as matrix and minor as clasts
Matrix contains very fine quartz grains
Matrix are grain rimming and pore filling
Air bubbles in matrix
Some clay matrix contains black material which could be hydrocarbon remnants or plant fragments.
Clay clasts are elongated

Muds: Fills pores and as matrix between pores

Micas: Very minor traces
Flakes found along grain contacts
Slightly deformed

Authigenic Minerals:	***Percentages***
Quartz cement	3%
Carbonate cement	2%

Quartz cement: Occur as overgrowths on detrital grains

Carbonate cement: Found between grains

***Porosity*:** Porosity is poor
Primary and secondary porosity is not easily defined
Connectivity is poor which can be seen by the lack of blue dye Figure E-1

***Texture*:** Very Fine Grained (<0.1mm average) [x4 magnification]

Moderately sorted
Mostly sub angular grains
Low Sphericity therefore mostly oblong shapes
Grains are tightly packed
Grain contacts are sutured
Grain supported and matrix supported

Name: Subarkose (Sandstone)

Comments: There are few pores which are filled with black material representing stresses inflicted upon the rock (which is perpendicular to the length of the stylolite) and clays, muds and cements. This can be seen in Figure E-1 in PPL in the centre of the image.
This slide displays a highly deformed rock due to the lack of porosity and permeability.

FIGURES E. Sample: SWC I 23 Depth: 2793.00m

Figure E-1- PPL

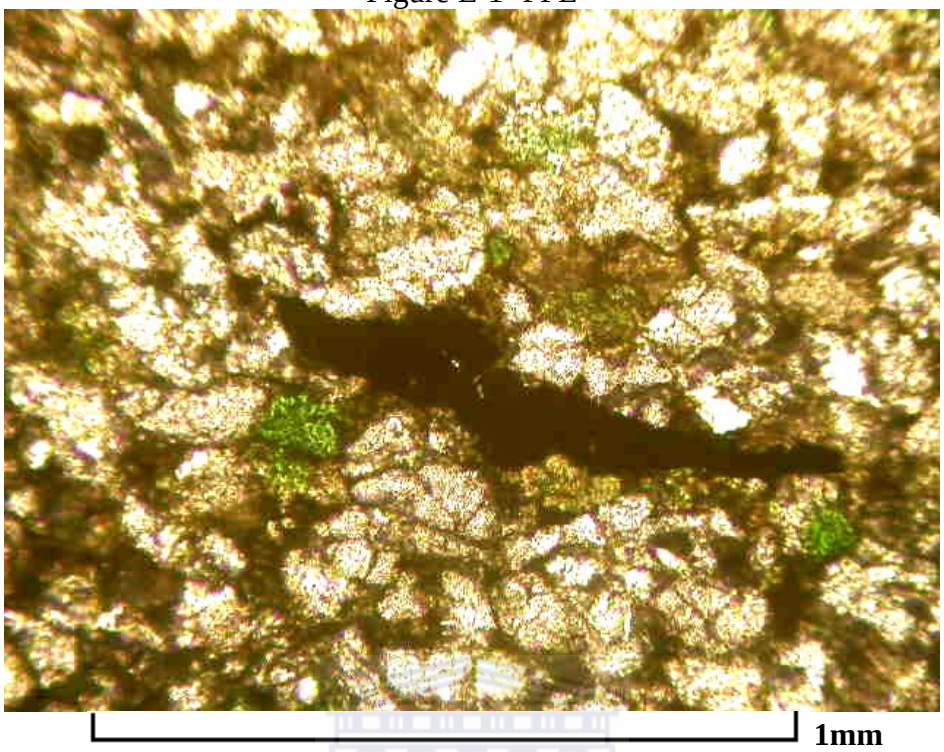

Scale (Magnification x10)

Figure E-2- XPL

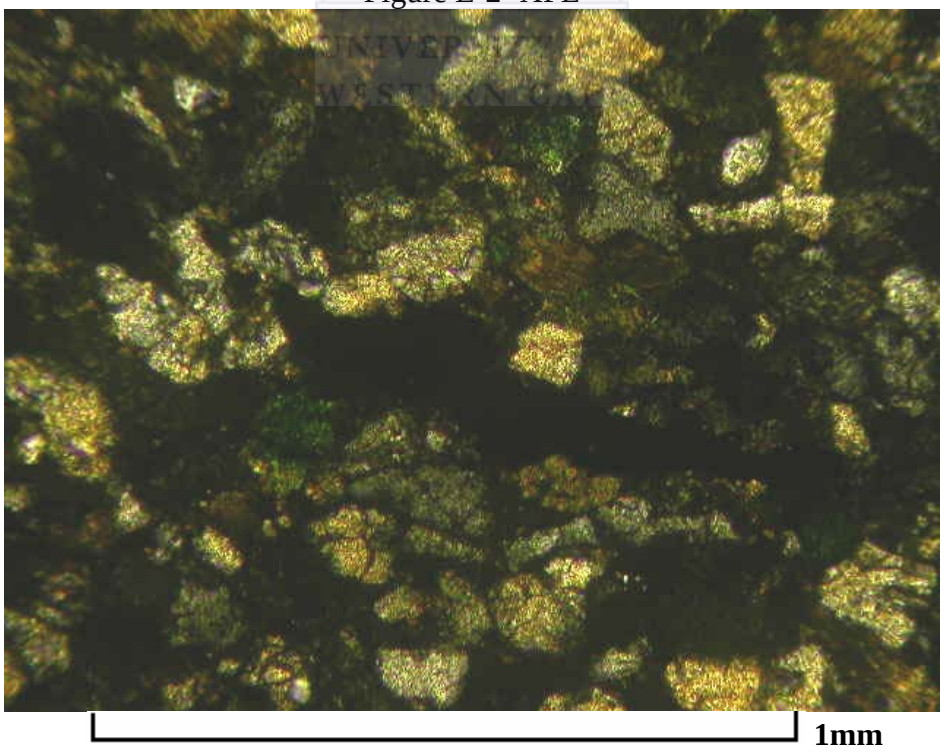

Scale (Magnification x10)

Sample: SWC I 21 **Depth: 2808.00m**

Composition: Framework minerals:	***Percentages***
Quartz	65%
Feldspar	10%
Lithic fragments	5%
Glauconite	3%

Quartz: Monocrystalline and polycrystalline
Cracked grains
Planar and undulose extinctions
Grains are angular in shape
Grains are sutured together where in contact

Feldspar: Cracked grains
No visible twinning features
Dissolution of feldspar has taken place

Lithic Fragments: Fine sedimentary rock fragments
Fine quartz grains in clay matrix

Glauconite: A minor constituent almost an accessory
Pellet shapes are not distinct

Ductile Minerals:	***Percentages***
Clays	5%
Micas	<1%

Clays: Occur as matrix
Contains fine quartz grains with air bubbles

Micas: Occur as flakes
Deformation caused bending of flakes

Authigenic Minerals:	***Percentages***
Quartz cement	6%
Carbonate/ dolomite cement	5%

Quartz cement: Occur as overgrowths on detrital grains

Carb/dol cement: Appear clear in PPL and pastel in XPL (Figures F) as grain coatings

***Porosity*:** Porosity is poor
Permeability is poor
Primary and secondary porosity has almost entirely been destroyed by deformation

***Texture*:** Fine grained (0.5mm average) [x4 magnification]
Rock is poorly sorted
Grain shapes are angular to sub angular
Sphericity is low
Grains are tightly packed

Grains are supported predominantly by matrix but are grain supported as well
Grain contacts are long and sutured

Name: Subarkose (Sandstone)

Comments: Traces of yellow material can be found in the thin section, seen in XPL-Figure F-2. These are trace material precipitated out of solution moving through the rock. These appear as remnants on the grains
Sample underwent alteration seen by cracked grains (Figure F-2 XPL view)

FIGURES F. Sample: SWC I 21 Depth: 2808.00m

Figure F-1- PPL

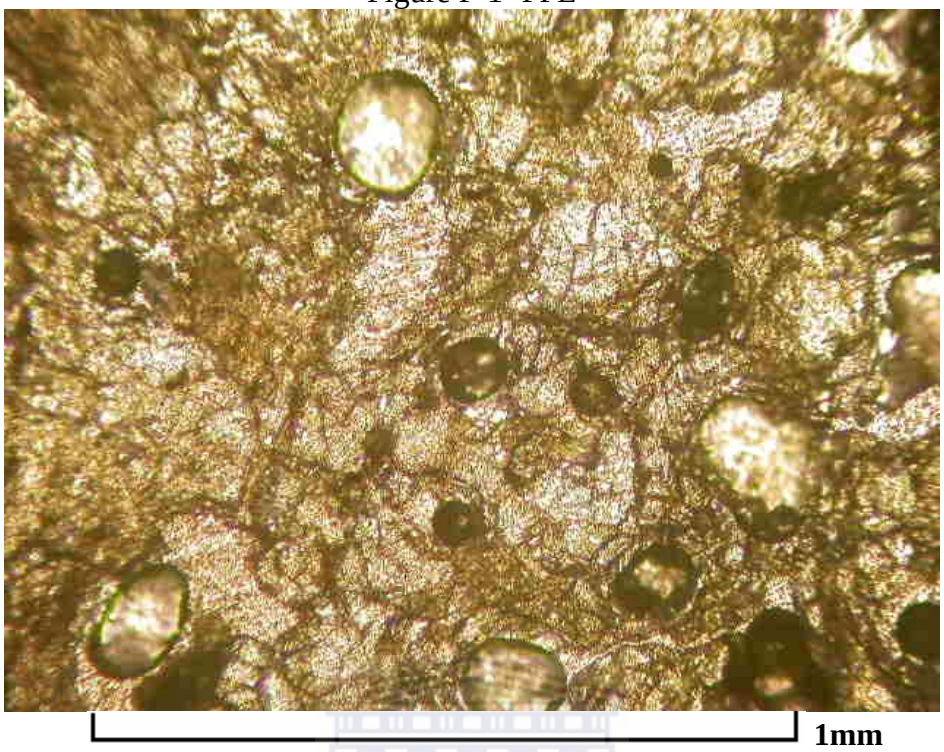

Scale (Magnification x10)

Figure F-2- XPL

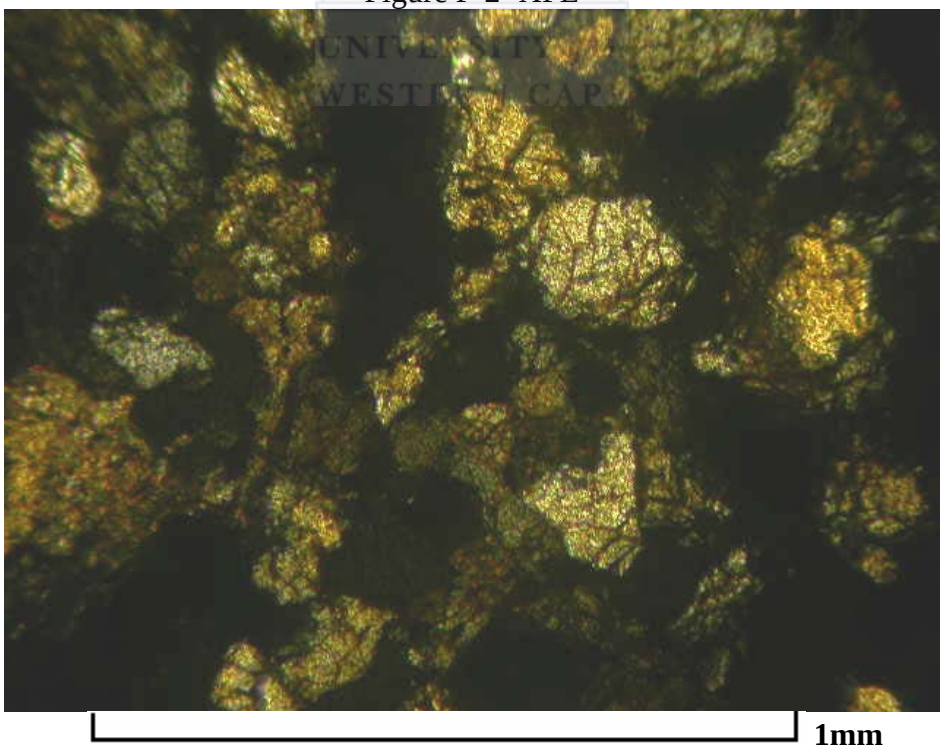

Scale (Magnification x10)

Sample: SWC I 20 **Depth: 2809.00m**

Composition: Framework minerals:	***Percentages***
Quartz	65%
Feldspar	10%
Lithic fragments	5%
Glauconite	3%

Quartz: Monocrystalline and polycrystalline
Planar extinction predominates
Colourful specks on grains (Figure G-2)
Long and sutured contacts

Feldspar: Cracked grains (thin section process)
No distinct twinning features
Dissolution of grains is noted

Lithic fragments: Fine Quartz and mica grains in a clay matrix

Glauconite: Pellets are not distinct
Partial dissolution through cracks

Ductile Minerals:	***Percentages***
Clays	5%
Micas	1%

Clays: Occur as matrix between grains (claystone)
Contains fine quartz and micas
Grain rimming (Detrital) and pore filling

Micas: Very fine grains clumped together to form one consolidated clast (seen in Figure G-1 in PPL)
Most likely biotite and chlorite

Authigenic Minerals:	***Percentages***
Quartz cement	5%
Clays	6%

Quartz cement: As overgrowths on detrital grains

Clays: Fills pores

***Porosity*:** Displays average porosity and permeability
Blue dye penetrates connecting pores (seen in Figure G-1 in PPL)
Pores contain gas bubbles due to mounting medium
Pores are mostly isolated
Intergranular porosity dominates

***Texture*:** Fine grain to medium grain sizes
(0.8mm Average) [x4 magnification]
Sorting is moderate to poor
Grain shapes are angular to sub angular
Sphericity of grain are low

Grains are tightly packed together
The support is by matrix and grains
Grain contacts are long and sutured

Name: SubArkose (Sandstone)

Comments: The porosity at the edges of the thin section seems to be better than average. The pores appear interconnected with blue dye penetrating it. This could be due to the preparation of the sample as moving towards the center of the thin section becomes more cemented by the clays. The following two figures represent a general view of the sample.

FIGURES G. Sample: SWC I 20 Depth: 2809.00m

Figure G-1- PPL

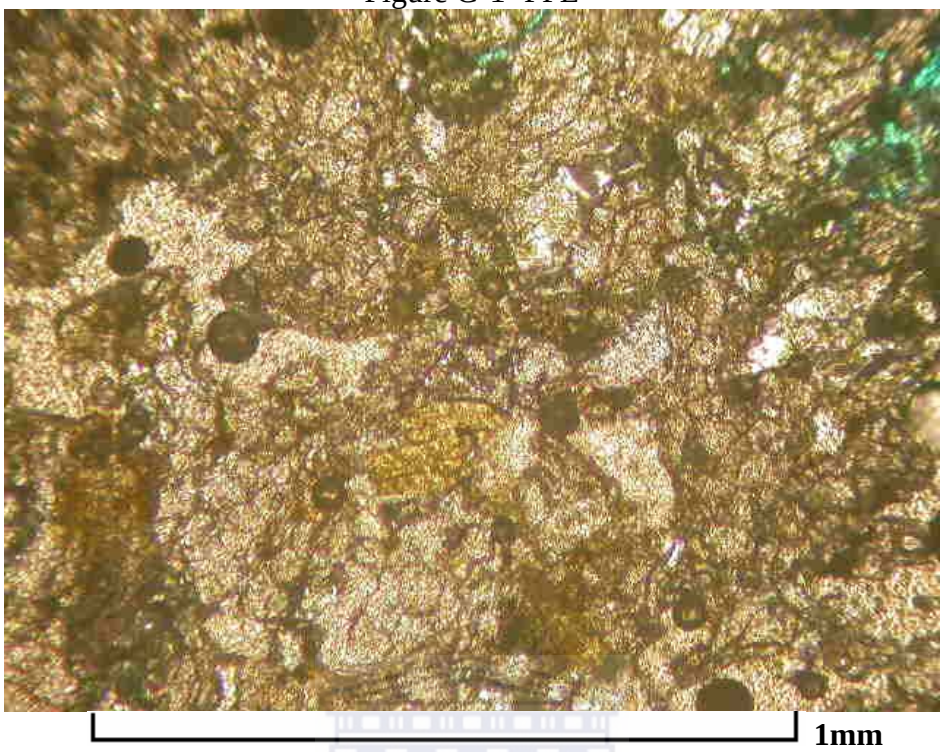

Scale (Magnification x10)

Figure G-2- XPL

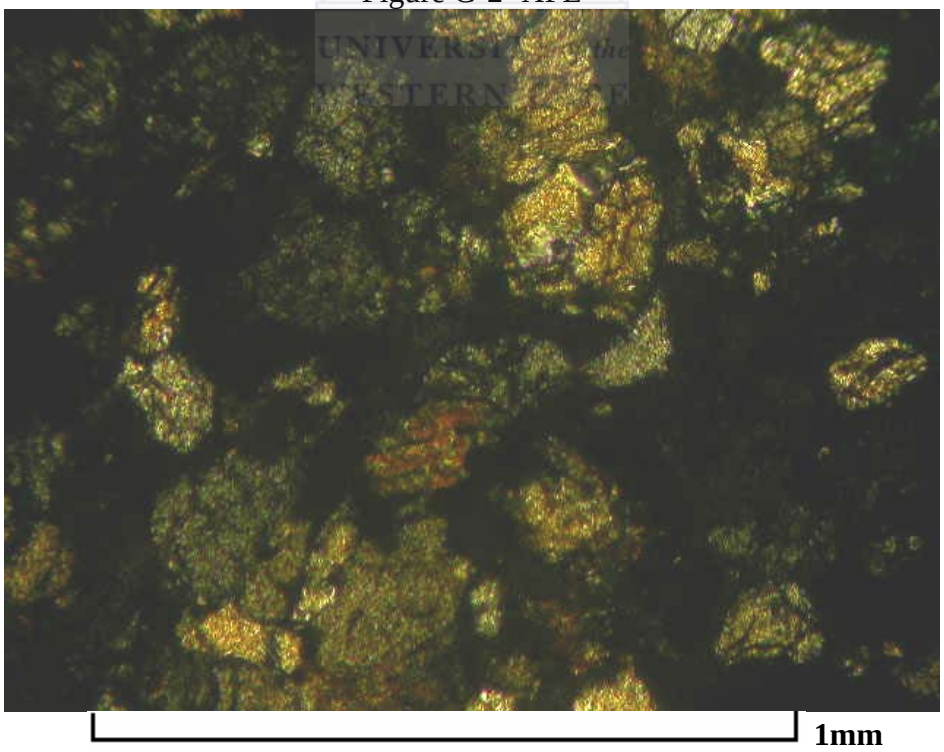

Scale (Magnification x10)

Sample: SWC I 19 **Depth: 2810.00m**

Composition: Framework minerals:	***Percentages***
Quartz	70%
Feldspar	10%
Lithic fragments	5%
Glauconite	5%

Quartz: Monocrystalline and polycrystalline
Sutured grain contacts
Few grains are coated with yellow remnants
Boundaries have black lining

Feldspar: Cracked
Dissolution of grains

Lithic fragments: Green matrix (PPL Figure H-1) is clay with chlorite component
Fine quartz grains
Fine mica specks (Chlorite source very light in colour)

Ductile Minerals:	***Percentages***
Clays	6%
Micas	1%

Clays: Occur as matrix between grains
Contain mica flakes
Some clays rim the grains

Micas: Occur only as specks in the matrix

Authigenic Minerals:	***Percentages***
Quartz cement	3%

Quartz Cement: Occur as overgrowths on detrital grains

***Porosity*:** Patchy porosity (not the same throughout the thin section)
Good porosity found mostly on one side of the slide
Macro and micropores
Primary and secondary porosity
Good connectivity (seen by blue dye in Figure H-3)

***Texture*:** Fine to medium grain size (0.8mm average) [x4magnification]
Sorting is moderate to poor
Grain shapes are angular to sub angular
The grains have low sphericity and are mainly oblong
Grains are tightly packed
Rock is matrix supports
Grain contacts are long and sutured

Name: SubArkose (Sandstone)

Comments: The slide appears highly scratched. The feldspar grains are highly dissolved
Grains and pores are coated with clays which are detrital and authigenic. The slide represents porosity and permeability that is concentrated on one end of the slide. This is illustrated by the following Photographs which shows a section with low porosity and permeability, in PPL and XPL, and a section with good porosity and permeability, in PPL and XPL. Carbonate clasts appear pastel in XPL (Figure H-4)

FIGURES H. Sample: SWC I 19 Depth: 2810.00m

Figure H-1- PPL

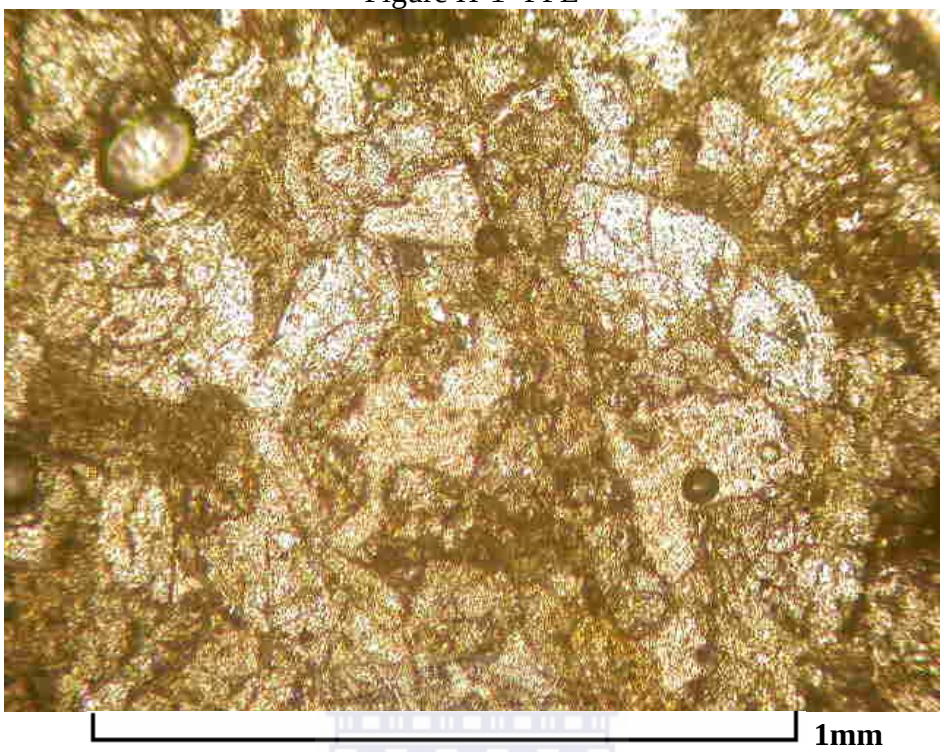

Scale (Magnification x10)

Figure H-2- XPL

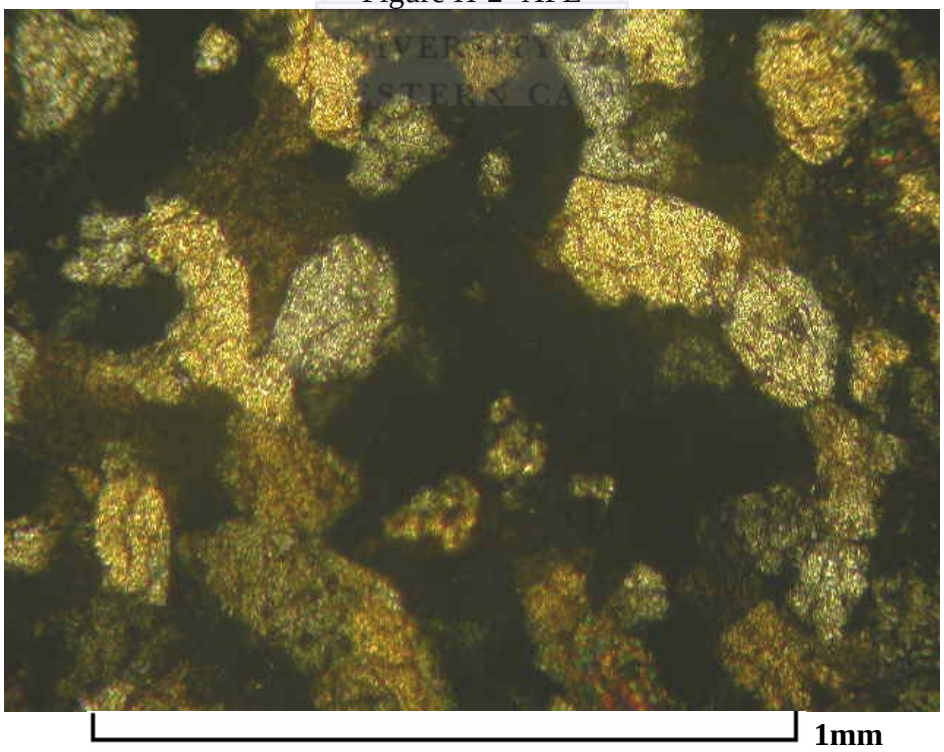

Scale (Magnification x10)

Figure H-3- PPL

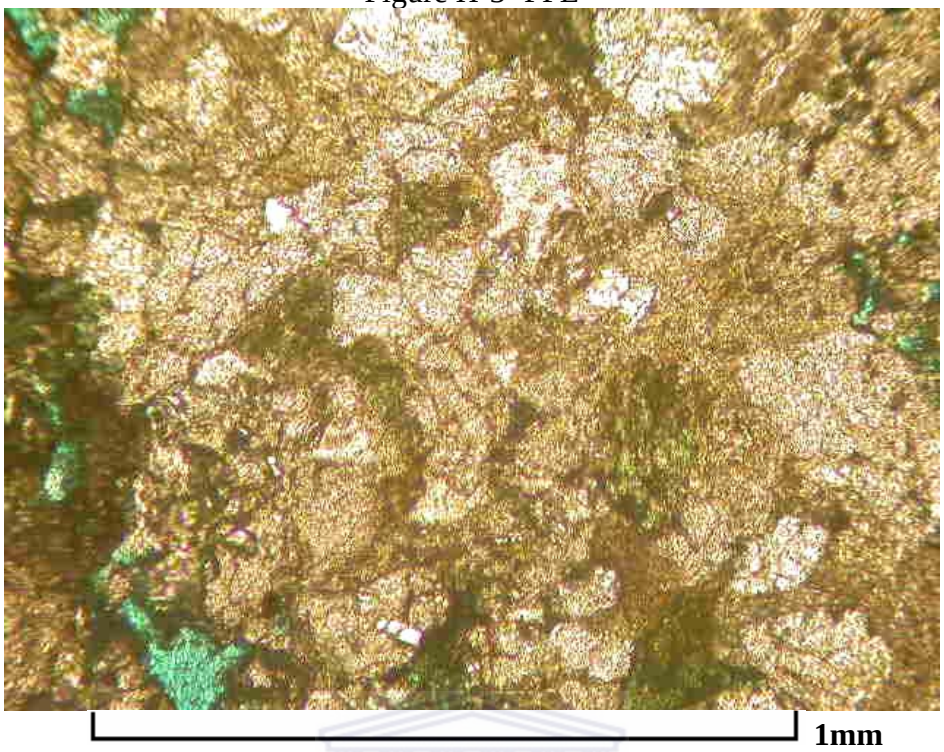

Scale (Magnification x10)

Figure H-4- XPL

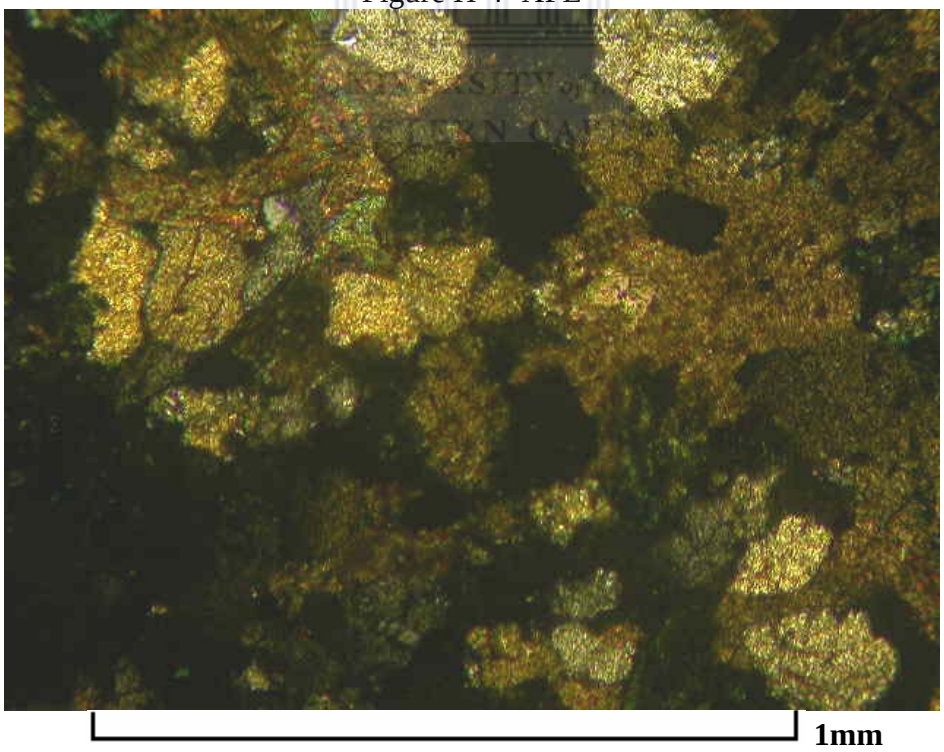

Scale (Magnification x10)

Sample: SWC I 17 **Depth: 2814.00m**

Composition: ***Framework minerals:*** ***Percentages***

Quartz	65%
Feldspar	15%
Lithic fragments	4%
Glauconite	5%

Quartz: Most grains are cracked
Grains are composite polycrystalline
Grain contacts are long and sutured

Feldspar: Most grains are cracked
Twinning features are visible (Figure I-2 upper right corner of field of view)

Lithic fragments: Fine quartz grains in clay matrix

Glauconite: Pellet are found between grains and in pores

Ductile Minerals: ***Percentages***

Clays	5%
Micas	1%

Clays: Occur as matrix and grain rimming clays
Matrix contains elongated crystals possibly dolomite traces and mica flakes
Rimming clays occur between detrital grains

Micas: Contain large mica flakes, which are deformed
Smaller flakes are found inside clay matrix

Authigenic Minerals: ***Percentages***

Quartz cement	3%
Carbonate cement	2%

Quartz cement: Occur as overgrowths on detrital grains

Carbonate cement: Appear clear in PPL and pastel in XPL (Figures F)
Occur as grain Coatings

***Porosity*:** Porosity is good
Pores are widely distributed over thin section
Good connectivity indicated by blue dye in Figure I-1
Pores are intergranular, intragranular and moldic

***Texture*:** Fine grains (0.5mm average) [x4 magnification]
Sorting is moderate
Grain shape is sub angular
Sphericity is low (mostly oblong grains)
Packing of grains is moderate
Rock mostly grain supported
Grain contacts are long and sutured

Name: SubArkose (Sandstone)

Comments: The overall porosity and permeability of the slide is good with many pores produced by dissolution of feldspar grains and some filled by cements. This can be seen by partially filled pores in Figure I-1- PPL in the bottom center of the view.

FIGURES I. Sample: SWC I 17 Depth: 2814.00m

Figure I-1- PPL

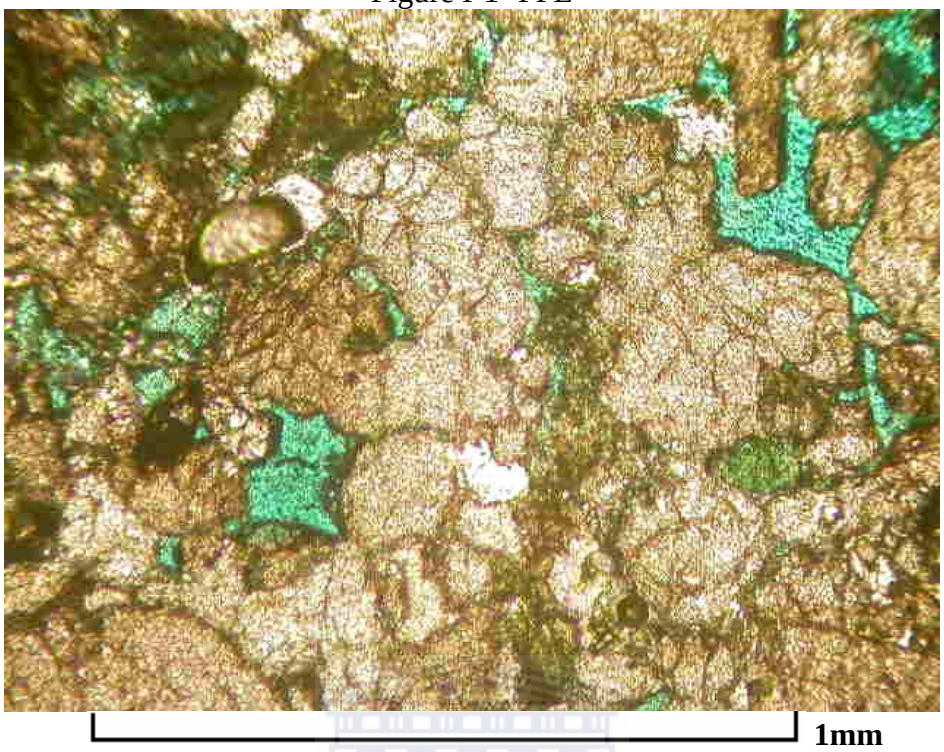

Scale (Magnification x10)

Figure I-2- XPL

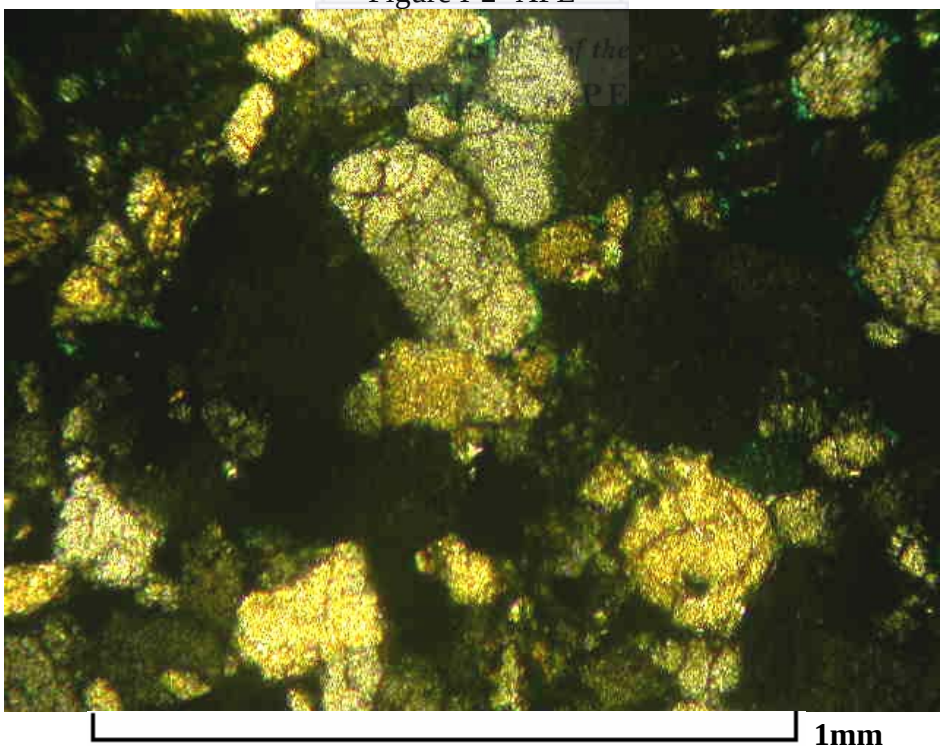

Scale (Magnification x10)

Sample: SWC I 15 **Depth: 2818.00m**

Composition: Framework minerals:	***Percentages***
Quartz	65%
Feldspar	10%
Lithic Fragments	3%
Glauconite	1%

Quartz: Grains are cracked and hard to distinguish
Extinctions are planar and yellow

Feldspar: Grains are cracked and highly altered.
No visible twinning features are present

Lithic fragments: Fine quartz grains in clay matrix material

Glauconite: Very minor constituent
Grains are as pellets
Some grains are noted as partially dissolved (cannot be seen in photomicrograph)

Ductile Minerals:	***Percentages***
Clays	10%
Muds	5%
Micas	1%

Clays: Grain rimming and pore filling properties

Muds: Dust seen around certain grains

Micas: Fine fragments found in the matrix

Authigenic Minerals:	***Percentages***
Quartz cement	5%

Quartz cement: Occur as overgrowths on detrital grains

***Porosity*:** Porosity is average
Intergranular pore types
Pores are found in cements
Connectivity is average
Permeability increases towards the sample edge

***Texture*:** Fine to medium grain sizes (0.8mm average) [x4magnification]
Sorting is poor to moderate
Grain shapes are sub angular
Sphericity of the grains is low
Grain packing is moderately tight
Grain to grain contacts are long with no suturing

Name: SubArkose (Sandstone)

Comments: Most of the primary porosity is lost and secondary porosity is isolated making the porosity together with the permeability quite poor. There is connectivity but on a small scale and not throughout the sample. Porosity and connectivity can be seen in Figure J-1 by the presence of blue dye in PPL but is not representative of the entire sample. A XPL view of the same section is shown by Figure J-2 and porosity is difficult to distinguish from the extinct grains.

FIGURES J. Sample: SWC I 15 Depth: 2818.00m

Figure J-1- PPL

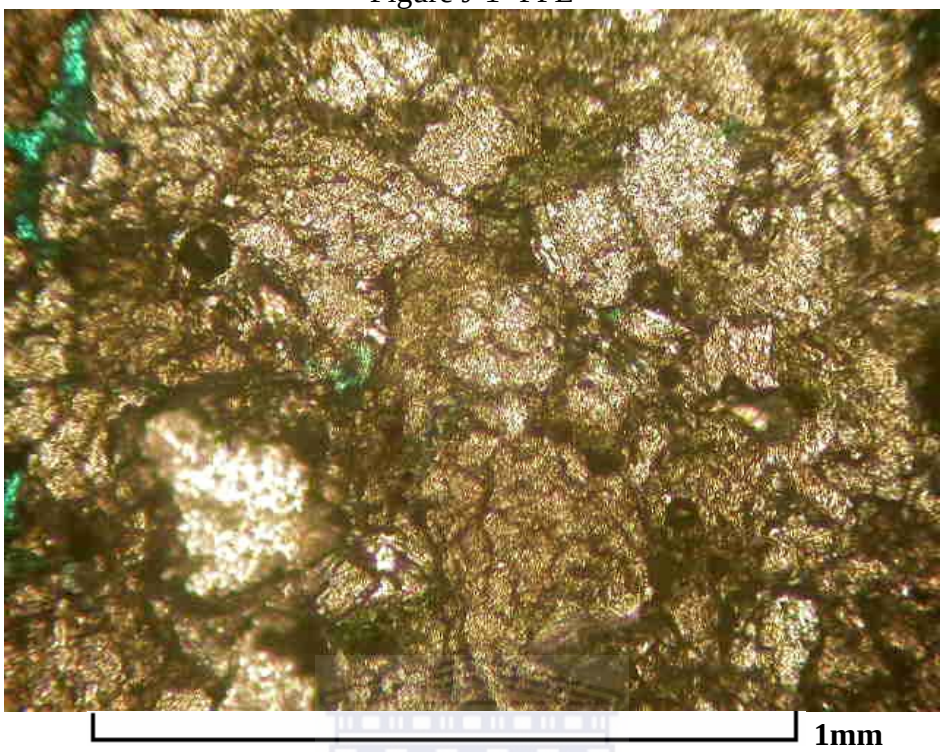

Scale (Magnification x10)

Figure J-2- XPL

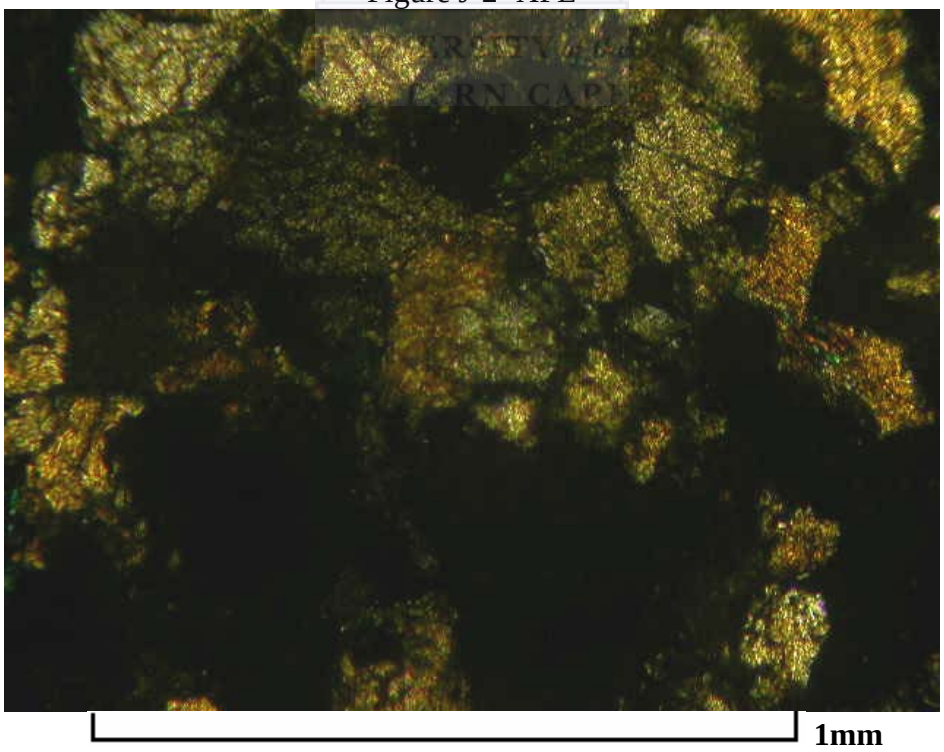

Scale (Magnification x10)

Sample: SWC I 14 **Depth: 2820.00m**

Composition: Framework minerals:	***Percentages***
Quartz	65%
Feldspar	10%
Lithic Fragments	5%
Glauconite	5%

Quartz: Monocrystalline grains
Grains are very tightly compacted
Extinctions are yellow
Some grains have dark boundaries

Feldspar: Grains are cracked
No visible twinning
Grains are partially overgrown by clay
Inclusions in grains are not spherical (not gas)

Lithic fragments: Fine quartz grains and fine mica fragments
Fine grains surrounded by matrix

Glauconite: Very few pellets visible

Ductile Minerals:	***Percentages***
Clays	5%
Micas (minor)	<1%

Clays: Occur on grains and in pores as coatings and as matrix
Matrix contains fine crystals possibly quartz as extinctions are observes when the stage is turned
Fine micas seen as brilliant colors in XPL

Micas: Muscovite and biotite due to its clear and brown colors in PPL and brilliant colours in XPL
Occur as fragments, no flakes present

Authigenic Minerals:	***Percentages***
Quartz cement	7%
Carbonate cement	3%

Quartz cement: Occur as overgrowths on detrital grains, can be seen by overprints of original grain shapes and by the extinctions of overgrowths and detrital grains being different.

Carbonate cement: Noted as pore filling

***Porosity*:** Porosity is average
Cements destroyed filled the pores
Connectivity is average
Pore throat are blocked by clays

***Texture*:** Fine grains (0.5mm average) [x4 magnification]
Grains have been moderately sorted
Grain shapes are fairly sub angular

Sphericity of the grains is low
Packing of grains is moderate
Support is mostly grain to grain
Contacts appear long between grains with most contacts along the length of grains

Name: Subarkose (Sandstone)

Comments: There are traces of black muddy material found in the pores and speckles of black muddy material found on glauconitic pellets partially dissolved. (Figure K-1 top- centre view of photograph).

FIGURES K. Sample: SWC I 14 Depth: 2820.00m

Figure K-1- PPL

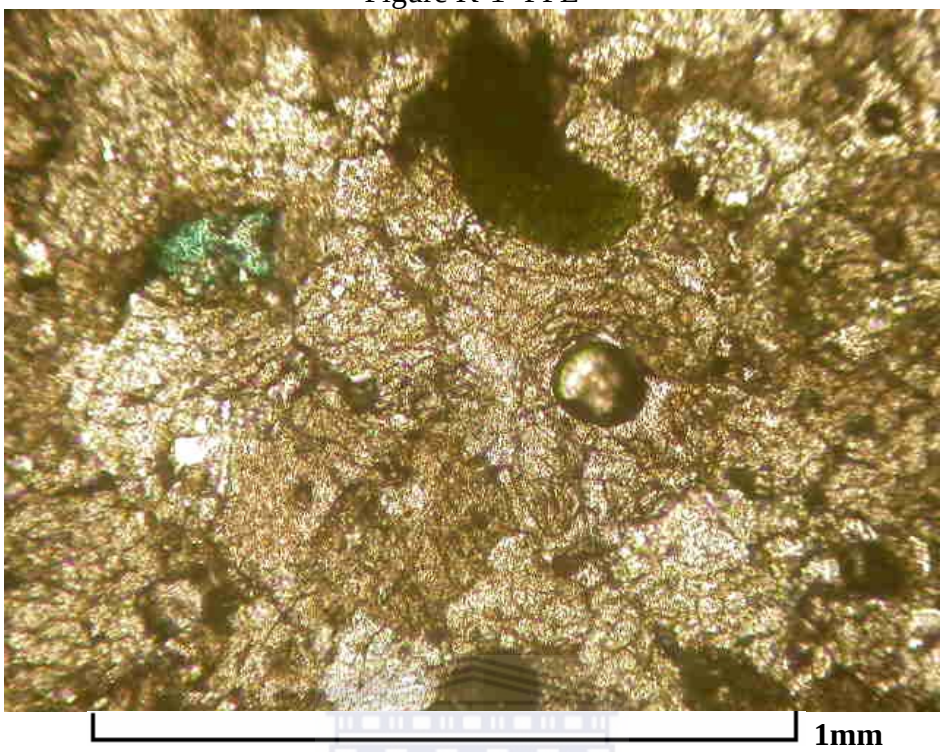

Scale (Magnification x10)

Figure K-2- XPL

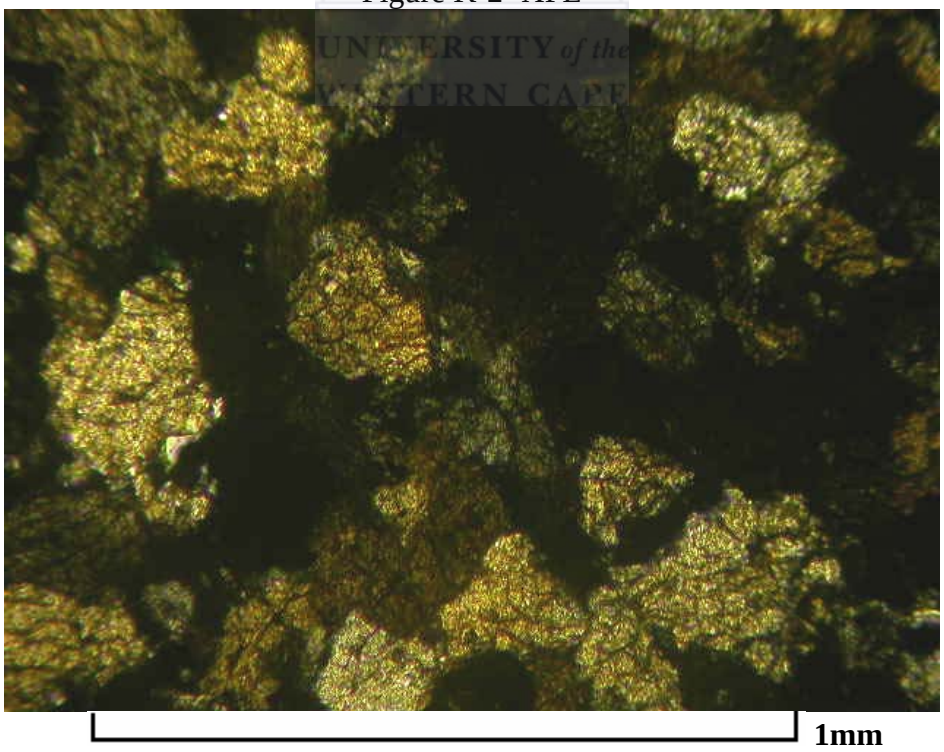

Scale (Magnification x10)

Sample: SWC I 13 **Depth: 2822.00m**

Composition: ***Framework minerals:*** ***Percentages***

Quartz	>50%
Feldspar	15%
Lithic fragments	*not visible*
Glauconite	5%

Quartz: Monocrystalline forms
Grains are sub angular but angular grains are present
Quartz is cracked due to alteration

Feldspar: Grains are cracked
Altered grains are partially dissolved

Lithic fragments: Not prominent in this sample

Glauconite: Partially dissolved pellets

Ductile Minerals: ***Percentages***

Clays	8%

Clays: Matrix has fine traces of micas with tiny quartz crystals and is found between grains as coatings
Clays fill secondary pore structures and contain gas bubbles which appears black in PPL and XPL (Figures L-1 and L-2 bottom-centre of photograph)

Authigenic Minerals: ***Percentages***

Quartz cement	5%
Carbonate cement	3%

Quartz cement: Occur as overgrowths on detrital grains. These overgrowths are seen outside the dust rims.

Carbonate cement: Found between grains with pores (either man-made or natural gas bubbles)
Pores can be seen in top half of photograph in Figure L-1)

***Porosity*:** Good porosity
Intergranular and intragranular
Good connectivity

***Texture*:** Fine grained (0.5mm average) [x4 magnification]
Grains are moderately sorted
Grain shapes are sub angular
Sphericity of grains are low
Grain packing is fairly loose
Main support is grain to grain
Grain contacts are long and concavo-convex

Name: Subarkose (Sandstone)

Comments: Porosity and permeability increases in the sample apposed to the previous sample due to the loose packing of the grains. Overall reservoir quality is good for this sample. There are stylolites present which represents pressure solution.

FIGURES L. Sample: SWC I 13 Depth: 2822.00m

Figure L-1- PPL

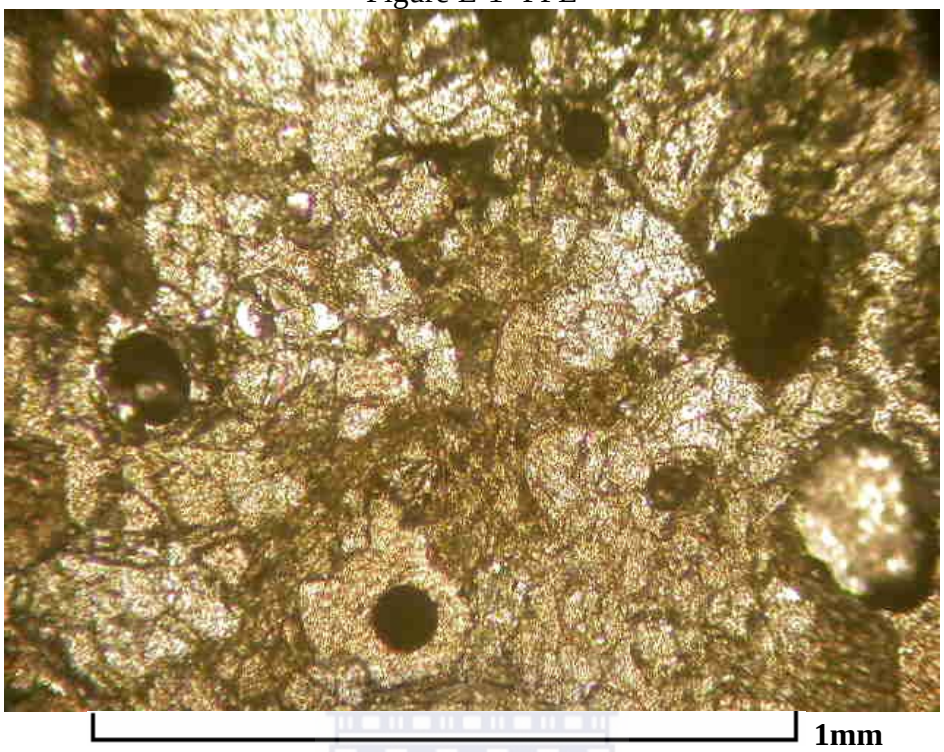

Scale (Magnification x10)

Figure L-2- XPL

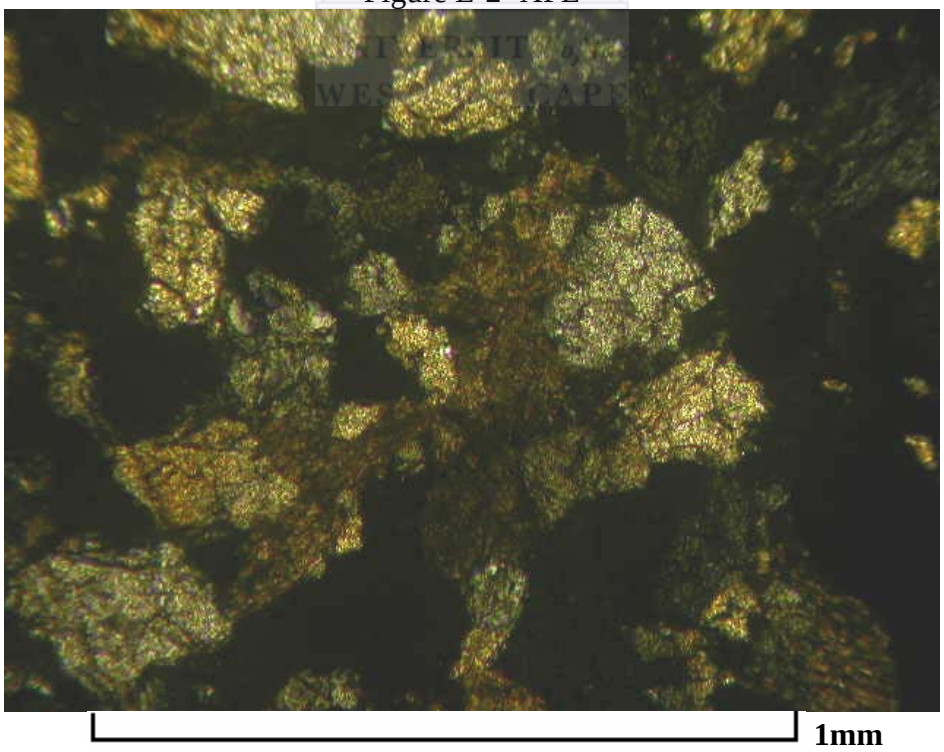

Scale (Magnification x10)

Sample: SWC I 12 **Depth: 2823.00m**

Composition: ***Framework minerals:*** ***Percentages***

Quartz	60%
Feldspar	20%
Lithic fragments	7%
Glauconite	3%

Quartz: Grains have been altered
Grains are mainly polycrystalline type
Undulose and planar extinctions

Feldspar: Grains are highly altered (cracked)
No visible twinning features

Lithic fragments: Fine quartz and mica crystals in clay matrix (sedimentary origin)

Ductile Minerals: ***Percentages***

Clays	5%

Clays: Found between grains
Contains gas bubbles from mounting medium
Grains appears brown in PPL (Figure M-1 in centre of photograph) and dark brown with colourful speckles in XPL (Figure M-2 in centre of photograph)

Authigenic Minerals: ***Percentages***

Quartz cement	5%

Quartz cement: Occur as overgrowths on detrital grains

***Porosity*:** Good porosity
Intergranular and intragranular pores
Good connectivity

***Texture*:** Fine grained (0.5 average) [x4 magnification]
Moderately sorted grains
Grain shape is angular to sub angular
Sphericity is low with oblong/elongated grains
Grain packing is fairly tight
Main support is grain to grain
Grain contacts display long and concavo-convex boundaries

Name: Subarkose (Sandstone)

Comments: Sample contains stylolites indicating minor straining within the rock.

FIGURES M. Sample: SWC I 12 Depth: 2823.00m

Figure M-1- PPL

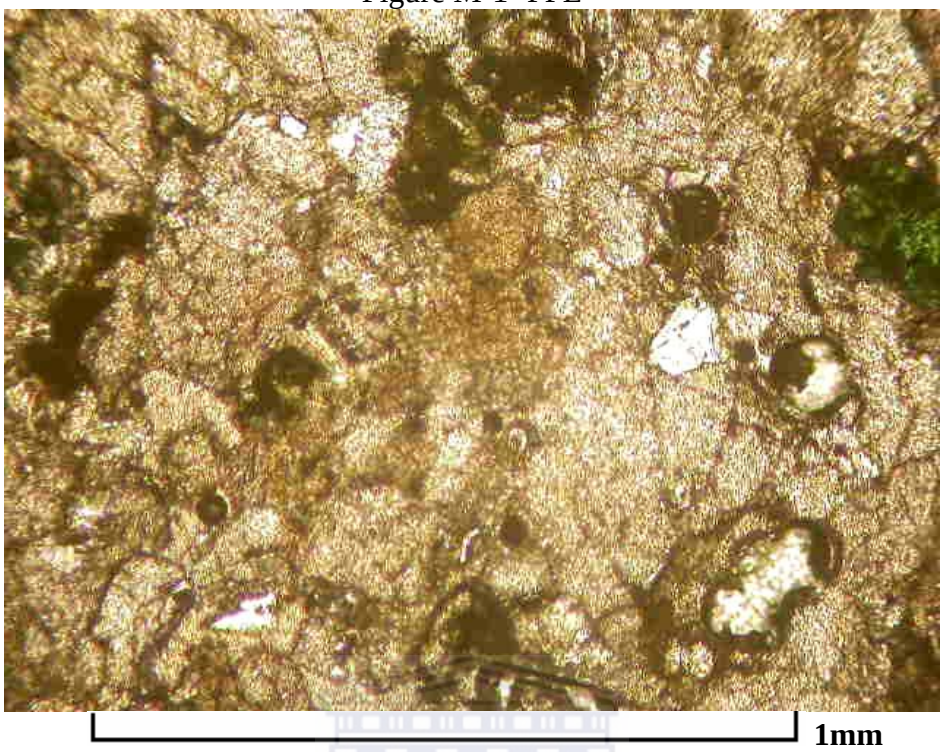

Scale (Magnification x10)

Figure M-2- XPL

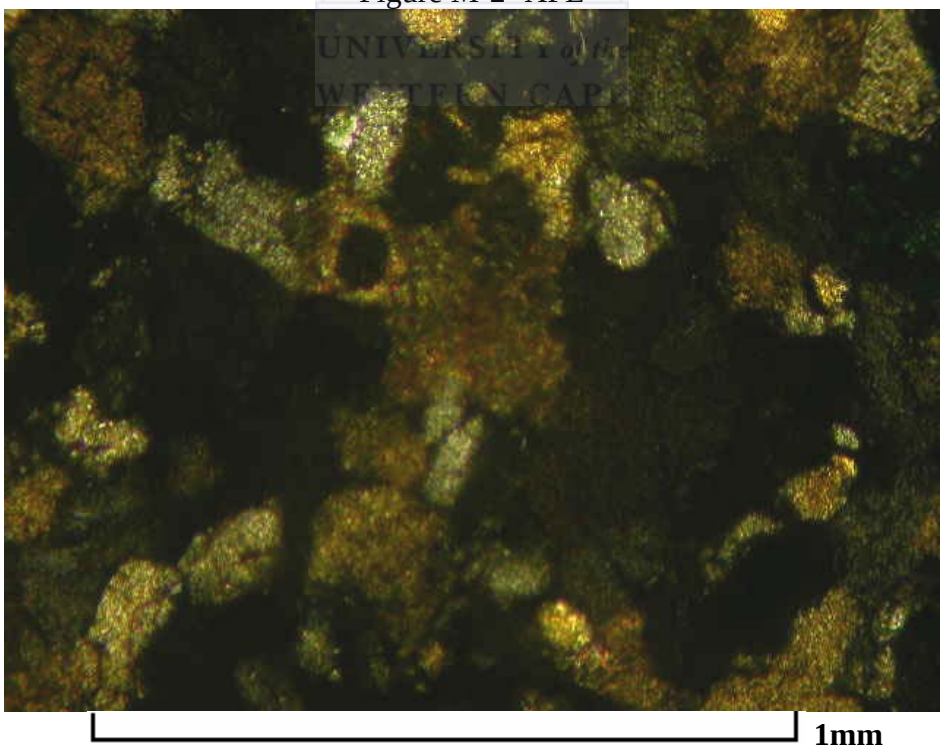

Scale (Magnification x10)

Sample: SWC I 9 **Depth: 2827.50m**

Composition: ***Framework minerals:*** ***Percentages***

Quartz	60%
Feldspar	20%
Lithic fragments	1%
Glauconite	3%

Quartz: Grains are altered (cracked)
Monocrystalline type with planar and undulose extinction
Polycrystalline type with undulose extinction
Some grains show euhedral crystal forms with overgrowths

Feldspar: Grains are altered (highly cracked)
Some grains show twinning features

Lithic fragments: Fine quartz grains in clay matrix

Glauconite: Pellets found in pores showing dissolution occurred around the grains and some pellets are in the process of being dissolved

Ductile Minerals: ***Percentages***

Clays	2%
Micas	1%

Clays: Clay makes up the matrix in sample
Matrix contains very fine quarts crystals

Micas: Micas occur as deformed flakes
Clear in colour in PPL and brilliant colours in XPL

Authigenic Minerals: ***Percentages***

Quartz cement	5%
Carbonate cement	8%

Quartz cement: Quartz occur as overgrowths on detrital grain

Carbonate cement: Found between grains and rims the micro-fracture in the centre of the photograph in Figure N-1 PPL and N-2 XPL

***Porosity*:** Porosity is good to very good
Porosity is enhanced by the micro-fractures
Primary porosity is intergranular and secondary porosity is intragranular and generated by the micro-fracture
Connectivity is good
Major connectivity can be observed between micro-fracture

***Texture*:** Fine grained (0.3mm average) [x4 magnification]
Sorting of grains is moderate to well
Grain shape is sub angular
Sphericity is very low with most grains having elongated shapes

Grain packing is fairly tight
Main support is grain to grain
Grain contacts are long and concavo-convex

Name: Subarkose (Sandstone)

Comments: A fracture (seen in Figure N-1 in centre of photograph) enhances the porosity and permeability of a rock. This could be a horizontal reservoir-quality enhancer if extensive micro-fracturing exists in the area.

FIGURES N. Sample: SWC I 9 Depth: 2827.50m

Figure N-1- PPL

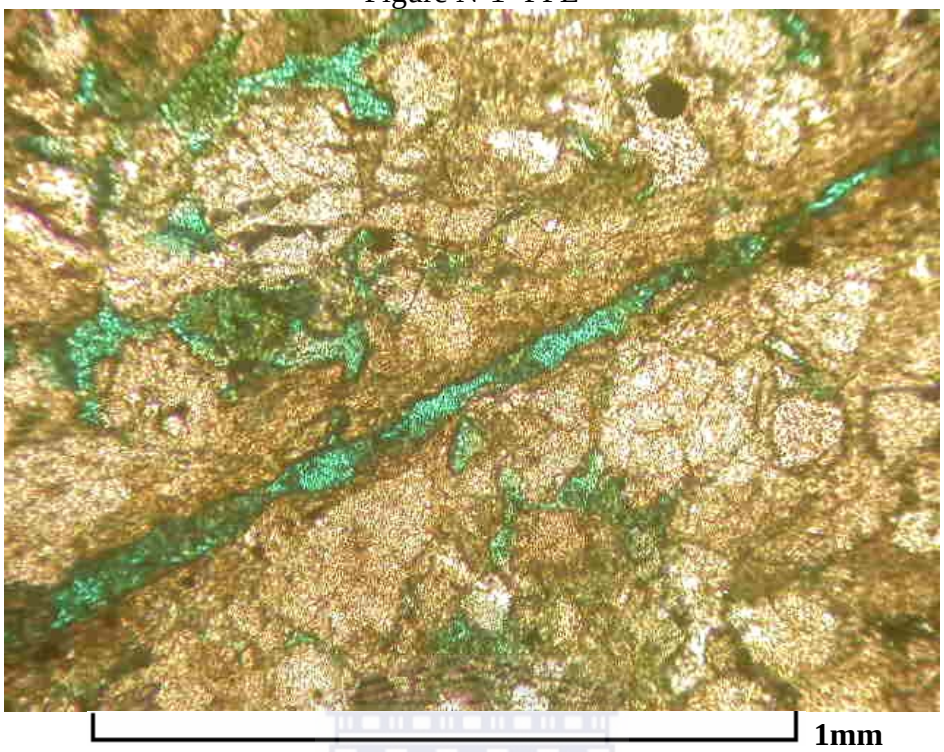

Scale (Magnification x10)

Figure N-2- XPL

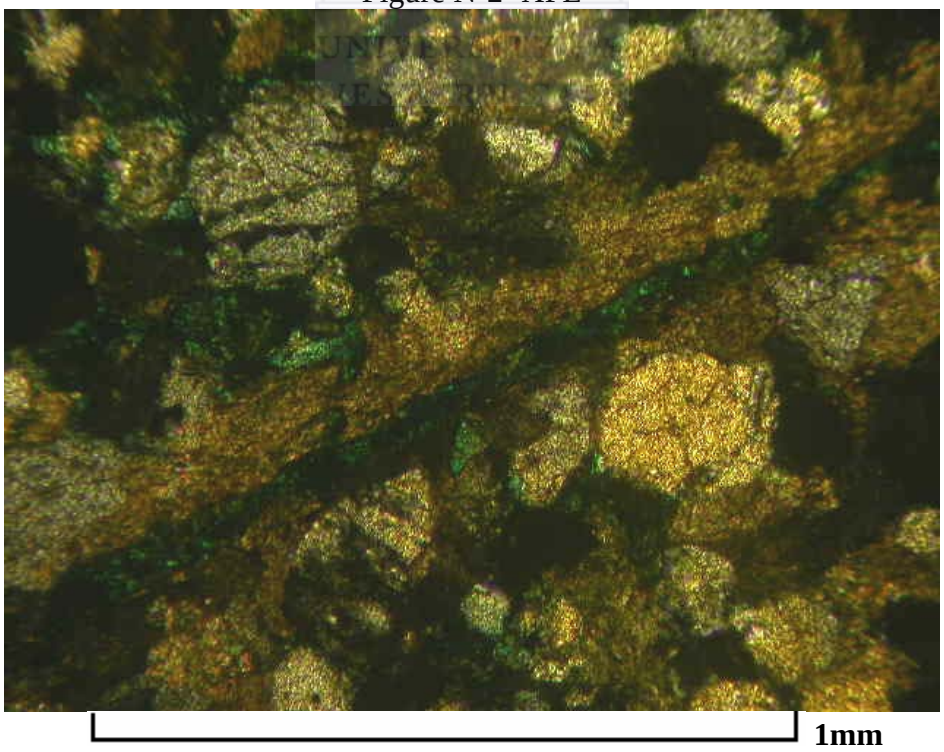

Scale (Magnification x10)

Sample: C1:1 **Depth: 2828.00m**

Composition: ***Framework minerals:*** ***Percentages***

Quartz	60%
Feldspar	20%
Lithic fragments	10%

Quartz: Grains are monocrystalline with planar extinctions and polycrystalline with undulose extinctions
Grains contain vacuoles
Polycrystalline grains are euhedral to subhedral

Feldspar: Grains are cloudy (PPL) and patchy
Inclusions are found in grains
Predominantly orthoclase with few microcline grains shown by twinning features

Lithic fragments: Predominantly sedimentary origins
Fine quartz crystals in clay matrix

Glauconite: Occur as pellet between grains and in pores (Figure O-1)

Ductile Minerals: ***Percentages***

Clays	2%
Micas	<1%

Clays: Clays are predominantly grain rimming

Micas: Fibrous grains which are slightly deformed
Seen clear in PPL and displaying brilliant colours in XPL

Authigenic Minerals: ***Percentages***

Quartz cement	2%
Carbonate cement	3%
Dolomite cement	2%

Quartz cement: Occur as overgrowths on detrital grains and also overprints glauconitic pellets (seen in Figure O-1 in PPL bottom left of photograph and seen as extinct black grain in Figure O-2 in XPL)

Carbonate cement: Found between grains
Clear in PPL, pastel in XPL (Figure O-1 and Figure O-2)
Main feature shows a fractured pore with cements formed around grain edges. This is seen in Figures O-1 and O-2.

Dolomite cement: Distinct cubic grains are evident along the pore (Figure O-1)
These are clear in PPL (Figure O-1 centre view) and green in XPL (Figure O-2 centre- right view)

***Porosity*:** Excellent porosity
Intergranular and intragranular as well as moldic (formed by dissolution of detrital grains)
Connectivity is excellent
Pores formed by micro-fracturing as seen in Figures O-1 and O-2

***Texture*:** Fine grained (0.5mm average) [x4 magnification]
Sorting of grains is poor
Grain shapes are sub angular to sub rounded
Sphericity is medium with very few elongated grains
Grain packing is uneven displaying sections that has been tightly packed and loosely packed. The overall packing of grains is moderate
Grain support is by clay matrix
Grain contacts are tangential and concavo-convex

Name: Subarkose (Sandstone)

Comments: The overall porosity and permeability of the thin section is excellent. Grains on the edges of pores appear to have inclusions this could be due to flow through the pores at the time or it could be as a result of the mounting medium. Zircon grains exist as an accessory mineral.

Figures O-3 and O-4 show mudstone clasts which are found in pores. This is a form of lithic fragment. It has a clay-to-mud matrix with very fine grains of quartz. A pore, to the immediate left of the clasts is observed with a gas bubble (from the mounting medium). These mud clasts are seen being partially dissolved, as in the immediate left of the pore in Figure O-3 in PPL. Most of the view in XPL is dark brown to black as most quartz grains are extinct and pores with the mud remains black.

Dolomite cementation (centre view of figure O-1) in the pore or micro fracture was formed by the invasion of a solution passing through it, which occurred after fracturing took place.

FIGURES O. Sample: C1:1 **Depth: 2828.00m**

Figure O-1- PPL

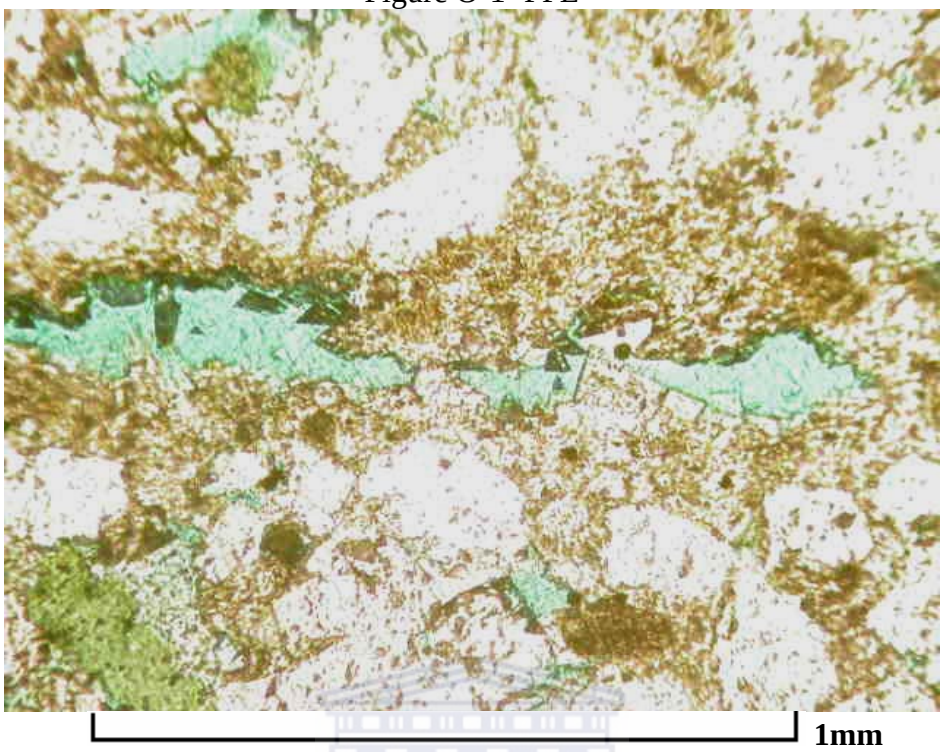

Scale (Magnification x10)

Figure O-2- XPL

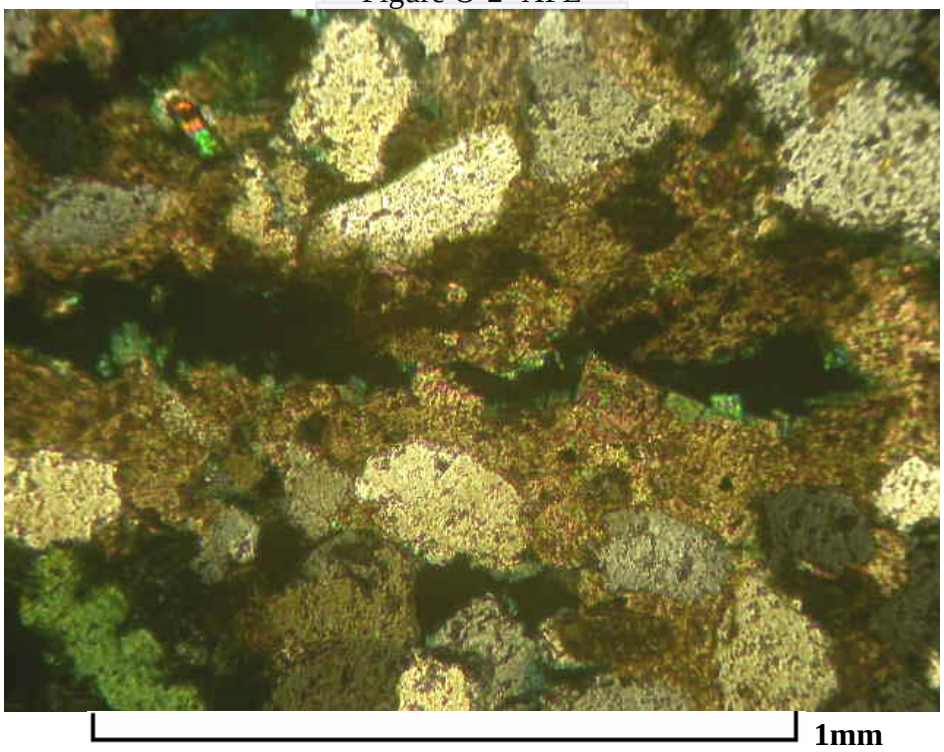

Scale (Magnification x10)

Figure O-3- PPL

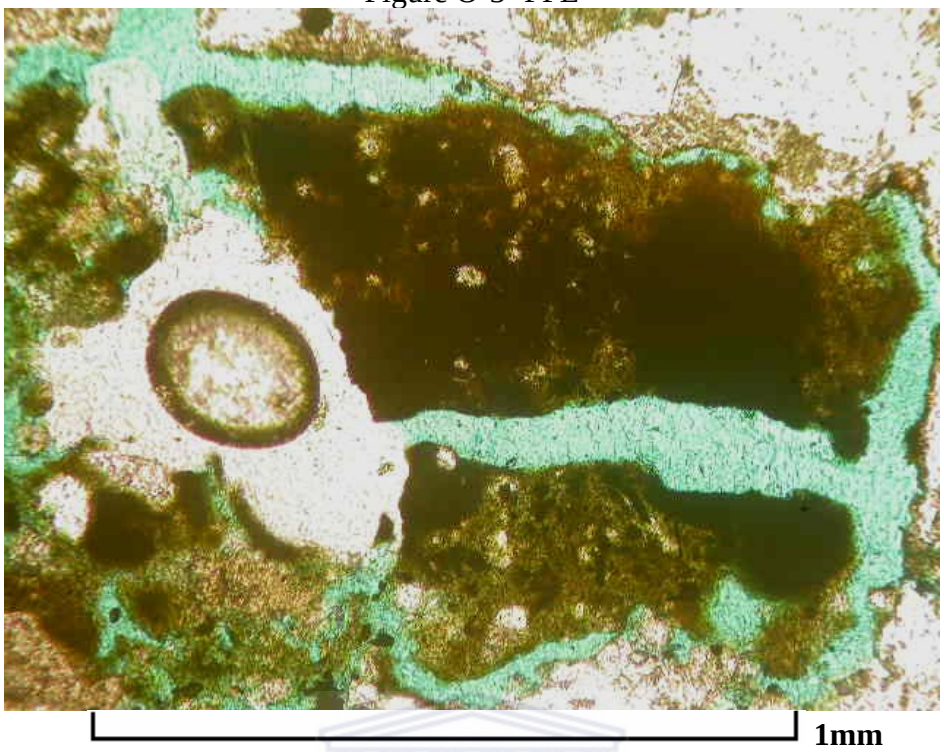

Scale (Magnification x10)

Figure O-4- XPL

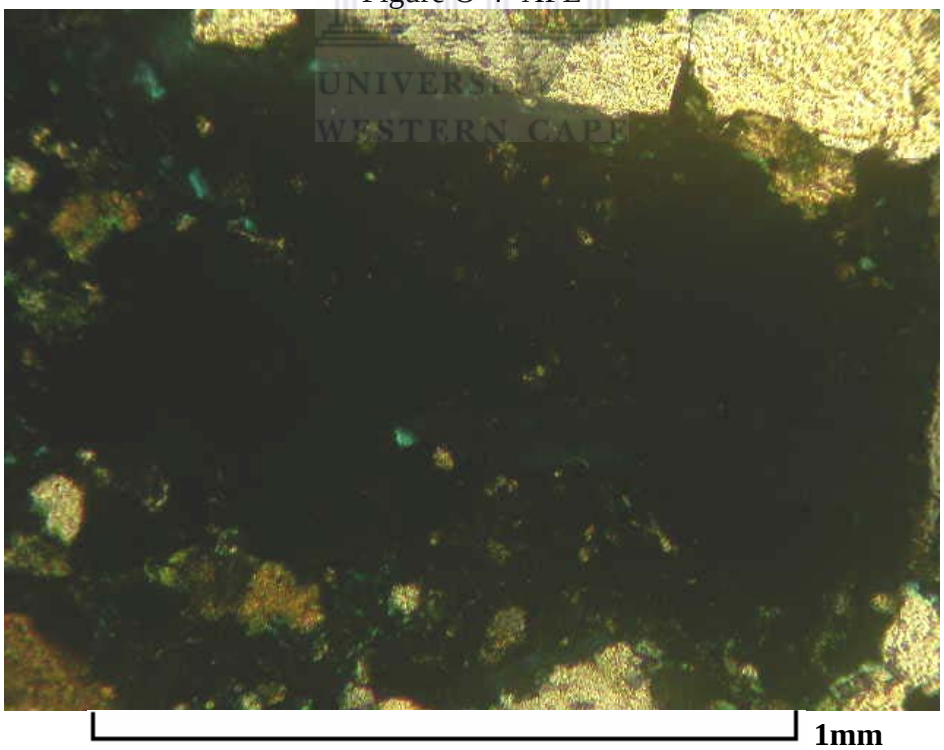

Scale (Magnification x10)

Sample: C1:2 **Depth: 2828.64m**

Composition: ***Framework minerals:***	***Percentages***
Quartz	60%
Feldspar	10%
Lithic fragments	5%
Glauconite	5%

Quartz: Monocrystalline and polycrystalline forms
Grain contacts are sutured together
Grains display planar and undulose extinctions in XPL

Feldspar: Microcline and orthoclase grains
Section shows twinning features
Grain alteration is not clear

Lithic fragments: Minor lithic fragments
Very fine quartz and feldspar grains in clay matrix

Glauconite: Found as pellets between grains

Ductile Minerals:	***Percentages***
Clays	11%
Micas	1%

Clays: Clays occur as matrix, as pore filling and in lithic fragments
Matrix is dominant type
Clays contain mud component
Viewed as brown in PPL and dark brown to black in XPL.

Micas: Very fine fragments not fibres in matrix

Authigenic Minerals:	***Percentages***
Quartz cement	5%
Clays	3%

Quartz cement: Occur as overgrowths on detrital grains

Clays: Clay grains coats the pores and reduces porosity

***Porosity*:** Porosity is average
Mostly isolated pores are found which are filled with black material (muds or hydrocarbon remnants)
Elongated pores show stress direction
Connectivity is poor
All connected pores have been filled with clays and cements

***Texture*:** Very fine grained material (0.05mm average) [x4 magnification]
Sorting of grains is moderate
Grain shapes are sub angular to sub rounded
Sphericity is medium
Packing of grains is very tight
Rock is grain and matrix supported

Grain contacts are sutured

Name: Subarkosic Claystone

Comments: The overall porosity and permeability is poor as most of the primary and some of the secondary porosity has been destroyed by either clays, mud or cements. This can be clearly seen in Figures P-1, P-2, P-3 and P-4 in PPL and XPL. P-3 shows stylolites in the centre right corner.
There are laminations across the thin section sample. These are defined by the darker material

FIGURES P. Sample: C1:2 **Depth: 2828.64m**

Figure P-1- PPL

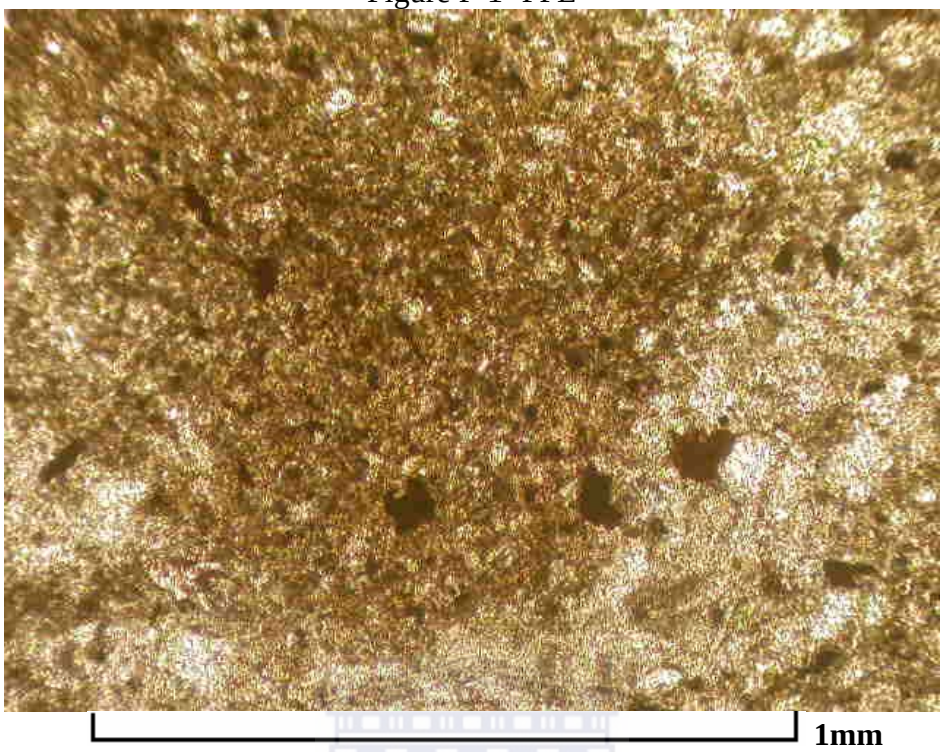

Scale (Magnification x10)

Figure P-2- XPL

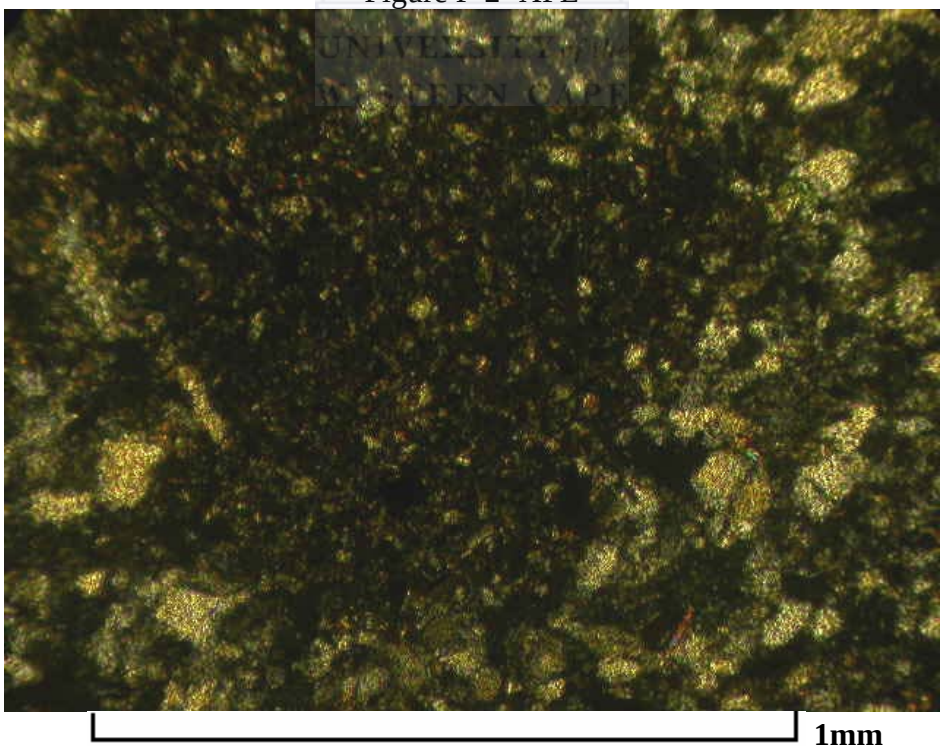

Scale (Magnification x10)

Figure P-3- PPL

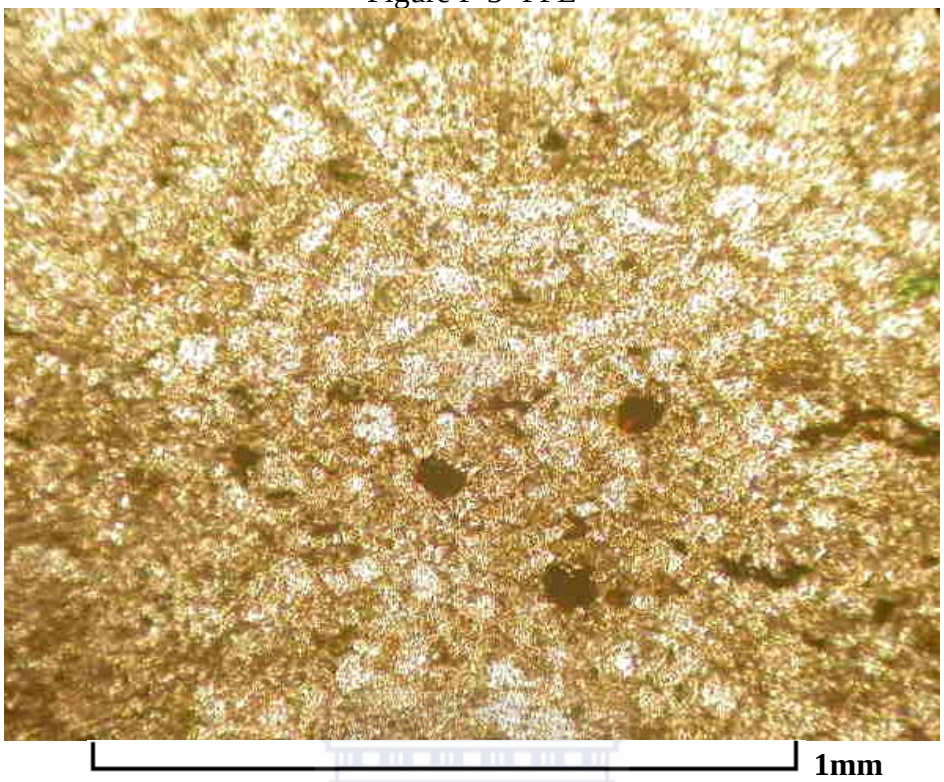

Scale (Magnification x10)

Figure P-4- XPL

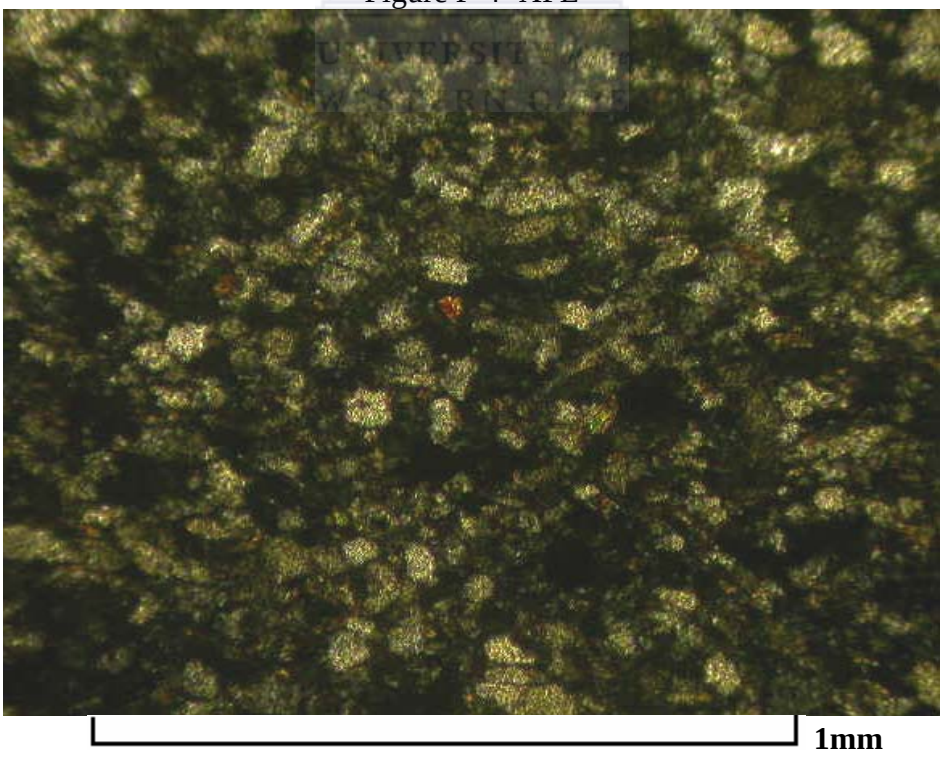

Scale (Magnification x10)

Sample: C1:3 **Depth: 2829.67m**

Composition: ***Framework minerals:*** ***Percentages***

Quartz	60%
Feldspar	15%
Lithic fragments	7%
Glauconite	3%

Quartz: Monocrystalline and polycrystalline
Planar and undulose extinctions seen in both forms
Extinctions are yellow (Figure Q-4)
Some grains are cracked displaying alteration
(Figure Q-2 and Q-4)

Feldspar: Grains are altered (cracked)
Some grains display twinning features characteristic of plagioclase

Lithic fragments: Very fine quartz in clay matrix

Glauconite: Fine pellets found between grains

Ductile Minerals: ***Percentages***

Clays	8%
Micas	2%

Clays: Grain rimming and pore filling is the dominant type of clays present
These appear brown in PPL and dark brown to black in XPL (figures Q-1 and Q-2)

Micas: Muscovite and biotite
Micas are not deformed
Appear clear and brown in PPL and brilliant in XPL

Authigenic Minerals: ***Percentages***

Quartz cement	3%
Carbonate cement	2%

Quartz cement: Occur as overgrowths on detrital grains

Carbonate cement: Found between grains and fills secondary porosity (Figure Q-4 XPL view, centre towards the left)

***Porosity*:** Porosity is average
Primary porosity destroyed by authigenic minerals
Connectivity of pores is good
Most clay blocks the pore throats

***Texture*:** Very fine to fine grained (0.05mm average) [x4 magnification]
Sorting of grains is moderate
Grain shapes are angular to sub angular
Sphericity of grain are very low thus most grains are elongate
Grain packing is tight
Main support is by matrix with minor grain support
Grain contacts are long

Name: SubArkosic Claystone

Comments: A feature seen in the thin section sample (not photographed) displays a granulation seam. Pores are along the same area. Black material is visible in the seam along with finer material caused by friction. The granulation seam does not affect the porosity and permeability of the whole thin section. Figure Q-2 displays extinctions which are yellow in colour this could be a remnant coating of migrating fluid as the entire grains have not been altered but nearly changed colour. The thin section represents average porosity and permeability.

FIGURES Q. Sample: C1:3 **Depth: 2829.67m**

Figure Q-1- PPL

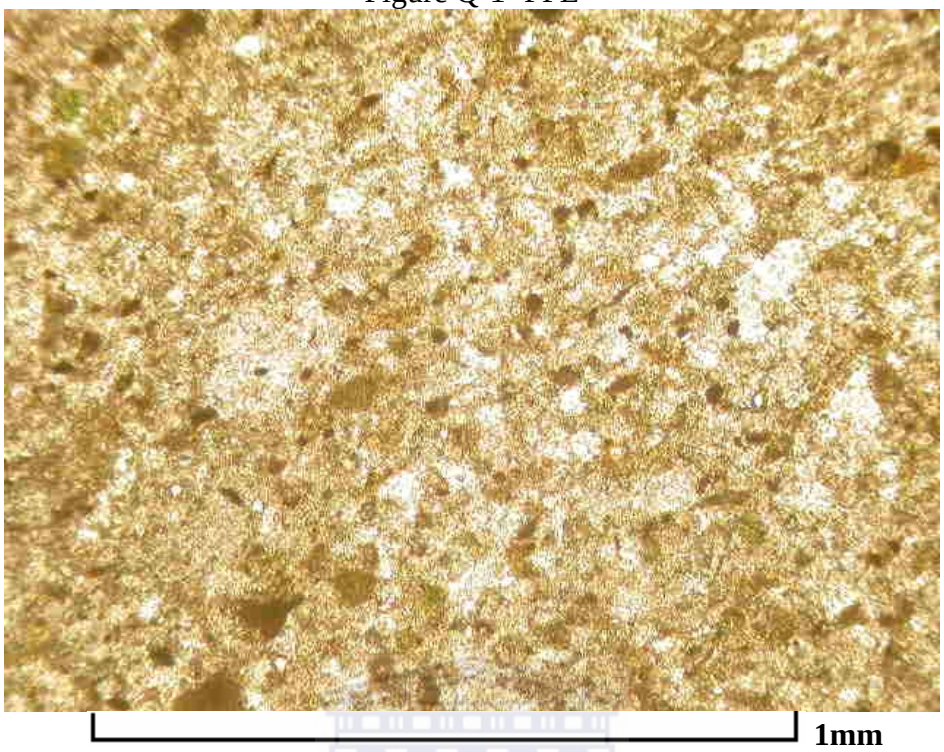

Scale (Magnification x10)

Figure Q-2- XPL

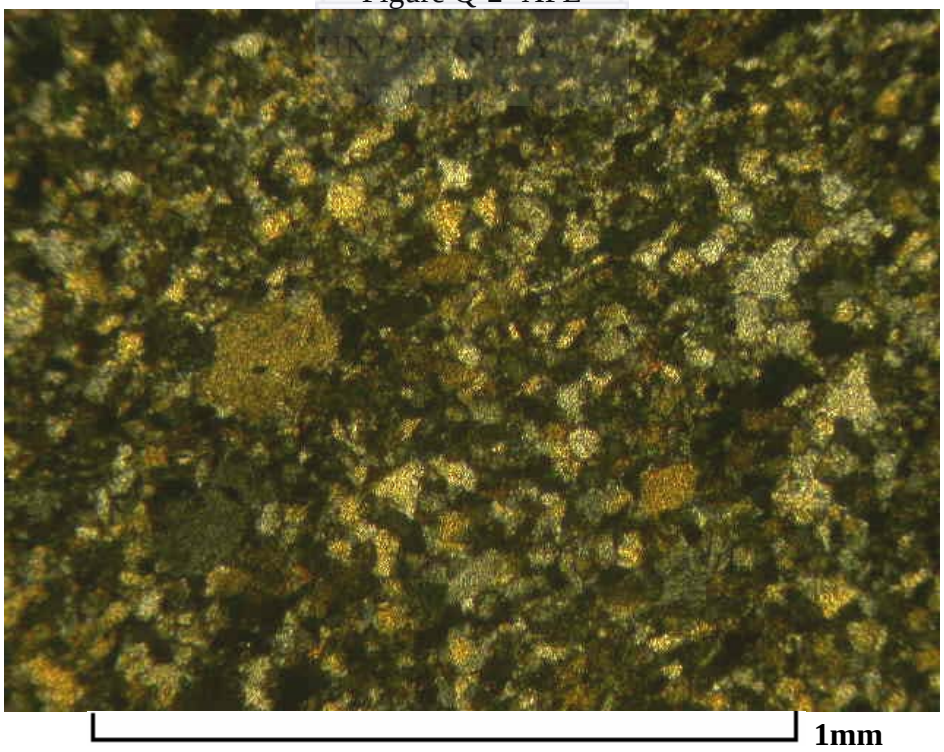

Scale (Magnification x10)

Sample: C1:4 **Depth: 2831.95m**

Composition: ***Framework minerals:***	***Percentages***
Quartz	60%
Feldspar	20%
Lithic fragments	5%
Glauconite	5%

Quartz:	Monocrystalline and polycrystalline Planar and undulose extinctions of grains Grains are coated with yellow to gold material which extincts to light gray Grain contacts are sutured
Feldspar:	Grains are cracked No visible twinning features Brown coatings on grains Some grains are partially dissolved
Lithic fragments:	Very fine quartz grains in matrix
Glauconite:	Pellets found between grains

Ductile Minerals:	***Percentages***
Clays	5%

Clays: Occur as coatings on feldspar grains
Clasts of clay found between grains

Authigenic Minerals:	***Percentages***
Quartz cement	3%
Carbonate cement	2%

Quartz cement: Occur as overgrowths on detrital grains
Carbonate cement: Occur as pore filling clasts between grains

***Porosity*:** Porosity is average
Secondary porosity reduced by material filling pores
Good connectivity

***Texture*:** Fine to medium grain sizes (0.8mm average) [x10 magnification]
Sorting of grains is moderate
Grain shapes are angular to sub angular
Sphericity of grains is low
Grain packing is fairly tight
Grain supported
Grain to grain contacts are long and tangential

Name: Subarkose (Sandstone)

Comments: There is dark brown to black material found in the pores between coated grains of quartz and feldspar. This is regarded as either muddy material (stylolites) or remnants of hydrocarbons. Feldspars which are partially dissolved display isolated micro-porosity. This can be seen in Figure R-1 and R-2 at the bottom left corner of the photograph.

FIGURES R. Sample: C1:4 **Depth: 2831.95m**

Figure R-1- PPL

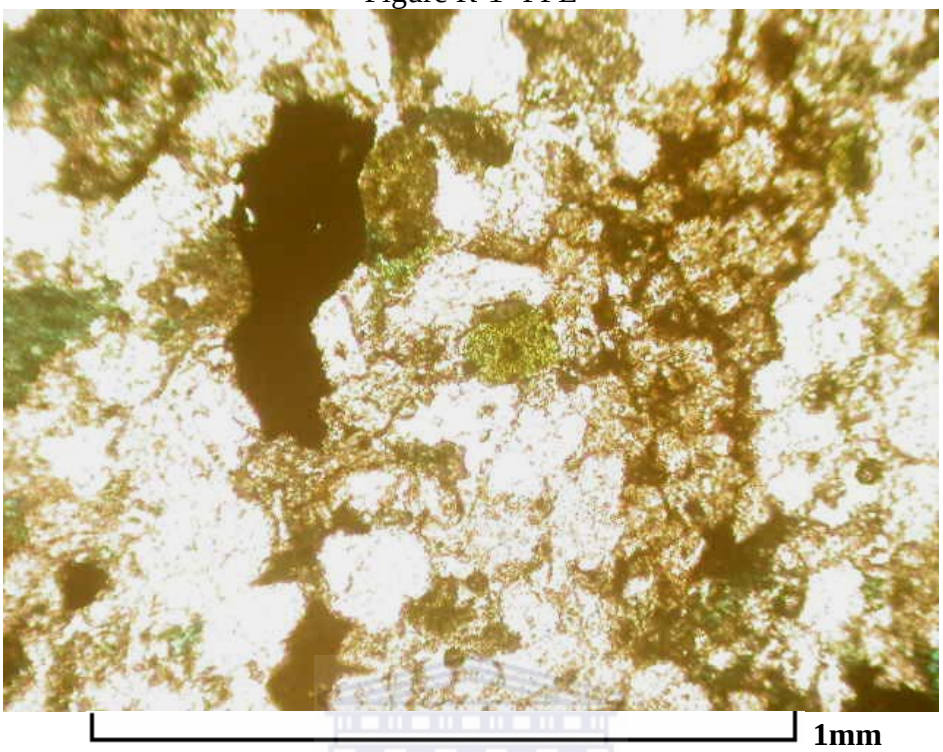

Scale (Magnification x10)

Figure R-2- XPL

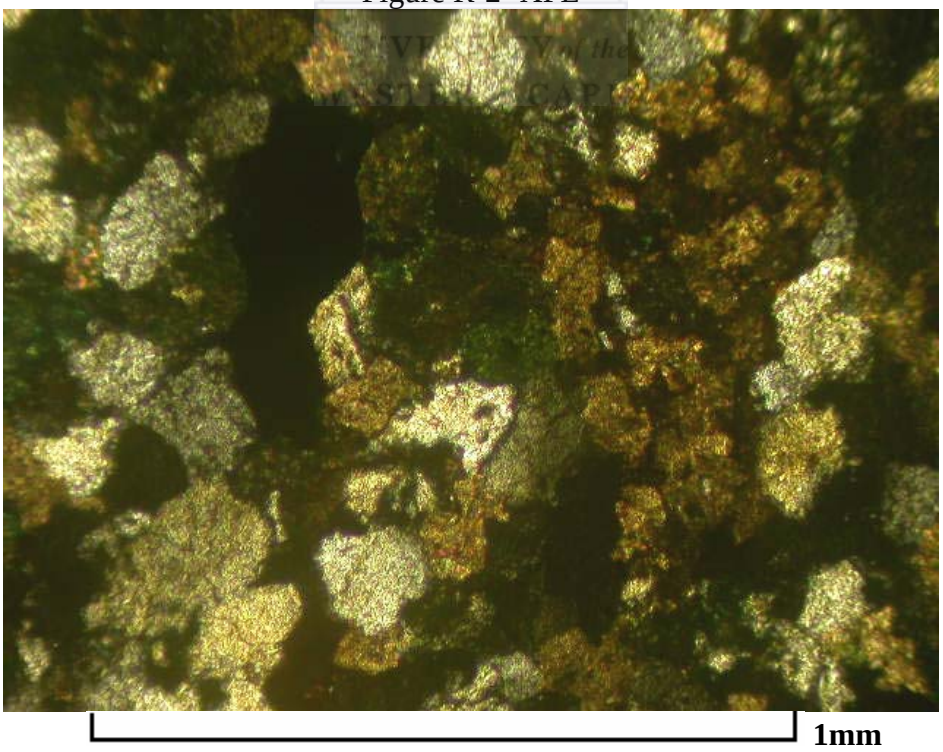

Scale (Magnification x10)

Sample: C 1:5 **Depth: 2832.87m**

Composition: Framework minerals:	***Percentages***
Quartz	60%
Feldspar	15%
Lithic fragments	10%
Glauconite	<1%

Quartz:	Crystal structure is euhedral
	Grain shape is sub angular
	Euhedral grains are detrital
	Grains contain needle-like vacuoles
Feldspar:	Grains are scratched or cracked
	No visible twinning present
	Contain many inclusions
	Orthoclase
Lithic fragments:	Very fine quartz grains in clay matrix
	Sedimentary origins
Glauconite:	Occur as pellets

Ductile Minerals:	***Percentages***
Clays	5%
Micas	3%

Clays:	Occur as clasts between grains
Micas:	As deformed flakes

Authigenic Minerals:	***Percentages***
Quartz cement	2%
Carbonate cement	4%

Quartz cement:	Overgrowths on detrital grains
Carbonate cement:	Clasts between grains and filling pores (Figure S-1 and S-2)

***Porosity*:** Porosity is very good
Mostly secondary porosity is filled with cement primary porosity is retained
Connectivity is very good

***Texture*:** Fine grained (0.5mmaverage) [x4 magnification]
Sorting of grains is moderate to poor
Grain shape is ranging from sub angular to sub rounded
Sphericity ranges from low to high
Packing of grains is fairly tight
Grain supported
Grain contacts are sutured

Name: SubArkose (Sandstone)

Comments: Pores are irregular this being an indication of a grain that has dissolved in that section. Glauconite is often observed along pores, this could be an indication of pressure solution of grains which formerly surrounded or was in contact with the glauconite. Overall porosity and connectivity of sample is very good.

FIGURES S. Sample: C 1:5 **Depth: 2832.87m**

Figure S-1- PPL

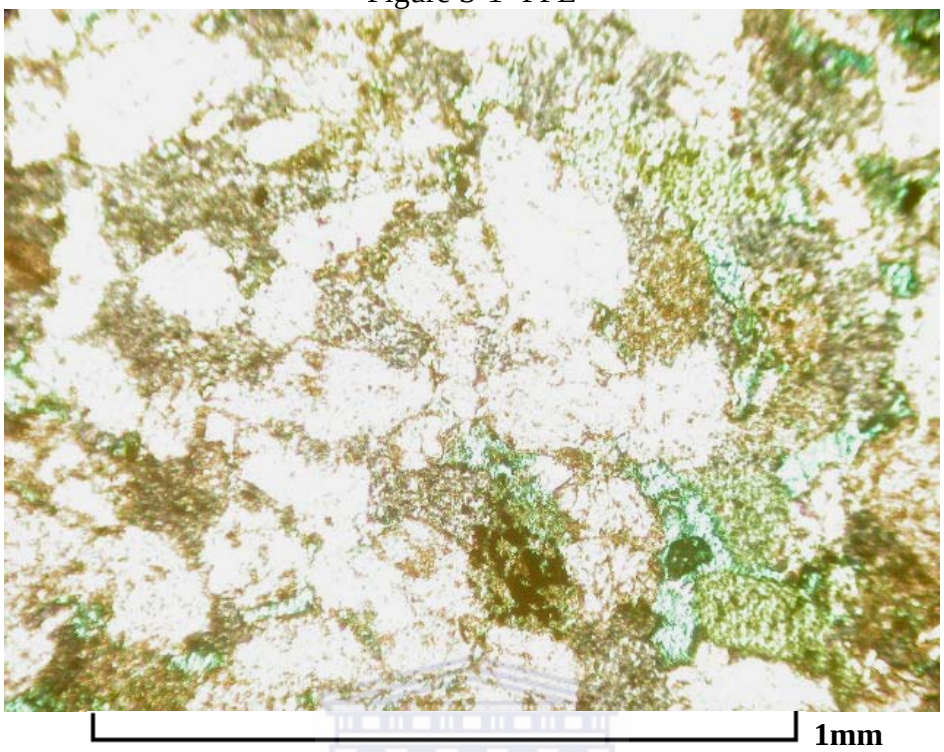

Scale (Magnification x10)

Figure S-2- XPL

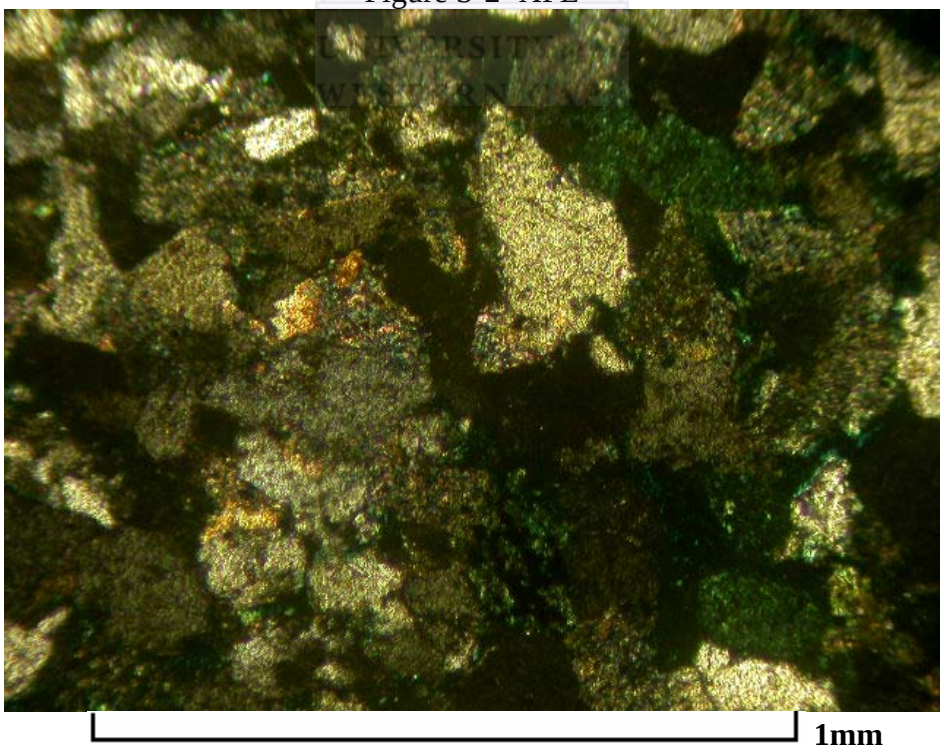

Scale (Magnification x10)

Sample: C 1:6 **Depth: 2833.89m**

Composition: Framework minerals:	***Percentages***
Quartz	60%
Feldspar	15%
Lithic fragments	10%
Glauconite	3%

Quartz: Monocrystalline dominates
Planar extinctions and occasional grains with undulose extinction
Individual crystals are sutures in polycrystalline grain
Vacuoles and needle inclusions in grains (Figure T-1 in bottom left field of photograph)

Feldspar: Partially dissolved grain
Cracked grains

Lithic fragments: Very fine quartz in clay matrix
Sedimentary rock fragment

Glauconite: Occur as pellets between grains

Ductile Minerals:	***Percentages***
Clays	5%
Micas	<1%

Clays: In the form of clasts found between grains

Micas: Flaked grains that is deformed

Authigenic Minerals:	***Percentages***
Quartz cement	<3%
Carbonate cement	3%

Quartz cement: Overgrowths on detrital grains

Carbonate cement: Grows between grains and fill pores

***Porosity*:** Porosity is average as a result of the clays and cements that reduce the pore amounts
Mostly isolated pores present
Angular pore shapes like grain thus secondary porosity dominant by dissolution.
Connectivity is poor as a result of reduced porosity

***Texture*:** Fine grained material
Grains are poorly sorted
Grain shapes are angular to sub angular
Sphericity of grains are low
Grains are tightly packed
Rock supported by grains and cement
Grain contacts are sutured and concavo-convex

Name: Subarkose (Sandstone)

Comments: Grains have dusty rims. Traces of black material are noted in pores at the boundary of the thin section sample.

FIGURES T. Sample: C 1:6 **Depth: 2833.89m**

Figure T-1- PPL

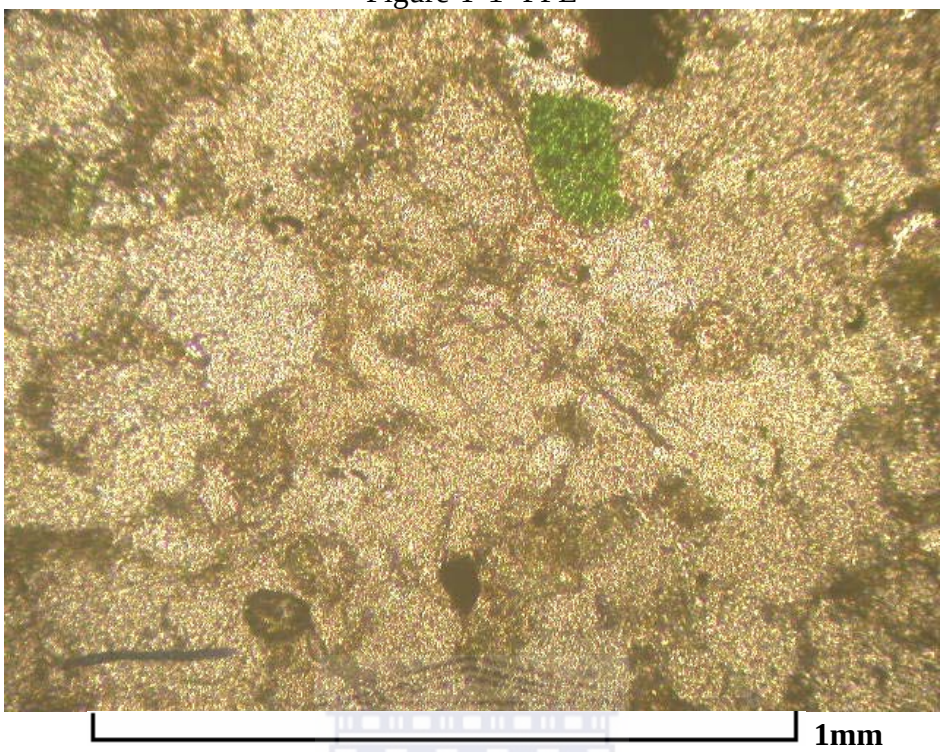

Scale (Magnification x10)

Figure T-2- XPL

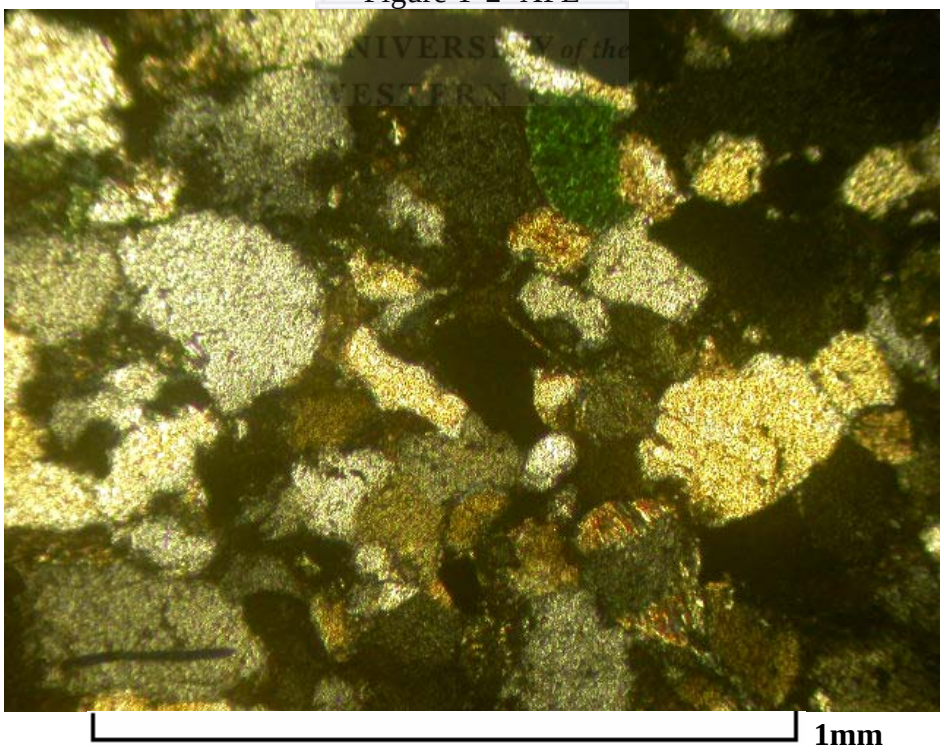

Scale (Magnification x10)

Sample: C 1:7 **Depth: 2834.08m**

Composition: Framework minerals:	***Percentages***
Quartz	60%
Feldspar	15%
Lithic fragments	10%
Glauconite	2%

Quartz: Monocrystalline and polycrystalline
Planar and undulose extinctions of grains
Concavo-convex and sutured contacts

Feldspar: No twinning of grains visible
Some grains are dissolved giving secondary porosity

Lithic fragments: Very fine quartz in clay matrix

Glauconite: Occur as pellets
A very large pellet is seen (Figure U-1) in thin section
The grain appears to be situated in a large pore which was formed by dissolution of surrounding grains.
There is black material (speckles) on the grain surface which could be a remnant of hydrocarbons which passed through the section

Ductile Minerals:	***Percentages***
Clays	5%
Micas	2%

Clays: Found between grains and in lithic fragments
Displays grain rimming properties

Micas: Occur as flakes deformed around crystal boundaries

Authigenic Minerals:	***Percentages***
Quartz cement	2%
Carbonate cement	4%

Quartz cement: Overgrowths on detrital grains

Carbonate cement: Formed between grains

***Porosity*:** Porosity is good
Mostly isolated pores
Intergranular and intragranular
Connectivity is average to poor

***Texture*:** Fine grained (0.5mm average) [x4 magnification]
Grains are poorly sorted
Grain shapes are angular
Sphericity of grains is low to high
Packing of grains are moderate to tight
Grains are mostly supported by other grains
Grain contacts are long, tangential and sutured

Name: Subarkose (Sandstone)

Comments: Sample is fairly compacted and isolated pores dominate porosity. This can be seen in Figure U-2 which was taken in PPL. Pores contain gas bubbles from mounting medium.

FIGURES U. Sample: C 1:7 **Depth: 2834.08m**

Figure U-1- PPL

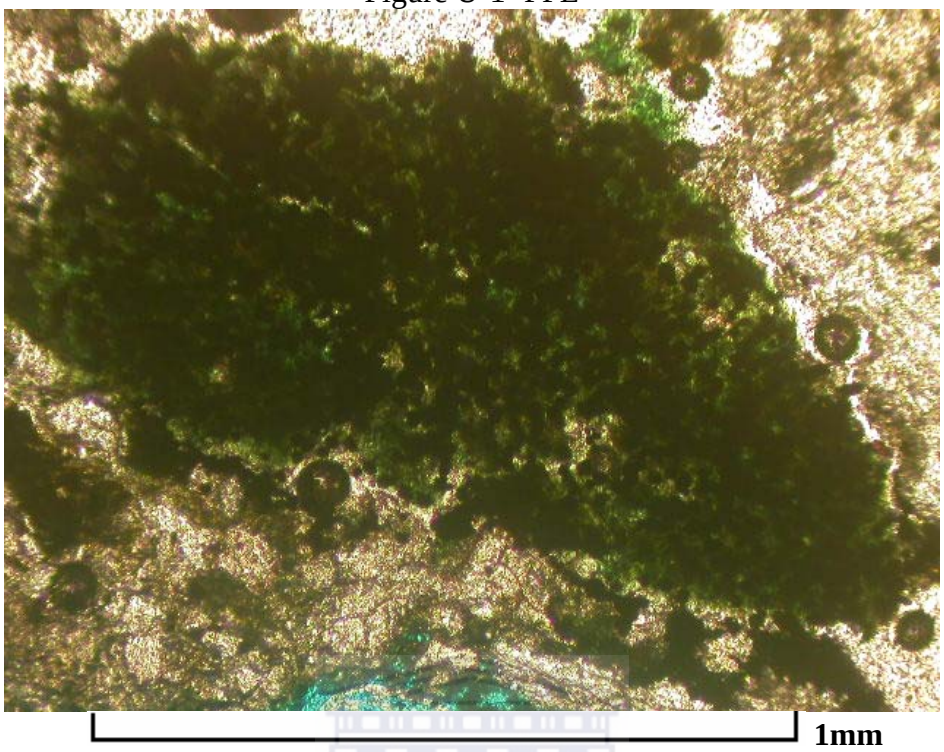

Scale (Magnification x10)

Figure U-2- PPL

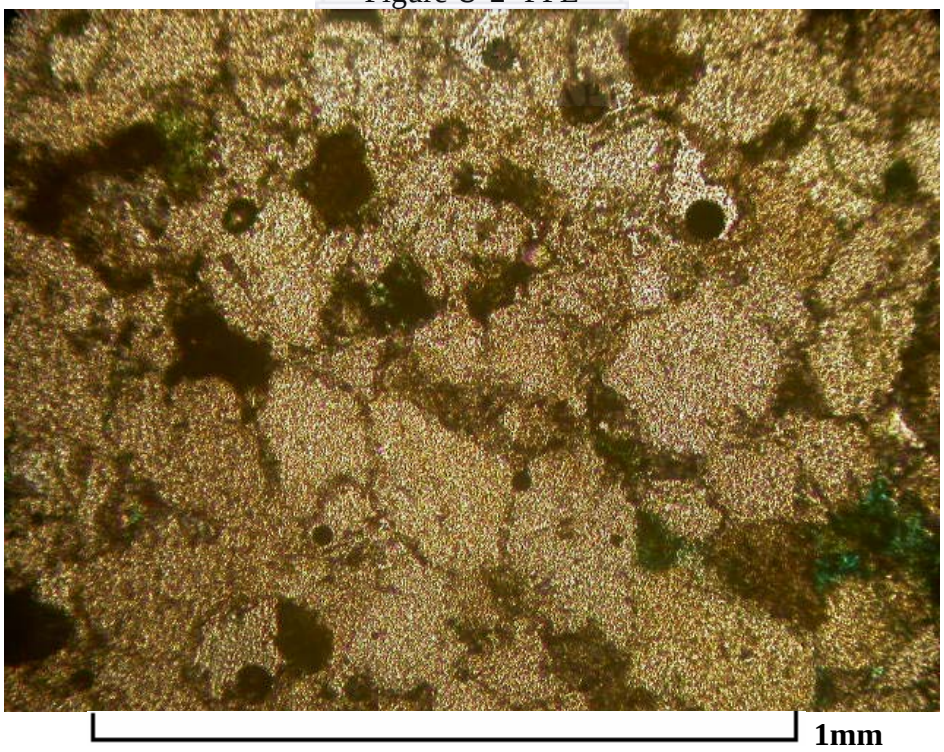

Scale (Magnification x10)

Sample: C 2:1 **Depth: 2835.05m**

Composition: Framework minerals:	***Percentages***
Quartz	60%
Feldspar	10%
Lithic fragments	8%
Glauconite	5%

Quartz: Monocrystalline and polycrystalline grain structures
Undulose and planar extinctions in XPL

Feldspar: Cracked grains
Some twinned grains were noted which indicates microcline is present in this sample

Lithic fragments: Occur as fine grained quartz in clay matrix indicating a sedimentary rock origin

Glauconite: Occur as pellets between grains

Ductile Minerals:	***Percentages***
Clays	10%
Micas	2%

Clays: High matrix content between grains
Filled with very fine quartz and mica grains
Deformation around grain boundaries (Figure V-1 and V-2 in centre of view)

Micas: Deformed flakes
Mica type not distinguished

Authigenic Minerals:	***Percentages***
Quartz cement	2%
Carbonate cement	3%

Quartz cement: Overgrowths on detrital grains

Carbonate cement: Found between grains as clasts and in clays

***Porosity*:** Porosity is good
Connectivity is good
Isolated pores are greater than connected pores
Fracture pore present

***Texture*:** Fine grained (0.5mm average) [x10 magnification]
Grains are poorly sorted
Grain shape is sub angular
Sphericity is low to high
Grains are moderately tight packed
Main grain support is matrix
Grain contacts are tangential and sutured

Name: Subarkose (Sandstone)

Comments: There are two “granulation” seams. One, more to the interior of the sample, is filled with dark brown to black muddy material (Figure V-1 and V-2 centre view). Some mica flakes are present which have been deformed (figure V-2) around grains.
The second seam (Figure V-3) is positioned at the edge of the slide. It is about 0.05mm [x10] wide and runs across the width of the slide. Fluid flow is improved, seen by the blue epoxy dye. There are traces of black material on the sides of the seam which could be a remnant of the hydrocarbon fluid that passed through it.

FIGURES V. Sample: C 2:1 **Depth: 2835.05m**

Figure V-1- PPL

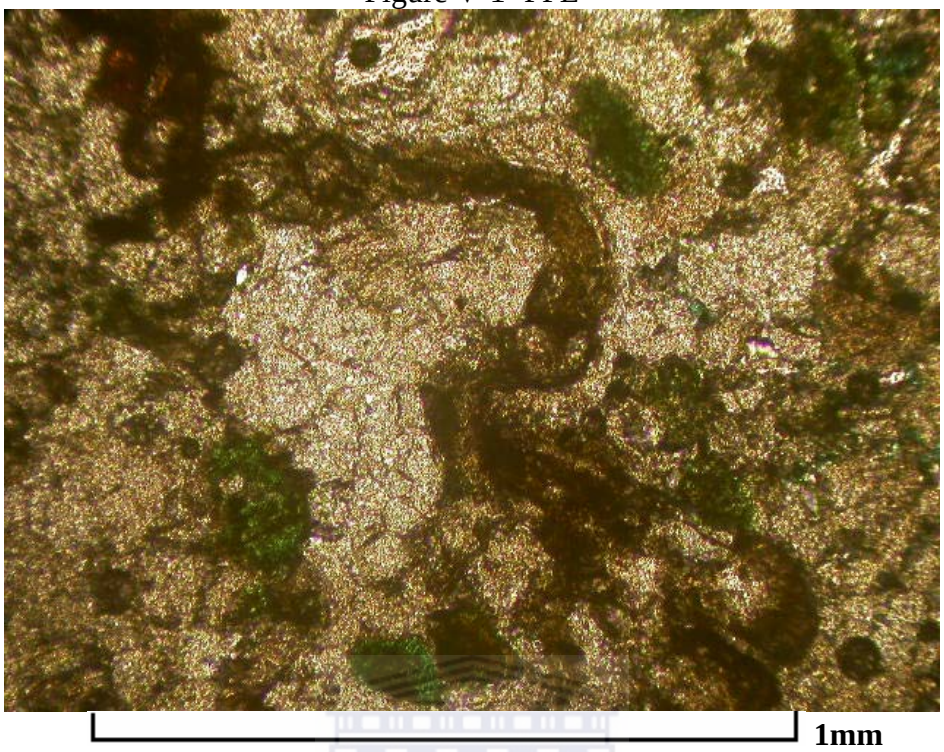

Scale (Magnification x10)

Figure V-2- XPL

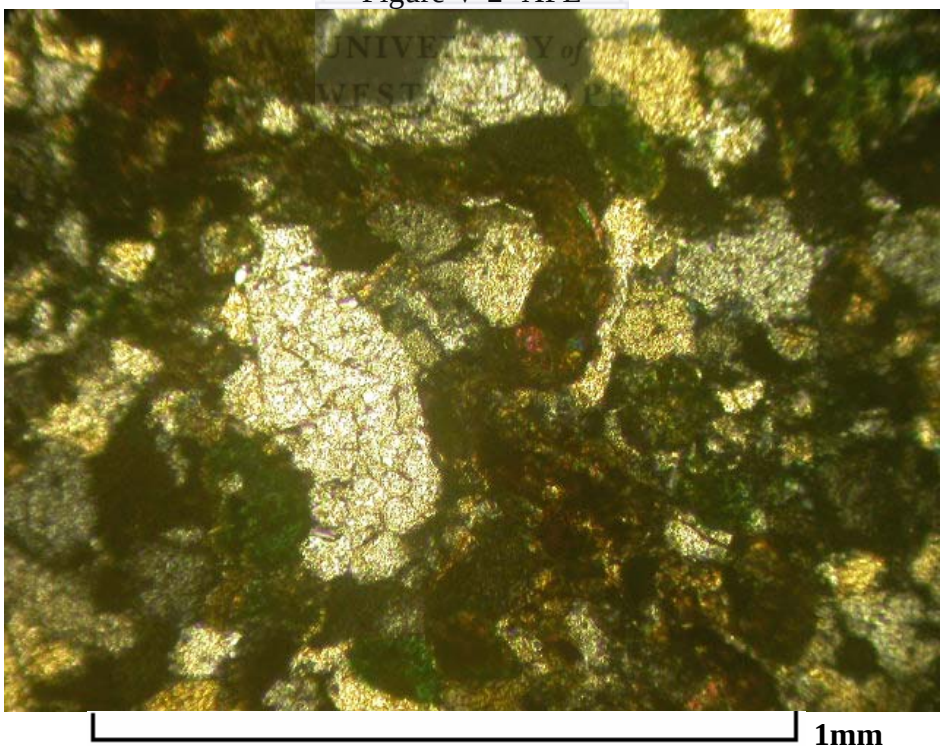

Scale (Magnification x10)

Figure V-3- PPL

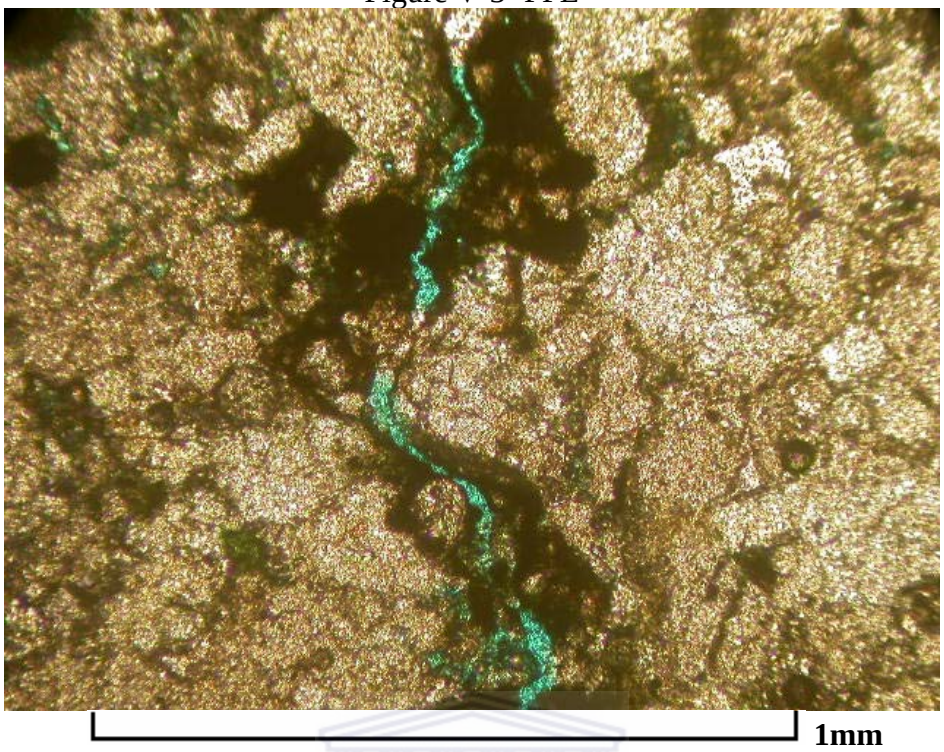

Scale (Magnification x10)

Figure V-4- XPL

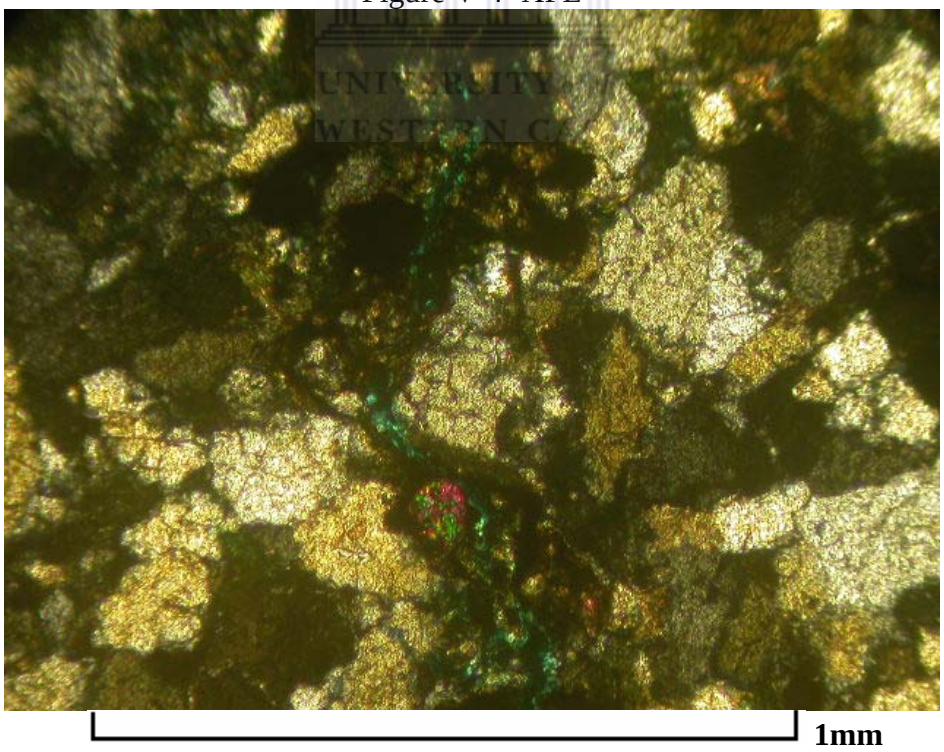

Scale (Magnification x10)

Sample: C 2:2 **Depth: 2835.96m**

Composition: Framework minerals:	***Percentages***
Quartz	60%
Feldspar	15%
Lithic fragments	10%
Glauconite	5%

Quartz:	Monocrystalline Grain contacts are concavo-convex and sutured Polycrystalline grains with undulose extinction
Feldspars:	Grains are cracked Some grains are partially dissolved
Lithic fragments:	Very fine quartz grains in clay matrix (sedimentary lithic fragment) Some fragments have only quartz fragments (metamorphic lithic fragment)
Glauconite:	Occur as pellets between grains

Ductile Minerals:	***Percentages***
Clays	5%
Micas	<1%

Clays:	Mainly as matrix and also pore-filling
Micas:	Minor constituent as grains

Authigenic Minerals:	***Percentages***
Quartz cement	1%
Carbonate cement	3%

Quartz cement:	Occur as overgrowths on all detrital grains
Carbonate cement:	Pore-filling

***Porosity*:** Porosity is good
Connectivity is good
Some isolated pores present containing black material
Some pores filled with clays and cement

***Texture*:** Fine grained (0.5mm average) [x10]
Grains are moderately sorted
Grain shapes are angular to sub angular
Sphericity of grains are ranging low to high
Grains are packed moderately tight
Rock is grain and matrix supported
Grain contacts are concavo-convex and sutured

Name: Subarkose (Sandstone)

Comments: When looking at Figures W-1 and W-2, the cements and clay matrix can be clearly seen between the grains however, the slide represents overall good porosity and permeability.

FIGURES W. Sample: C 2:2 **Depth: 2835.96m**

Figure W-1- PPL

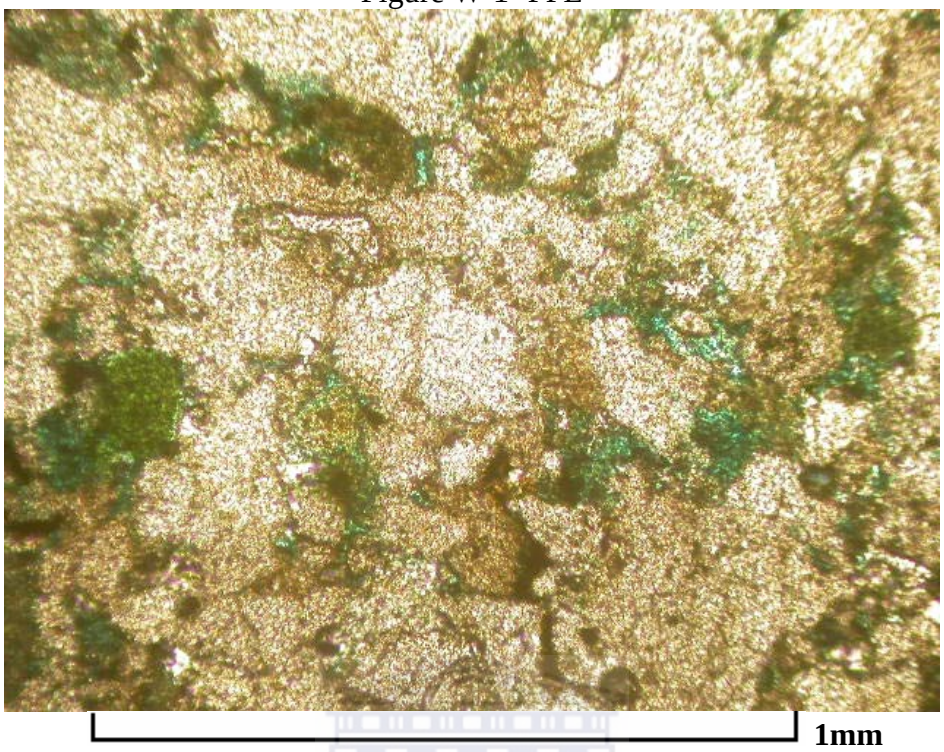

Scale (Magnification x10)

Figure W-2- XPL

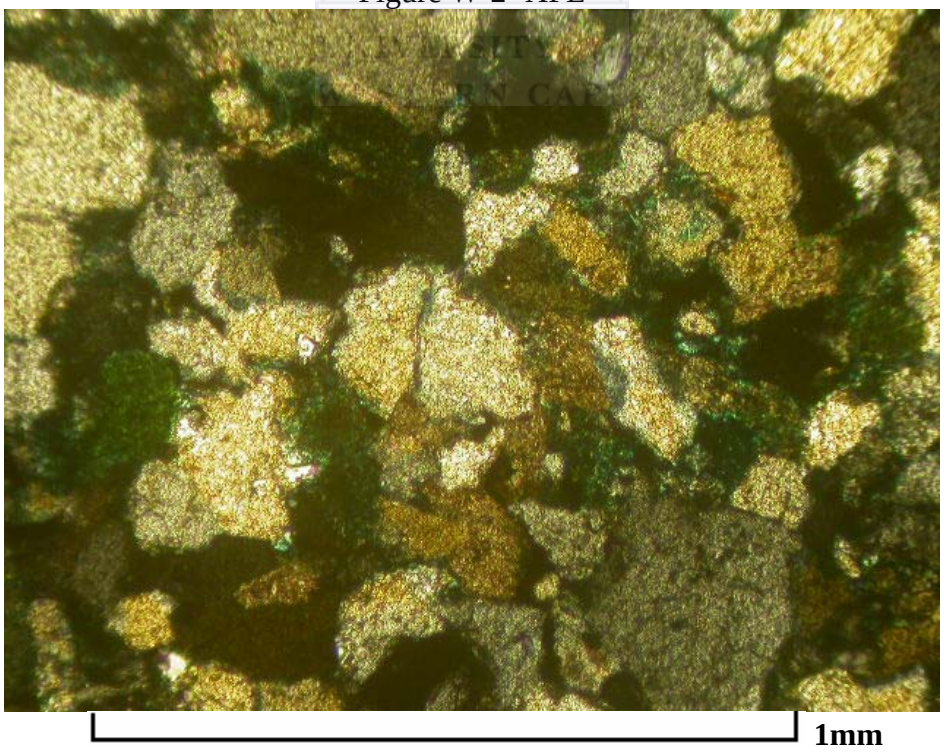

Scale (Magnification x10)

Sample: C 2:3 **Depth: 2836.95m**

Composition: ***Framework minerals:***	***Percentages***
Quartz	60%
Feldspar	15%
Lithic fragments	5%

Quartz: Most grains are cracked
Grains are composite polycrystalline
Grain contacts are long
Feldspar: Most grains are cracked
No twinning feature are visible
Lithic fragments: Very fine quartz in clay matrix (Sedimentary rock source)
Glauconite: Occurs as pellets between grains

Ductile Minerals:	***Percentages***
Clays	6%
Micas	<1%

Clays: Occur mostly as matrix and clasts between grains
Micas: Very minor constituent found in the matrix

Authigenic Minerals:	***Percentages***
Quartz cement	5%
Carbonate cement	5%

Quartz cement: Overgrowths on detrital grain
Carbonate cement: Found in pores

***Porosity*:** Porosity is good
Connectivity in centre of slide is average which becomes good towards the edges of the slide (could be artifact of thin section operation)
Some pores contain black material

***Texture*:** Fine grained (0.5mm average) [x10]
Grains are poorly sorted
Grain shapes are angular to sub angular
Sphericity ranges from low to high
Grain packing is from moderate to well
Grain support is by grains and matrix
Grain contacts are long and tangential

Name: Subarkose (Sandstone)

Comments: Overall porosity is good and permeability is average due to its patchy nature. Features of cracked grains and extinctions can be seen in Figures X-1 and X-2. The connectivity can be seen in PPL by the blue epoxy dye and as black patches in XPL. Stylolites are present.

FIGURES X. Sample: C 2:3 **Depth: 2836.95m**

Figure X-1- PPL

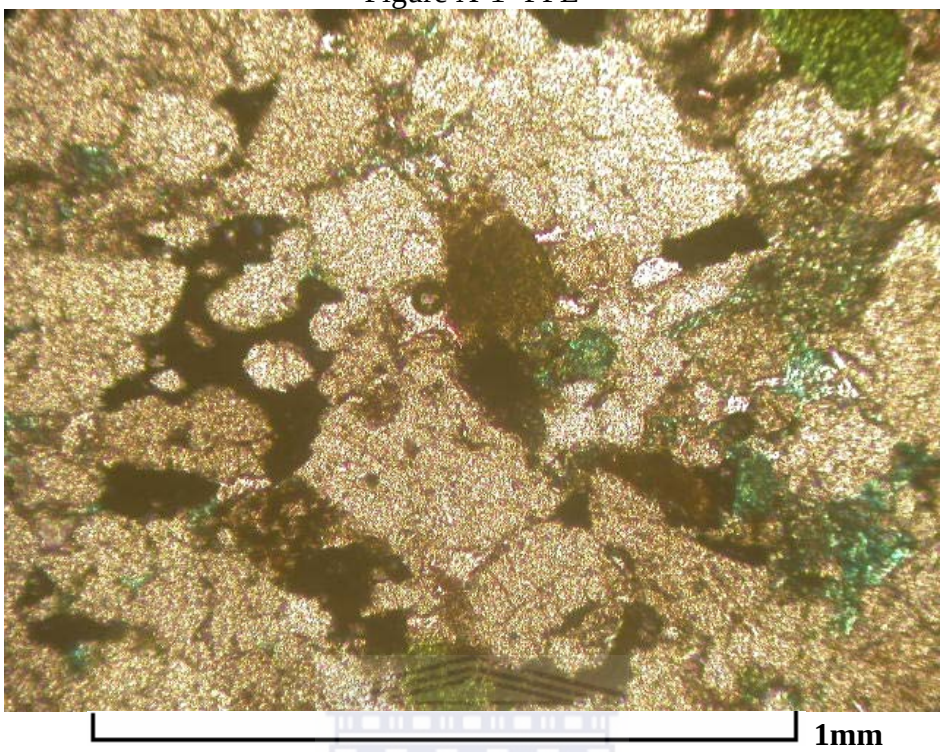

Scale (Magnification x10)

Figure X-2- XPL

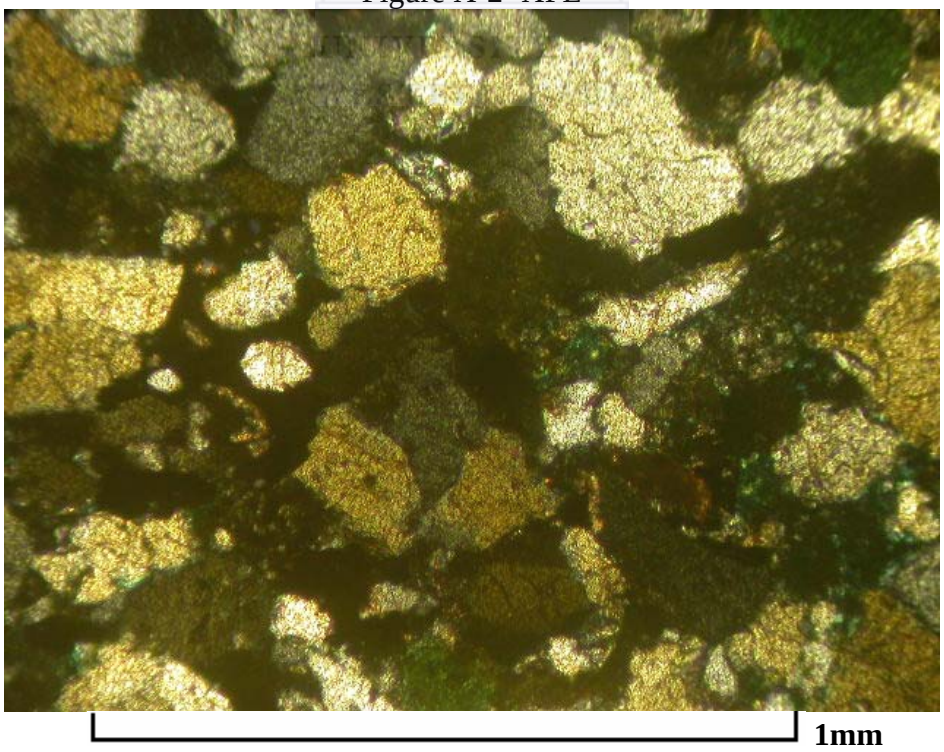

Scale (Magnification x10)

Sample: C 2:4 **Depth: 2837.95m**

Composition: Framework minerals:	***Percentages***
Quartz	60%
Feldspar	15%
Lithic fragment	10%
Glauconite	3%

Quartz:	Monocrystalline and polycrystalline grains
	Grains to grain contact mostly sutured
Feldspar:	Scratched grains due to weathering
	No visible twinning features
	Dissolution is evident
Lithic fragments:	Very fine grains in clay matrix (sedimentary LF)
	Clasts of sutured grain with no matrix (metamorphic LF)
Glauconite:	Occurs as pellets

Ductile Minerals:	***Percentages***
Clays	6%
Micas	1%

Clays:	Grain rimming clays
Micas:	Not well deformed flakes

Authigenic Minerals:	***Percentages***
Quartz cement	3%
Carbonate cement	2%

Quartz cement:	Overgrowths on detrital grains
Carbonate cements:	Pore-filling

***Porosity*:** Good porosity
Good connectivity
Some pores filled with quartz crystals but evidence of blue due suggest that permeability is not affected greatly

***Texture*:** Fine Grained (0.5mm average) [x4 magnification]
Grains are moderately sorted
Grain shapes are sub angular
Sphericity ranges from low to high
Packing of grains is moderately tight
Support is by grains and matrix
Grain contacts are long and sutured

Name: SubArkose (Sandstone)

Comments: Porosity and permeability is shown bye the presence of blue dye in the pores seen in Figure Y-1 in PPL. The pores appear black in Figure Y-2 in

XPL. A stylolite can be clearly seen in Figure Y-1 in the top-left of the thin section. Traces of precipitated pyrite were observed within the matrix. These appear ‘metallic in reflected light (not shown on photomicrograph).

FIGURES Y. Sample: C 2:4 **Depth: 2837.95m**

Figure Y-1- PPL

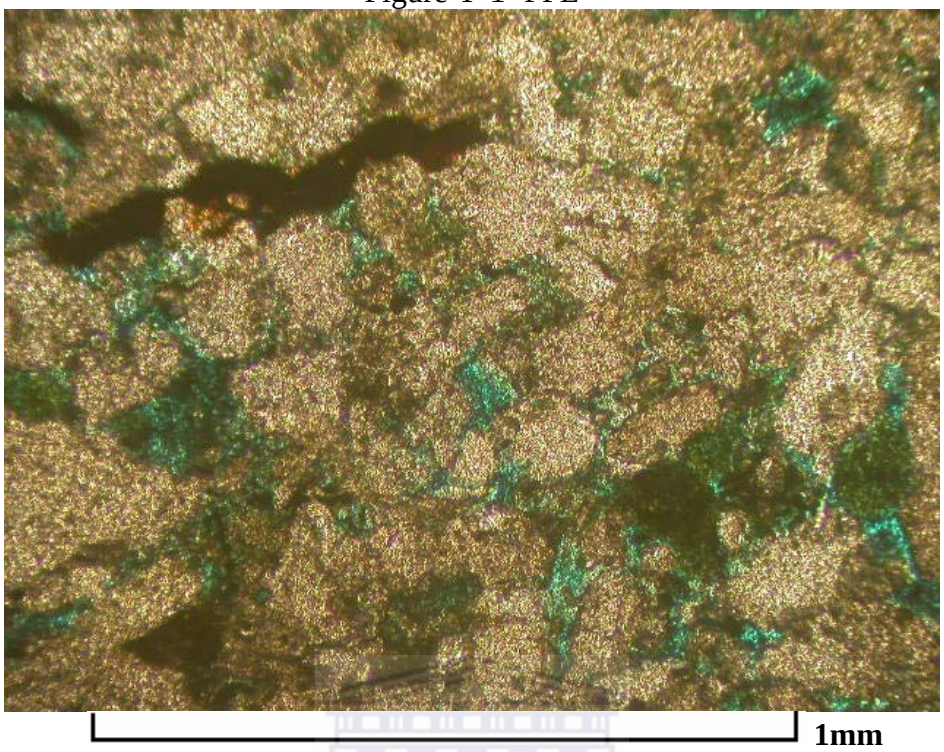

Scale (Magnification x10)

Figure Y-2- XPL

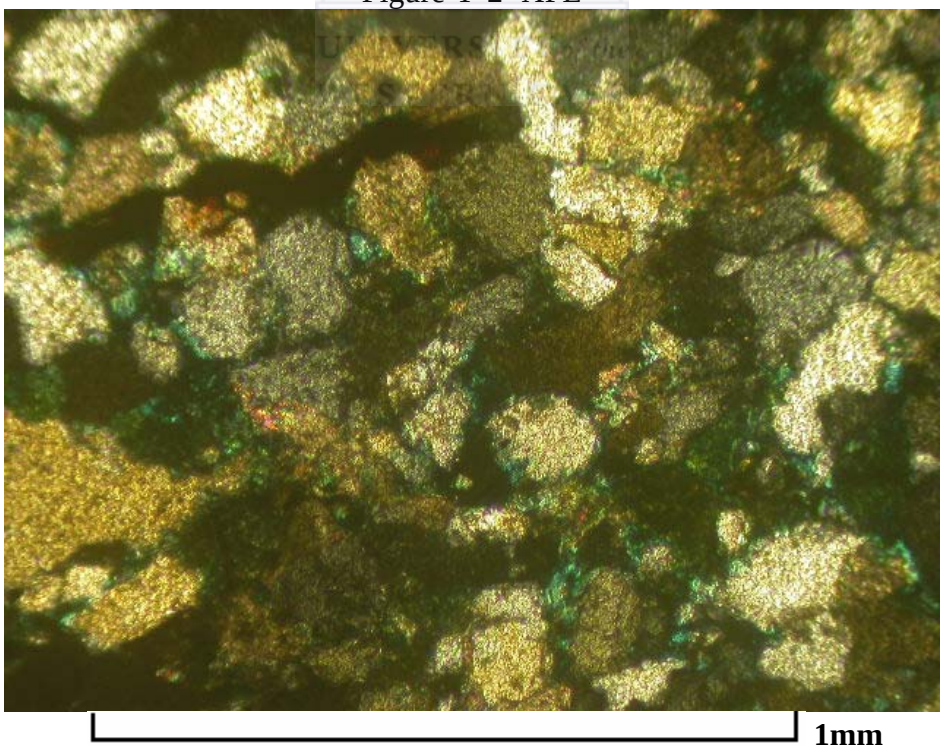

Scale (Magnification x10)

Sample: C 2:5 **Depth: 2839.00m**

Composition: Framework minerals:	***Percentages***
Quartz	60%
Feldspar	15%
Lithic fragments	5%
Glauconite	2%

Quartz:	Monocrystalline and polycrystalline grains Undulose and planar extinctions
Feldspar:	Twinning visible- microcline (Figure Z-2 in centre view) Some grains partially dissolved
Lithic fragments:	Very fine grains in clay matrix
Glauconite:	Pellets between grains

Ductile Minerals:	***Percentages***
Clays	5%
Micas	1%

Clays:	Found between grains
Micas:	Minor flakes between grains

Authigenic Minerals:	***Percentages***
Quartz cement	5%
Carbonate cement	5%
Silica cement	2%

Quartz cement:	Overgrowths on detrital grains
Carbonate cement:	Fills pores
Silica cement	Found in few pores as crystals

***Porosity*:** Porosity is average
Intergranular, intragranular and fractured porosity present
Connectivity is poor but enhanced by the presence of a granulation seam, but only on a local scale

***Texture*:** Fine grained (0.5mm average) [x4]
Grains are moderately sorted
Grain shape is angular
Sphericity ranges from low to high
Grains are tightly packed
Grains are supported by matrix and grains
Grain contacts are long and sutured

Name: Subarkose (sandstone)

Comments: There are traces of a brown muddy material between the grains. Figure Z-1 and Z-2 is a general representation of a granulation seam in the thin section. Figure Z-2 displays a sparry carbonate cement precipitated within a pore.

FIGURES Z. Sample: C 2:5 **Depth: 2839.00m**

Figure Z-1- PPL

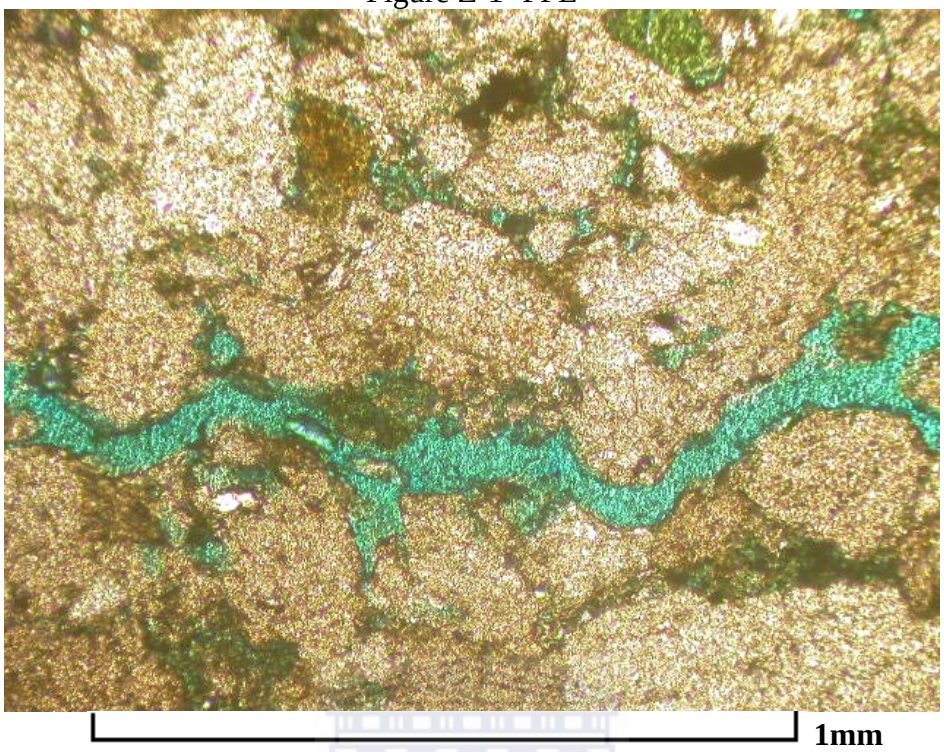

Scale (Magnification x10)

Figure Z-2- XPL

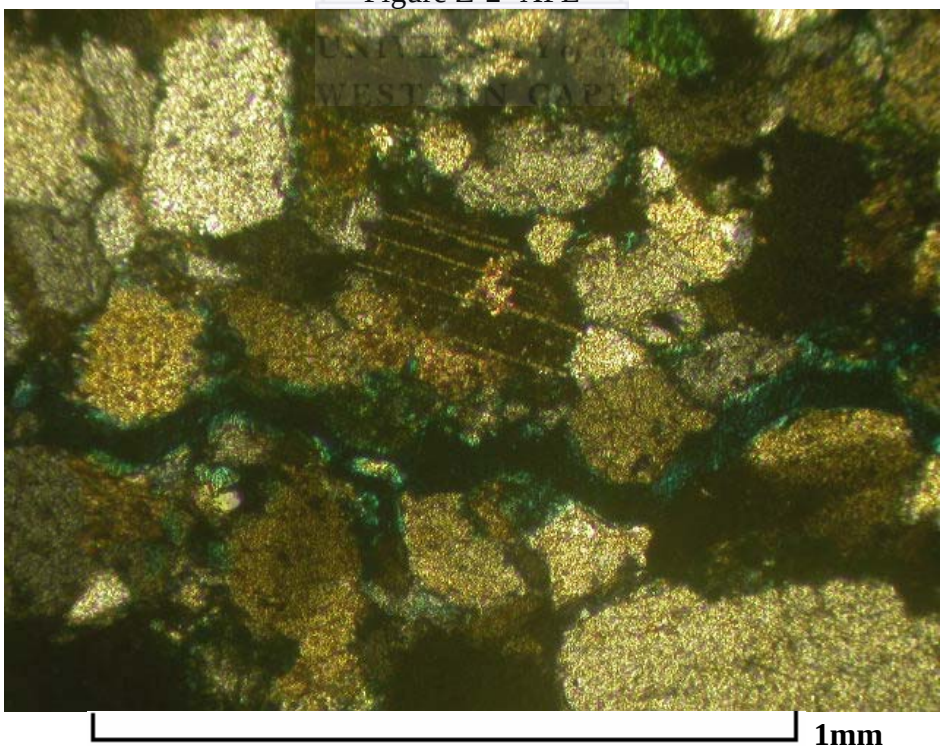

Scale (Magnification x10)

Sample: C 2:6 **Depth: 2840.00m**

Composition: ***Framework minerals:***	***Percentages***
Quartz	65%
Feldspar	10%
Lithic fragments	5%
Glauconite	3%

Quartz:	Monocrystalline and polycrystalline Planar and undulose extinction
Feldspar:	No visible twinning features Cracked grains Dissolution is evident
Lithic fragments:	Very fine grains in clay matrix
Glauconite:	Pellets between grains

Ductile Minerals:	***Percentages***
Clays	5%
Micas	1%

Clays:	Grain rimming clays
Micas:	Not well deformed flakes

Authigenic Minerals:	***Percentages***
Quartz cement	2%
Carbonate cement	3%

Quartz cement:	Overgrowths on detrital grains
Carbonate cements:	Pore-filling

***Porosity*:** Porosity is good
Connectivity is good
Small pore throats
Isolated and connected
Dark material in isolated pores

***Texture*:** Fine grained (0.5mm average) [x4]
Grains are moderately sorted
Grain shape is angular
Sphericity is from low to high
Grains are packed moderately tight
Support is by grains and matrix
Grain contacts are long and sutured

Name: Subarkose (Sandstone)

Comments: Figures AA-1 and AA-2 is a representation of the thin section

FIGURES AA. Sample: C 2:6 Depth: 2840.00m

Figure AA-1- PPL

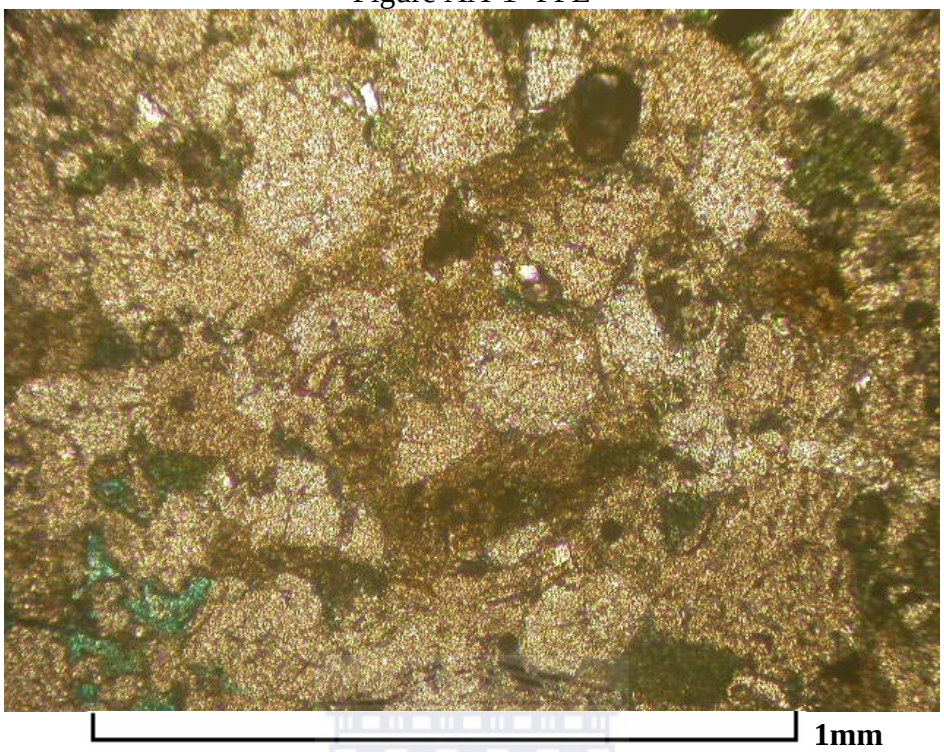

Scale (Magnification x10)

Figure AA-2- XPL

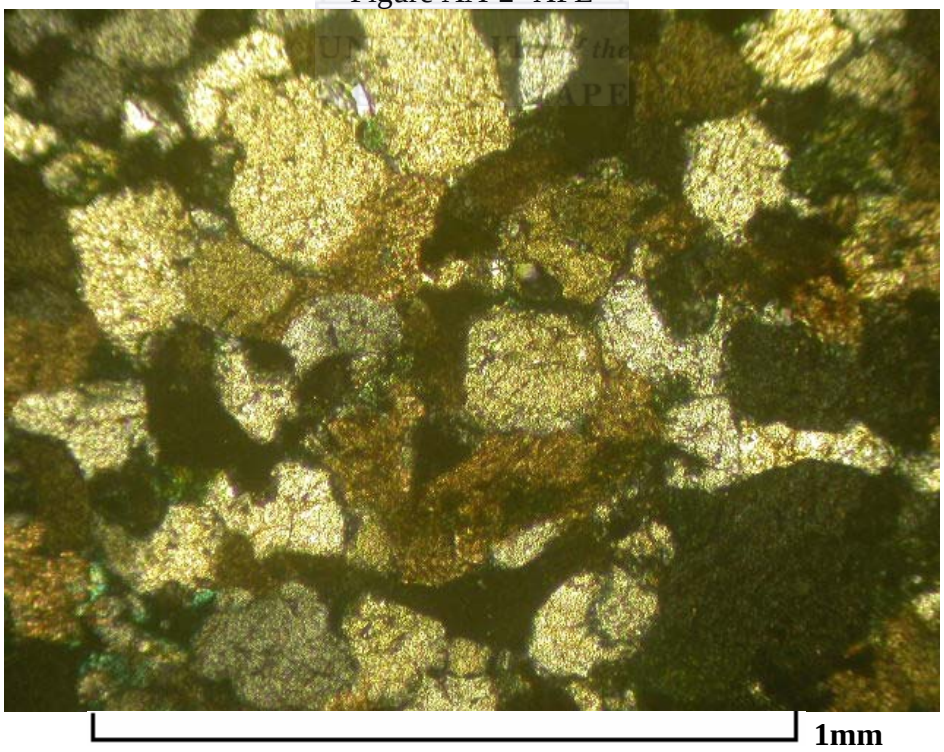

Scale (Magnification x10)

Sample: C 2:7 **Depth: 2841.03m**

Composition: Framework minerals:	***Percentages***
Quartz	65%
Feldspar	10%
Lithic fragments	10%
Glauconite	3%

Quartz: Grains are cracked and hard to distinguish
Extinctions are planar and yellow
Feldspar: Grains are cracked and highly altered.
No visible twinning features are present
Lithic fragments: Fine quartz grains in clay matrix material
Glauconite: Minor constituent
Grains are as pellets

Ductile Minerals:	***Percentages***
Clays	5%
Micas	1%

Clays: Grain rimming clays
Micas: Not well deformed flakes

Authigenic Minerals:	***Percentages***
Quartz cement	2%
Carbonate cement	2%

Quartz cement: Overgrowths on detrital grains
Carbonate cements: Pore-filling, large clast in centre view of Figure AB-2 in XPL

***Porosity*:** Average to good porosity
Good connectivity
Isolated pores, and interconnected pores
Pores are intergranular and intragranular
Primary and secondary porosity present

***Texture*:** Fine grained (0.5mm average) [x4 magnification]
Sorting of grains is moderate to well
Grain shape ranges from sub angular to sub rounded
Sphericity is low
Grains are packed moderately tight
The section is grain and matrix supported
Grain contacts are long and sutured

Name: Subarkose (sandstone)

Comment: Figure AB-2 shows a calcite cement in the centre view.

FIGURES AB. Sample: C 2:7 Depth: 2841.03m

Figure AB-1- PPL

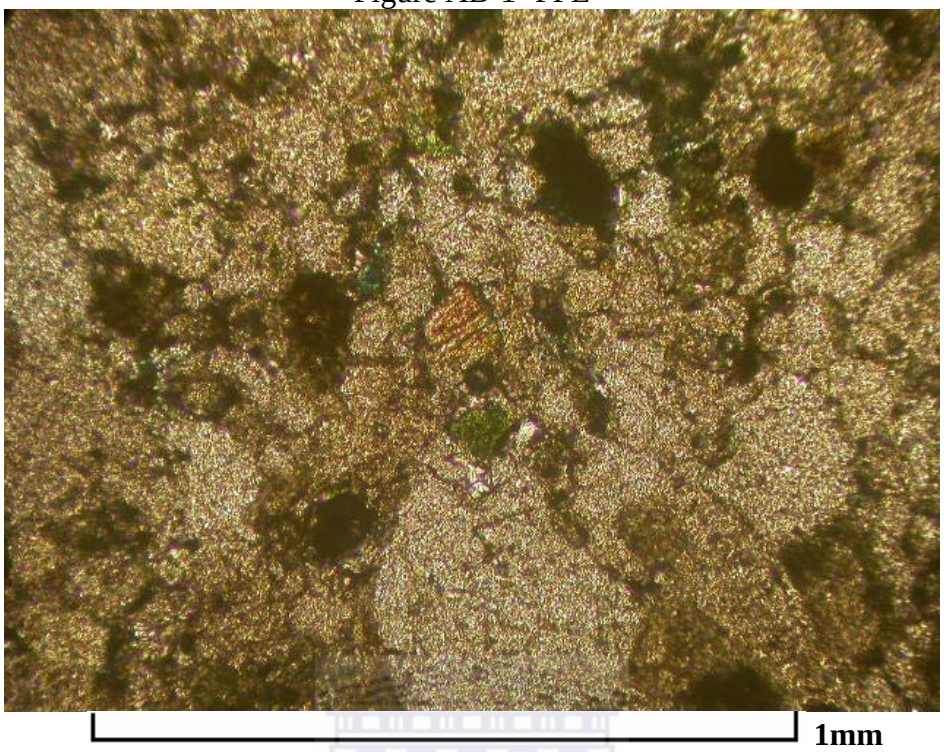

Scale (Magnification x10)

Figure AB-2- XPL

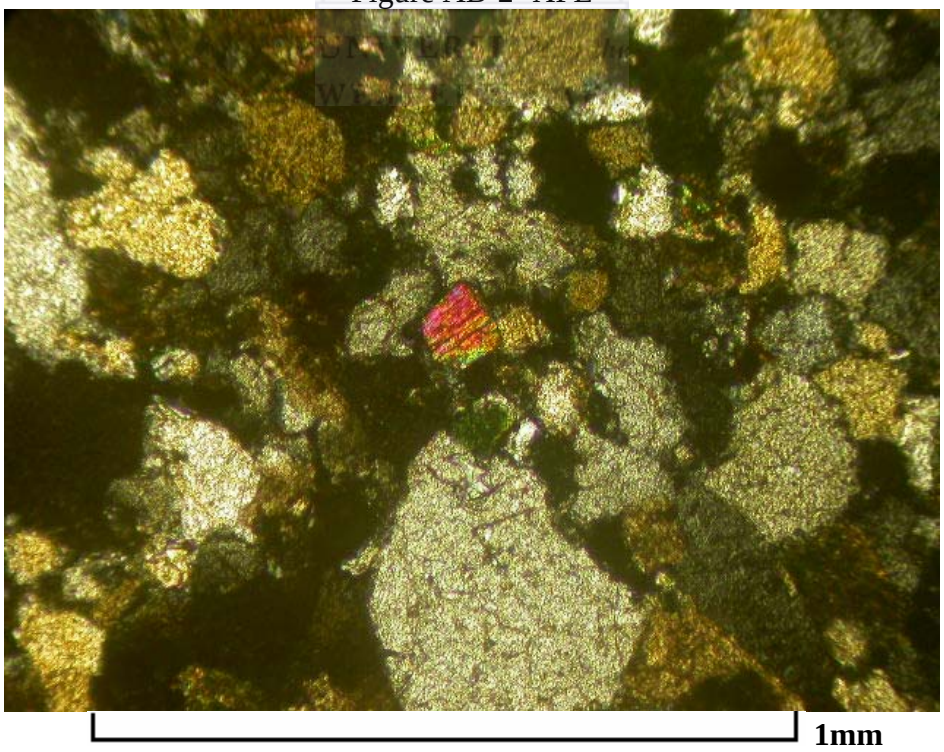

Scale (Magnification x10)

Sample: C 2:8 **Depth: 2842.05m**

Composition: Framework minerals:	***Percentages***
Quartz	65%
Feldspar	10%
Lithic fragments	10%
Glauconite	3%

Quartz: Monocrystalline and polycrystalline
Mostly undulose extinction
Yellow coatings on grain surfaces

Feldspar: Partially dissolved grains
No visible twinning features

Lithic fragments: Very fine grains in clay matrix and clasts of very fine sutured grains

Glauconite: Occur as pellets between grains

Ductile Minerals:	***Percentages***
Clays	5%
Micas	1%

Clays: Occur as matrix

Micas: Minor constituent of rock material as flakes and as tiny fragments in matrix

Authigenic Minerals:	***Percentages***
Quartz cement	2%
Carbonate cement	4%

Quartz cement: Occurs as overgrowths on detrital grains. These overgrowths are seen outside the dust rims.

Carbonate cement: Found between grains with pores (either man-made or natural gas bubbles)

***Porosity*:** Porosity is good
Connectivity is good
Secondary porosity by dissolution of grains
Cements found in pores

***Texture*:** Fine grained (0.5mm average) [x4 magnification]
Angular to sub angular grain shapes
Grains are moderately sorted
Grains are loosely packed
Support- grain to grain and matrix
Grain contacts are long and sutured

Name: SubArkose (Sandstone)

A general representation of the whole thin section is given by Figures AC-1 and AC2.

FIGURES AC. Sample: C 2:8 Depth: 2842.05m

Figure AC-1- PPL

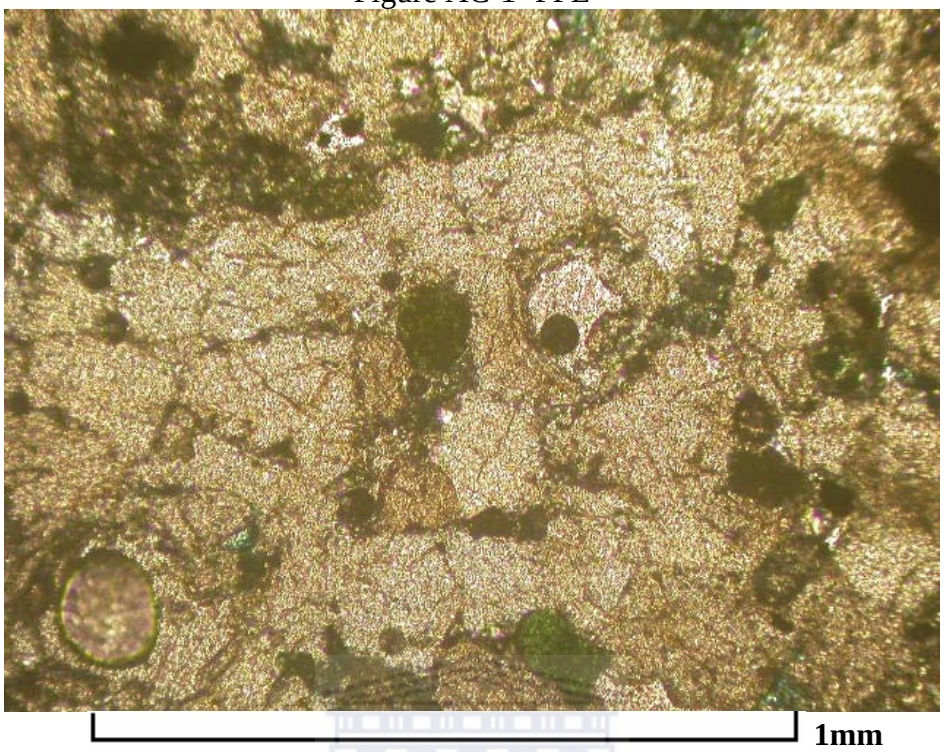

Scale (Magnification x10)

Figure AC-2- XPL

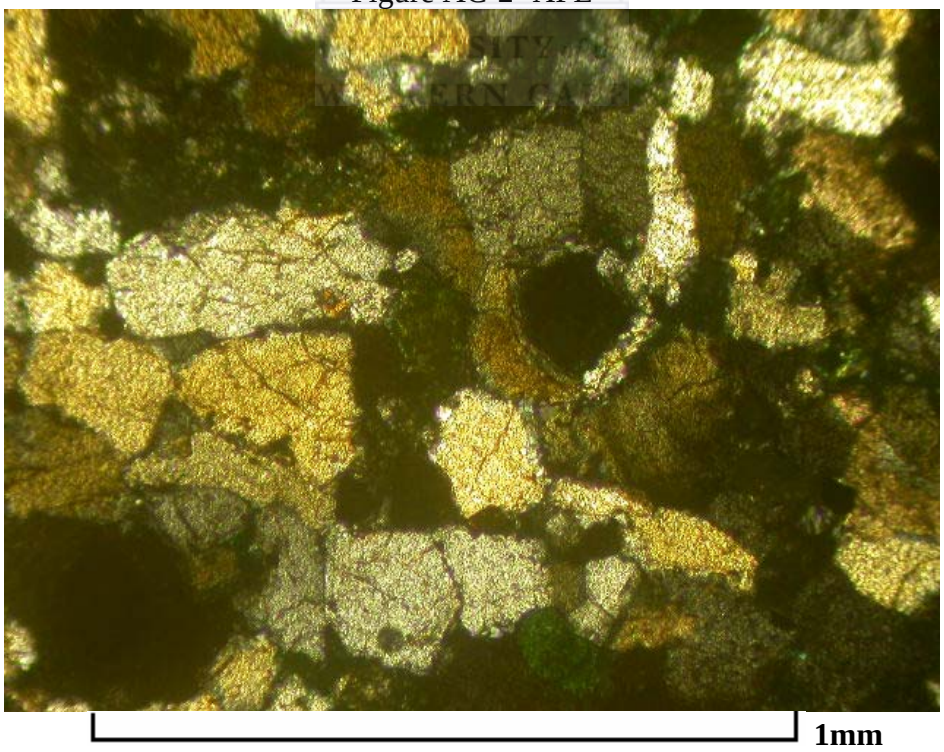

Scale (Magnification x10)

Sample: C 2:9 **Depth: 2842.96m**

Composition: Framework minerals:	***Percentages***
Quartz	65%
Feldspar	10%
Lithic fragments	10%
Glauconite	5%

Quartz:	Monocrystalline and polycrystalline Planar and undulose extinction
Feldspar:	No visible twinning features Scratched grains Dissolution is evident
Lithic fragments:	Very fine grains in clay matrix
Glauconite:	Pellets between grains

Ductile Minerals:	***Percentages***
Clays	4%
Micas	1%

Clays:	Occur as clasts between grains
Micas:	As deformed flakes

Authigenic Minerals:	***Percentages***
Quartz cement	2%
Carbonate cement	3%

Quartz:	Overgrowths on detrital grains
Carbonate cement:	Found between grains and in pores.

***Porosity*:** Excellent porosity
Good connectivity
Intergranular and intragranular pores
Connectivity throughout slide

***Texture*:** Fine grained (0.5mm average) [x4 magnification]
Grains are moderately sorted
Grain shapes are angular to sub angular
Sphericity ranges from low to high
Packing of grains are loose
Rock is mainly grain supported
Grain contacts are along the length of the grains with minor suturing

Name: Subarkose (Sandstone)

Comments: Overall porosity of the thin section is very good with many interconnected pores seen in Figures AD-1 and AD-2.

FIGURES AD. Sample: C 2:9 Depth: 2842.96m

Figure AD-1- PPL

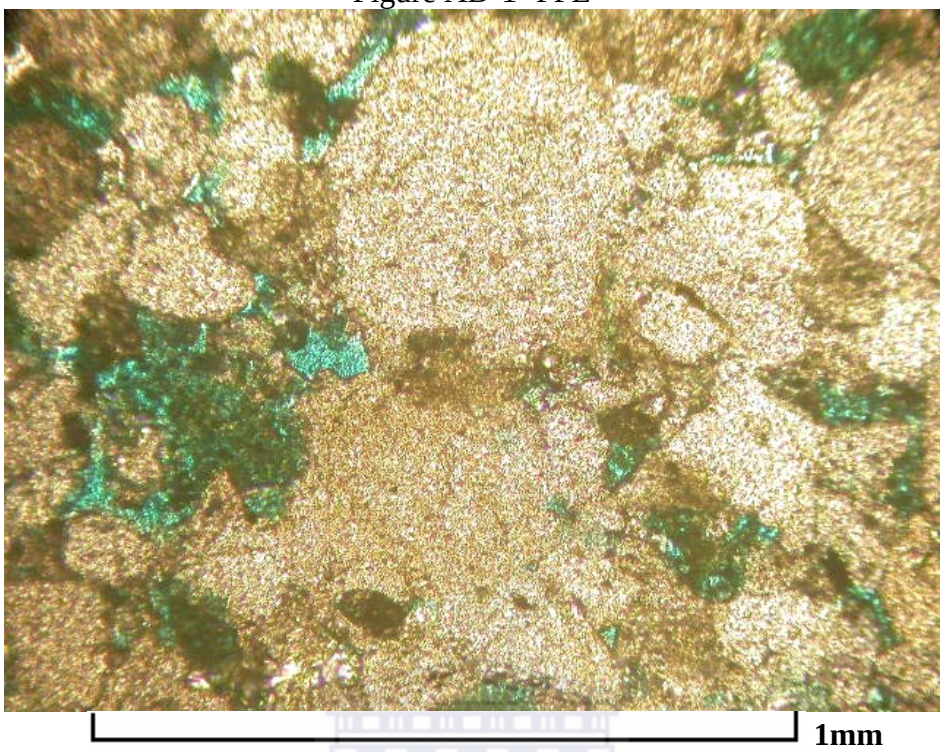

Scale (Magnification x10)

Figure AD-2- XPL

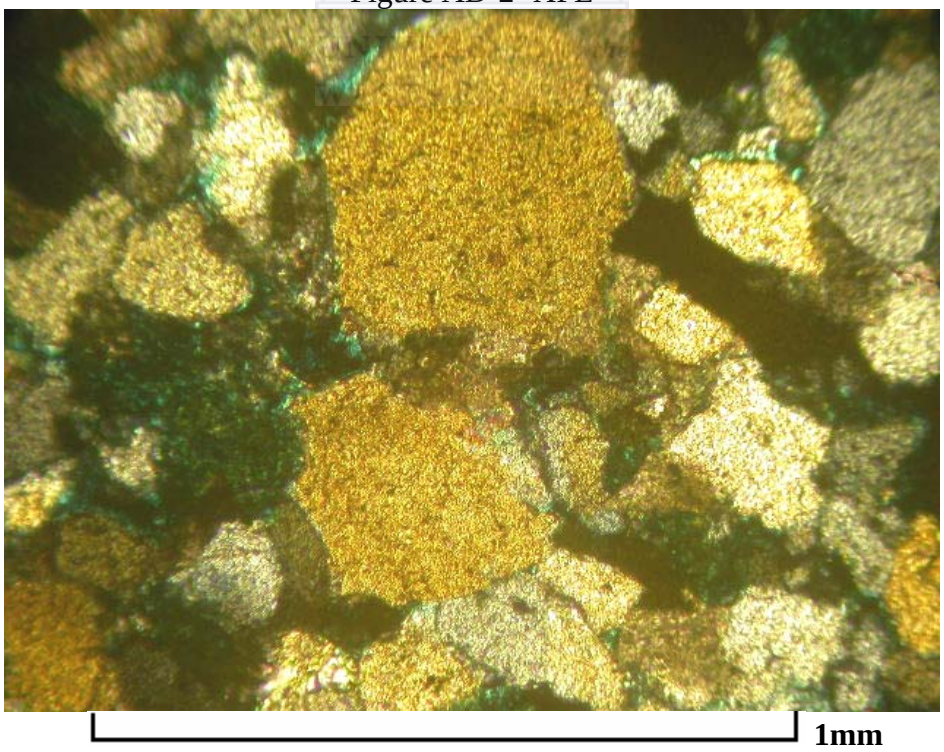

Scale (Magnification x10)

Sample: C 2:10 **Depth: 2867.00m**

Composition: ***Framework minerals:***	***Percentages***
Quartz	65%
Feldspar	15%
Lithic fragments	10%
Glauconite	3%

Quartz: Monocrystalline and polycrystalline
Planar and undulose extinctions
Vacuoles and needle inclusions visible in the grains (on higher magnification)

Feldspar: Grains are cracked
Partial dissolution of grains
No visible twinning

Lithic fragments: Very fine grains in clay matrix

Glauconite: Occur as pellets between grains

Ductile Minerals:	***Percentages***
Clays	3%
Micas	<1%

Clays: Occur as grain coatings and as few pore-filling clays

Micas: Very fine grains in clay matrix

Authigenic Minerals:	***Percentages***
Carbonate cement	3%

Carbonate cement: Found between grains as clasts

***Porosity*:** Average porosity
Average connectivity
Intergranular and intragranular

***Texture*:** Fine grained (0.1mm average) [x4 magnification]
Grains are moderately sorted
Grain shape is sub angular
Sphericity ranges from low to high
Grain packing is moderately tight
Grains are supported mainly by matrix
Grain contacts are long and tangential

Name: Subarkose (Sandstone)

Comments: A fracture in the thin section act as porosity and permeability enhancers but only for that section.

FIGURES AE. Sample: C 2:10 Depth: 2867.00m

Figure AE-1- PPL

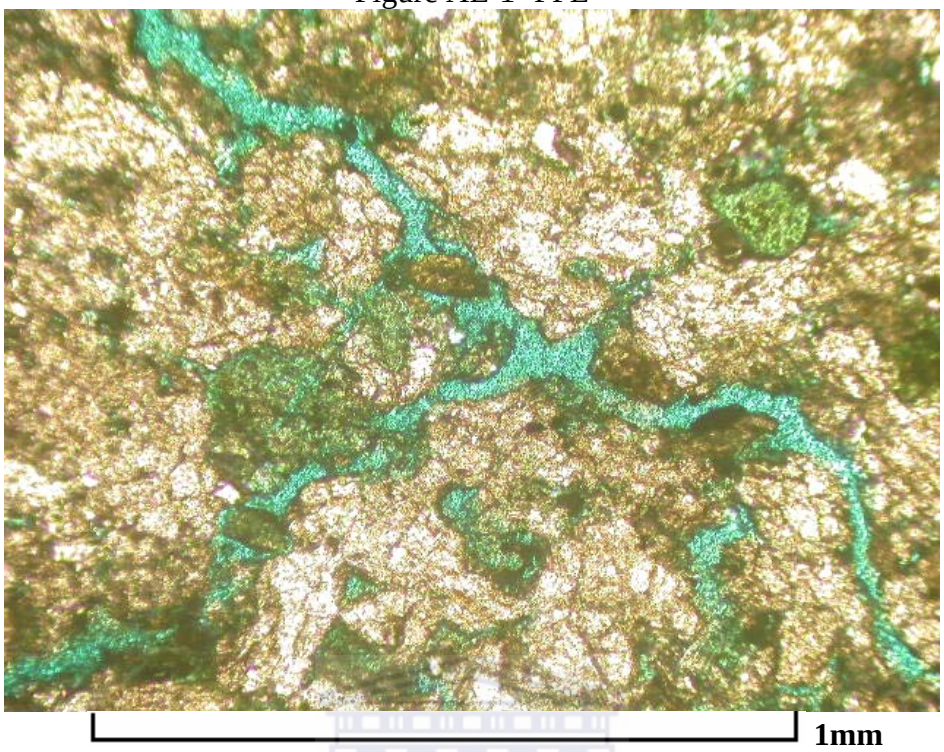

Scale (Magnification x10)

Figure AE-2- XPL

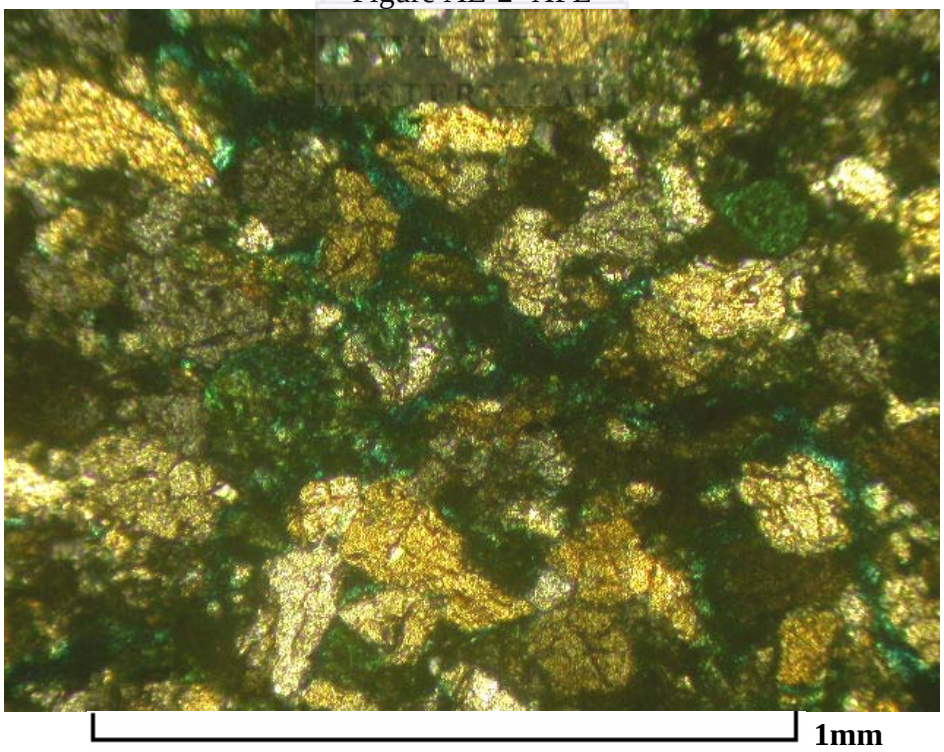

Scale (Magnification x10)

Sample: SWC 1 6 **Depth: 2868.00m**

Composition: Framework minerals:	***Percentages***
Quartz	70%
Feldspar	10%
Lithic fragments	5%
Glauconite	5%

Quartz:	Monocrystalline and polycrystalline Grains are highly compacted Grains are coated by clays Planar and undulose extinctions
Feldspar:	Grains are altered (cracked) Partial dissolution of grains take place
Lithic fragments:	Fine grains in clay matrix
Glauconite:	Occur as pellets between grains

Ductile Minerals:	***Percentages***
Clays	3%

Clays: Clay minerals coat the grains and fill the pores

Authigenic Minerals:	***Percentages***
Quartz cement	3%
Carbonate cement	4%

Quartz cement:	Overgrowths on detrital grains
Carbonate cement:	Carbonate cement between grains Some clasts fill secondary pores

***Porosity*:** Good porosity
Poor connectivity
Most pores are isolated
Main pore type is intergranular
Secondary porosity is poor

***Texture*:** Fine grained (0.5mm average) [x4 magnification]
Section contains moderate to well sorted grains
Grain shape is dominantly sub angular
Sphericity ranges from low to high
Grains are tightly packed
Rock is mostly grain supported
Grain contacts are concavo-convex and sutured

Name: Subarkose to Arenitic (Sandstone)

The following Figures (AF-1 and AF-2) is a general representation of the thin section.

FIGURES AF. Sample: SWC 1 6 Depth: 2868.00m

Figure AF-1- PPL

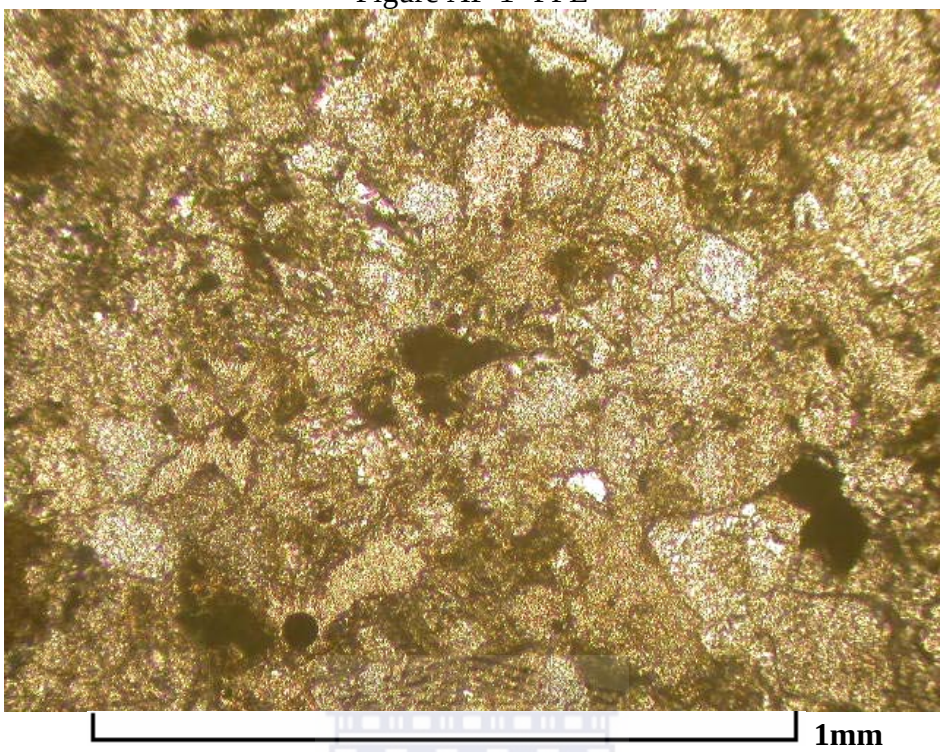

Scale (Magnification x10)

Figure AF-2- XPL

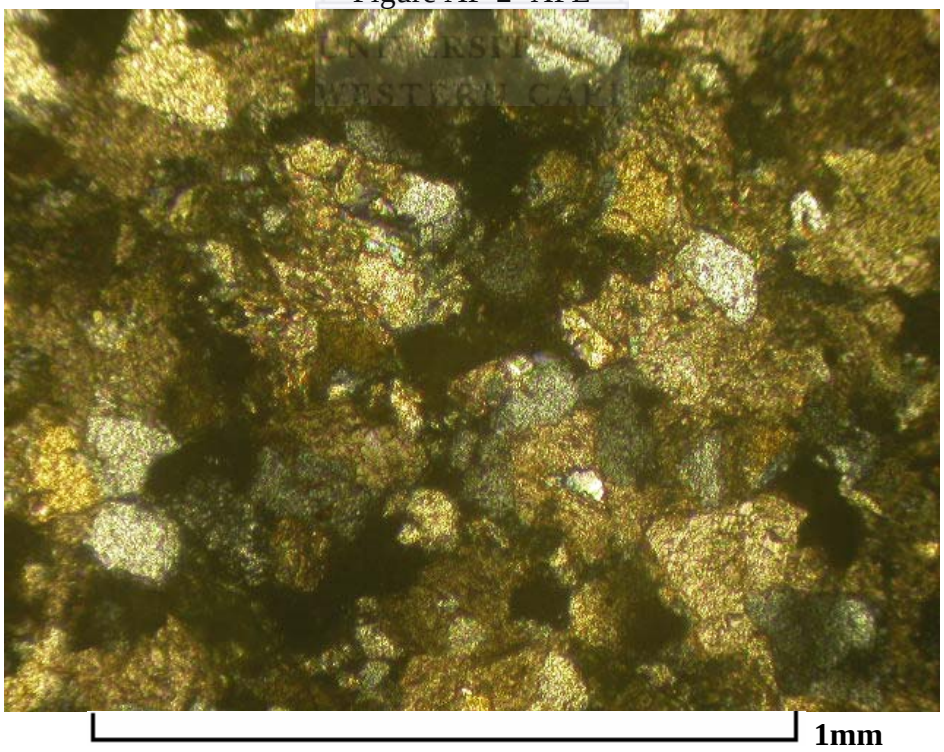

Scale (Magnification x10)

4.2 Summary of Petrographic Analysis

TABLE 1. DATA SUMMARY ON MINERALOGY

WELL	SAMPLE	DEPTH(m)	COMPOSITION Framework	Ductiles	Authegenic Minerals cements	Pressure solution features
E-BA1	SWC 1 40	2412	Qtz, flsp, LF , Glc.	clays	crb & qtz cements	none
E-BA1	SWC 1 39	2413.5	Qtz, flsp, LF , Glc.	clays, micas	crb & qtz cements	none
E-BA1	SWC 1 38	2418.5	Qtz, flsp, LF , Glc.	clays, micas	calc. & qtz cements	none
E-BA1	SWC 1 37	2435	Qtz, flsp, LF , Glc.	clays, micas	crb & qtz cements	stylolites
E-BA1	SWC 1 23	2793	Qtz, flsp, LF , Glc.	clays, micas	minor crb/dol., & qtz cements	Stylolites
E-BA1	SWC 1 21	2808	Qtz, flsp, LF , Glc.	clays, micas	qtz & dol. cement	none
E-BA1	SWC 1 20	2809	Qtz, flsp, LF , Glc.	clays, micas	crb & qtz cements	none
E-BA1	SWC 1 19	2810	Qtz, flsp, LF , Glc.	clays, micas	qtz cement	none
E-BA1	SWC 1 17	2814	Qtz, flsp, LF , Glc.	clays, micas	qtz and crb cements	none
E-BA1	SWC 1 15	2818	Qtz, flsp, LF , Glc.	clays, micas	qtz cement	traces
E-BA1	SWC 1 14	2820	Qtz, flsp, LF , Glc.	clays	qtz cement	traces
E-BA1	SWC 1 13	2822	Qtz, flsp, LF , Glc.	clays	crb & qtz cements	stylolites
E-BA1	SWC 1 12	2823	Qtz, flsp, LF , Glc.	clays	qtz cement	stylolites
E-BA1	SWC 1 9	2827.5	Qtz, flsp, LF , Glc.	clays, micas	qtz & crb/cal. Cements	none
E-BA1	C1:1	2828	Qtz, flsp, LF , Glc.	clays, micas	qtz & crb/dol. cements	none
E-BA1	C1:2	2828.64	Qtz, flsp, LF , Glc.	clays, micas	qtz and clays	stylolites
E-BA1	C1:3	2829.67	Qtz, flsp, LF , Glc.	clays, micas	qtz & crb cements	none
E-BA1	C1:4	2831.95	Qtz, flsp, LF , Glc.	clays	qtz & crb Cements	stylolites
E-BA1	C1:5	2832.87	Qtz, flsp, LF , Glc.	clays, micas	qtz & crb cements	none
E-BA1	C1:6	2833.89	Qtz, flsp, LF , Glc.	clays, micas	crb & qtz cements	none
E-BA1	C1:7	2834.08	Qtz, flsp, LF , Glc.	clays, micas	qtz & crb cements	none
E-BA1	C2:1	2835.05	Qtz, flsp, LF , Glc.	clays, micas	qtz & crb cements	none
E-BA1	C2:2	2835.96	Qtz, flsp, LF , Glc.	clays, micas	qtz & crb cements	none
E-BA1	C2:3	2836.95	Qtz, flsp, LF , Glc.	clays, micas	qtz & crb cements	stylolites
E-BA1	C2:4	2837.95	Qtz, flsp, LF , Glc.	clays	qtz & crb cements	stylolites, pyrite
E-BA1	C2:5	2839	Qtz, flsp, LF , Glc.	clays, micas	qtz, silica & crb cements	none
E-BA1	C2:6	2840	Qtz, flsp, LF , Glc.	clays, micas	qtz & crb cements	none
E-BA1	C2:7	2841.03	Qtz, flsp, LF , Glc.	clays, micas	qtz & crb cements	none
E-BA1	C2:8	2842.05	Qtz, flsp, LF , Glc.	clays, micas	qtz & crb cements	none
E-BA1	C2:9	2842.96	Qtz, flsp, LF , Glc.	clays, micas	qtz & crb cements	none
E-BA1	C2:10	2867	Qtz, flsp, LF , Glc.	clays	crb & clays	none
E-BA1	SWC 1 6	2868	Qtz, flsp, LF , Glc.	clays	qtz & crb cements	none

TABLE 2. TEXTURAL DATA SUMMARY

WELL	SAMPLE	DEPTH(m)	TEXTURE			
			GRAIN SIZE	SORTING (w/m/p)	GRAIN SHAPE	SPERICITY
E-BA1	SWC 1 40	2412	fg- 0.1mm ave.	moderate	angular	low
E-BA1	SWC 1 39	2413.5	fg- 0.5mm ave.	moderate	subangular	low
E-BA1	SWC 1 38	2418.5	fg- 0.5mm ave.	mod.to well	subangular	low
E-BA1	SWC 1 37	2435	fg- 0.5mm ave.	moderate	subangular	low
E-BA1	SWC 1 23	2793	vfg- <0.1mm av.	moderate	subangular	low
E-BA1	SWC 1 21	2808	fg- 0.5mm ave.	poor	angular to subangular	low
E-BA1	SWC 1 20	2809	fg - med.- 0.8mm	mod. to poor	angular to subangular	low
E-BA1	SWC 1 19	2810	fg - med.- 0.8mm	mod. to poor	angular to subangular	low
E-BA1	SWC 1 17	2814	fg- 0.5mm ave.	modrate	subangular	low
E-BA1	SWC 1 15	2818	fg to med.- 0.8av.	poor to moderate	subangular	low
E-BA1	SWC 1 14	2820	fg- 0.5mm ave.	moderate	subangular	low
E-BA1	SWC 1 13	2822	fg- 0.5mm ave.	moderate	subangular	low
E-BA1	SWC 1 12	2823	fg- 0.3mm ave.	moderate	angular to subangular	low
E-BA1	SWC 1 9	2827.5	fg- 0.3mm ave.	mod.to well	subangular	very low
E-BA1	C1:1	2828	fg- 0.5mm ave.	poor	subangular- subrounded	med
E-BA1	C1:2	2828.64	vfg- 0.05mm ave.	moderate	subangular- subrounded	med
E-BA1	C1:3	2829.67	vfg- 0.05mm ave.	moderate	angular to subangular	very low
E-BA1	C1:4	2831.95	fg - med.- 0.8mm	moderate	angular to subangular	low
E-BA1	C1:5	2832.87	fg- 0.5mm ave.	mod. to poor	subangular- subrounded	low - high
E-BA1	C1:6	2833.89	fg- 0.5mm ave.	poor	angular to subangular	low
E-BA1	C1:7	2834.08	fg- 0.5mm ave.	poor	angular	low - high
E-BA1	C2:1	2835.05	fg- 0.5mm ave.	poor	subangular	low - high
E-BA1	C2:2	2835.96	fg- 0.5mm ave.	moderate	angular to subangular	low - high
E-BA1	C2:3	2836.95	fg- 0.5mm ave.	poor	angular to subangular	low - high
E-BA1	C2:4	2837.95	fg- 0.5mm ave.	moderate	subangular	low - high
E-BA1	C2:5	2839	fg- 0.5mm ave.	moderate	angular	low - high
E-BA1	C2:6	2840	fg- 0.5mm ave.	moderate	angular	low - high
E-BA1	C2:7	2841.03	fg- 0.5mm ave.	mod. to well	subangular- subrounded	low
E-BA1	C2:8	2842.05	fg- 0.5mm ave.	moderate	angular to subangular	low
E-BA1	C2:9	2842.96	fg- 0.5mm ave.	moderate	angular to subangular	low - high
E-BA1	C2:10	2867	fg- 0.1mm ave.	moderate	subangular	low - high
E-BA1	SWC 1 6	2868	fg- 0.5mm ave.	mod. to well	subangular	low - high

TABLE 3. DATA SUMMARY ON FLUID FLOW ABILITY

WELL	SAMPLE	DEPTH(m)	COMPACTION PACKING	SUPPORT	GRAIN CONTACTS	POROSITY	CONNECTIVITY	OTHER FEATURES
E-BA1	SWC 1 40	2412	moderately tight	matrix & grain	long, tang., sutured	average	poor	
E-BA1	SWC 1 39	2413.5	moderately tight	matrix & grain	long, tang., sutured	good	poor	
E-BA1	SWC 1 38	2418.5	moderately tight	matrix	long	average	poor	
E-BA1	SWC 1 37	2435	moderately tight	matrix	long	poor	poor	
E-BA1	SWC 1 23	2793	tight	matrix	sutured	poor	poor	
E-BA1	SWC 1 21	2808	tight	matrix & grain	long and sutured	poor	poor	
E-BA1	SWC 1 20	2809	tight	matrix & grain	long and sutured	ave. - poor	ave. - poor	
E-BA1	SWC 1 19	2810	tight	matrix	long and sutured	good	good	
E-BA1	SWC 1 17	2814	moderate	grain	long and sutured	good	good	
E-BA1	SWC 1 15	2818	moderately tight	grain to grain	long	average	average	
E-BA1	SWC 1 14	2820	moderate	matrix	long	average	average	
E-BA1	SWC 1 13	2822	loose	grain	long, concavo-concex	good	good	
E-BA1	SWC 1 12	2823	fairly tight	grain	long, concavo-concex	good	good	
E-BA1	SWC 1 9	2827.5	fairly tight	grain	long, concavo-concex	good	good	Fractured
E-BA1	C1:1	2828	uneven	matrix	tang., concavo-convex	excellent	excellent	Fractured
E-BA1	C1:2	2828.64	very tight	matrix & grain	sutured	average	poor	Laminations
E-BA1	C1:3	2829.67	tight	matrix & grain	long	average	poor	Granulation Seam
E-BA1	C1:4	2831.95	fairly tight	grain	long, tang.	average	good	
E-BA1	C1:5	2832.87	tight	grain	sutured	v. good	excellent	
E-BA1	C1:6	2833.89	tight	grain & cem.	sutured and conc-conv.	average	poor	
E-BA1	C1:7	2834.08	moderate	grain	long, tang. & sutured	good	average- poor	
E-BA1	C2:1	2835.05	moderate	matrix	tang. & sutured	good	good	Granulation Seam
E-BA1	C2:2	2835.96	moderate	matrix & grain	conc.-convex, sutured	good	good	
E-BA1	C2:3	2836.95	mod. to well	matrix & grain	long & tang.	good	average	
E-BA1	C2:4	2837.95	moderate	matrix & grain	long & sutured	good	good	
E-BA1	C2:5	2839	tight	matrix & grain	long & sutured	good	average	Granulation Seam
E-BA1	C2:6	2840	moderate	matrix & grain	long & sutured	good	good	
E-BA1	C2:7	2841.03	moderate	matrix & grain	long & sutured	ave. - good	good	
E-BA1	C2:8	2842.05	loose	matrix & grain	long & sutured	good	good	
E-BA1	C2:9	2842.96	loose	grain	long, minor sutured	excellent	good	
E-BA1	C2:10	2867	moderate	matrix	long & tang.	average	average	Fractured
E-BA1	SWC 1 6	2868	tight	grain	conc.-convex, sutured	good	poor	

4.3 X-ray Diffractometry Analyses

SAMPLE 1.1 2828.00m

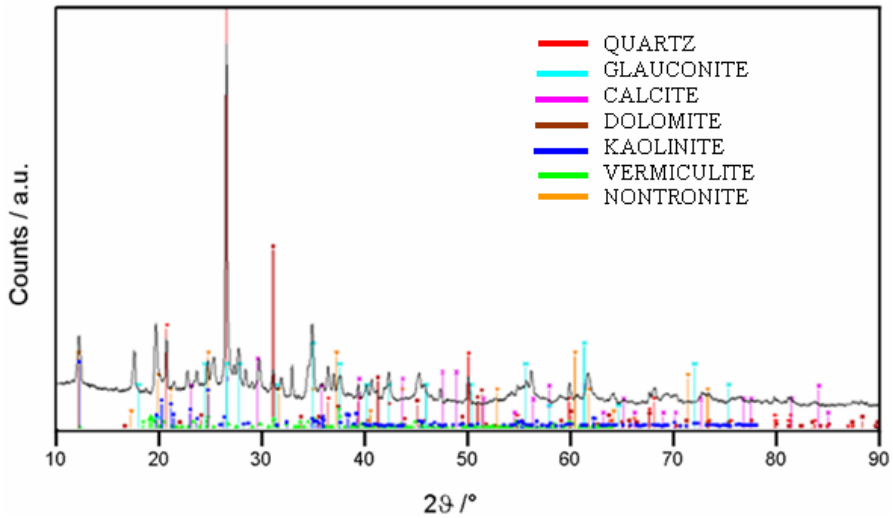

Sample 1 is characterized by quartz, and glauconite which form part of framework minerals within the sandstone. Calcite, dolomite are authigenic cements and kaolinite, vermiculite and nontrinite (smectite variety) are clays both detrital and authegenic.

SAMPLE 1.2 2833.89m

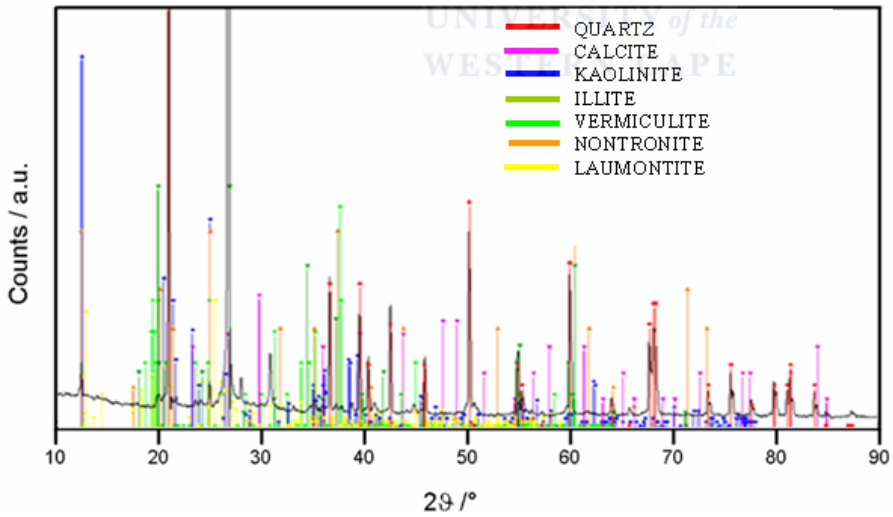

Sample 1.2 is characterized by framework quartz with a calcite component (cement). Illite, kaolinite, vermiculite and nontronite clays are present. Laumontite is present in this sample zeolite.

SAMPLE 1.3 2834.08m

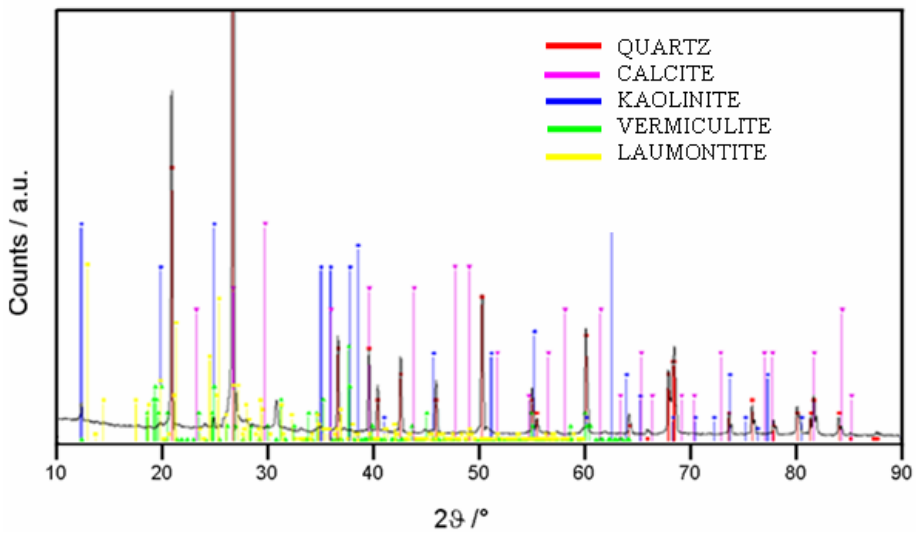

Sample 1.3 contains quartz, calcite, laumontite with kaolinite, vermiculite clays.

SAMPLE 1.4 2835.05m

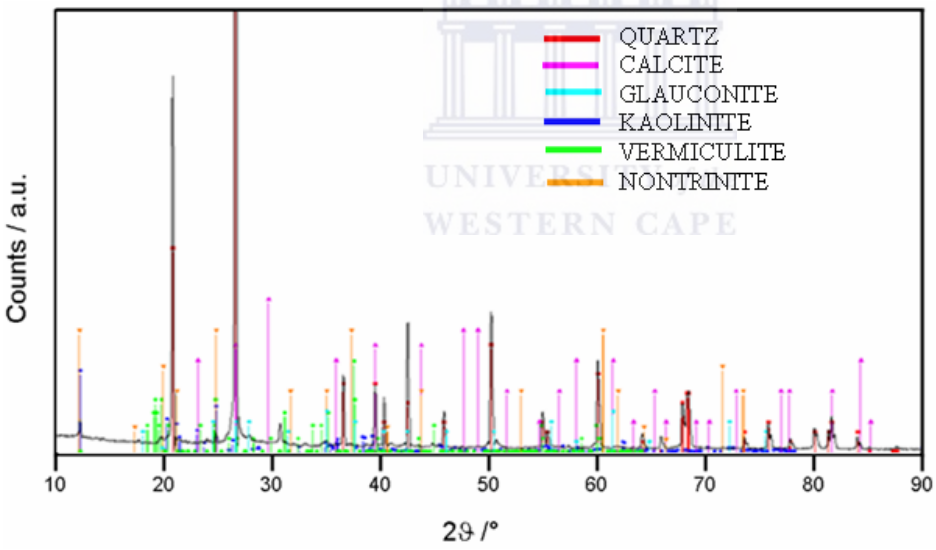

Sample 1.4 represents quartz and glauconite of framework minerals, calcite and kaolinite, vermiculite and nontronite clays.

SAMPLE 1.5 2836.95m

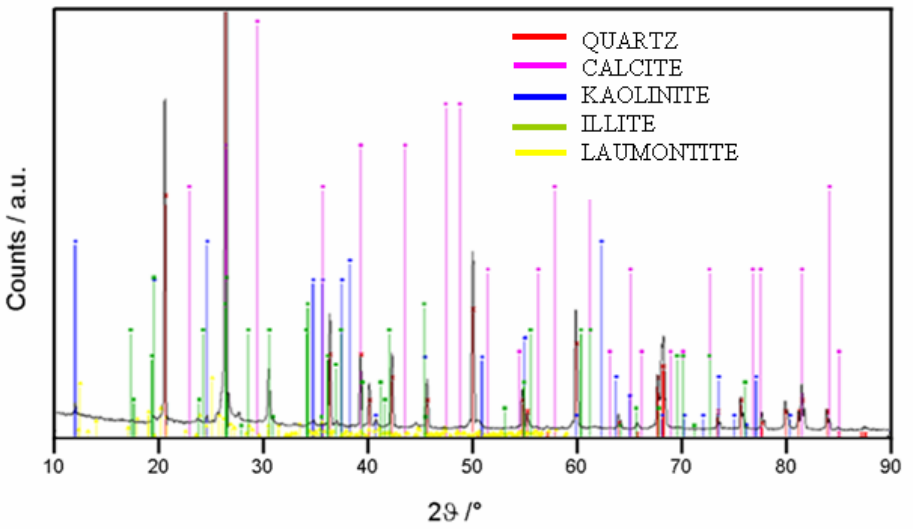

Sample 1.5 is characterized by quarts framework, calcite cement, laumontite and kaolinite and illite clays.

SAMPLE 1.6 2837.95m

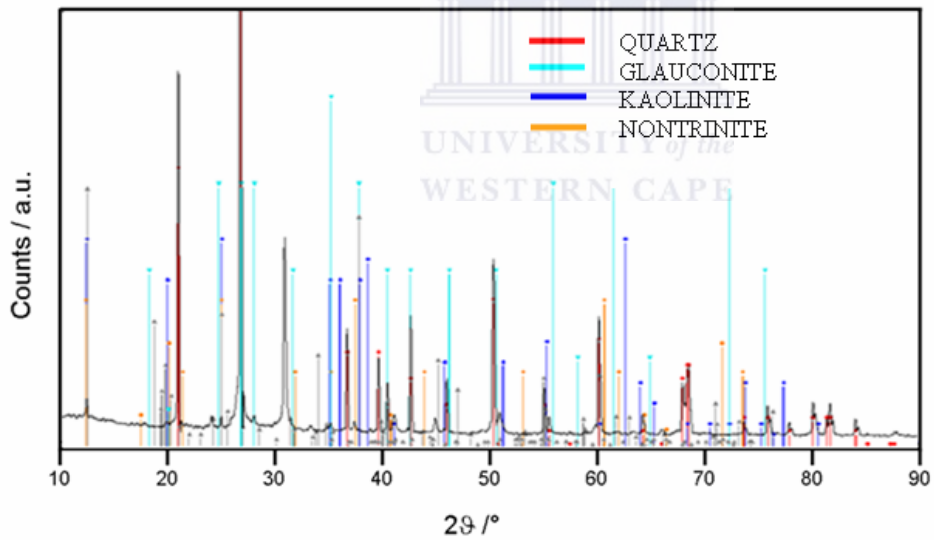

Sample 1.6 contains quartz and glauconite as framework minerals with kaolinite and nontronite clays.

SAMPLE 1.7 2842.05m

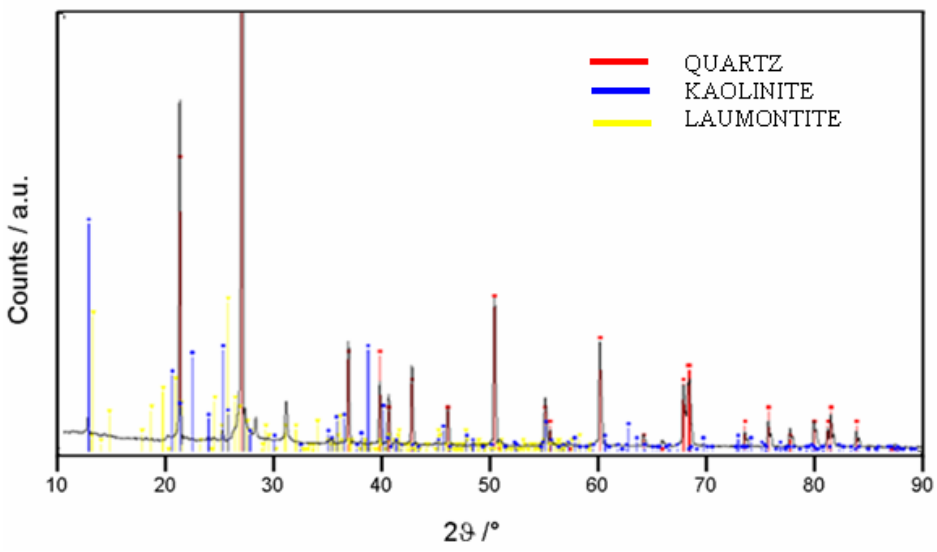

In sample 1.7 only quartz, kaolinite and laumontite were detected.

SAMPLE 1.8 2842.96m

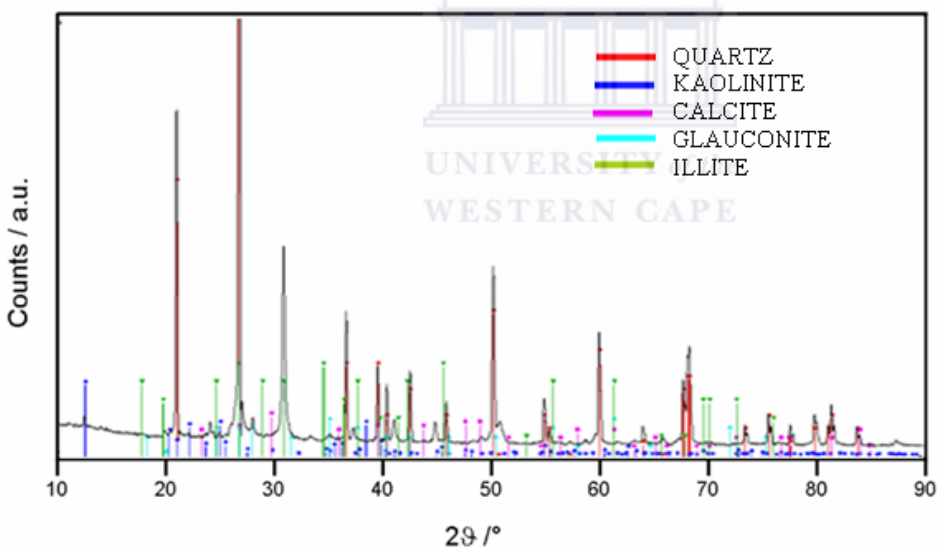

Sample 1.8 contains quarts, glauconite, calcite, kaolinite and illite clays.

4.4 Scanning Electron Microscopy Analyses

SAMPLE 2.1 Depth 2833.93m

(a)

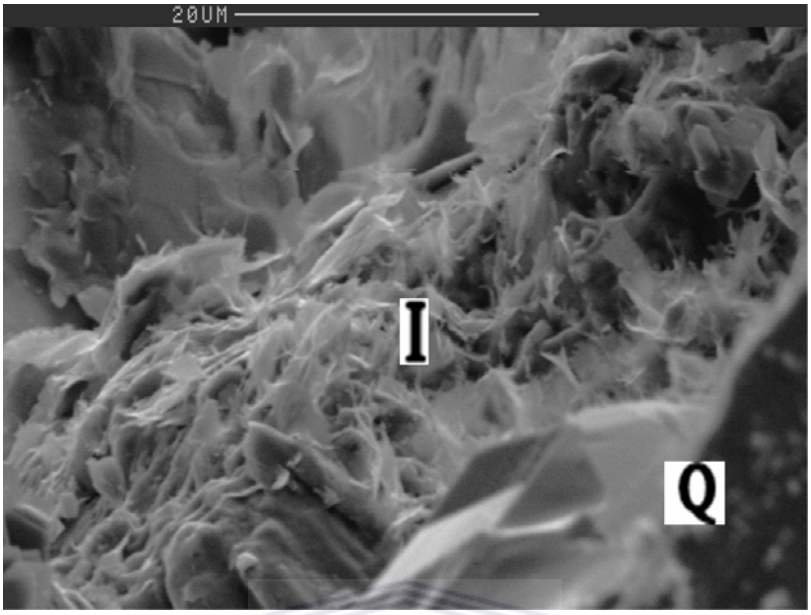

(b)

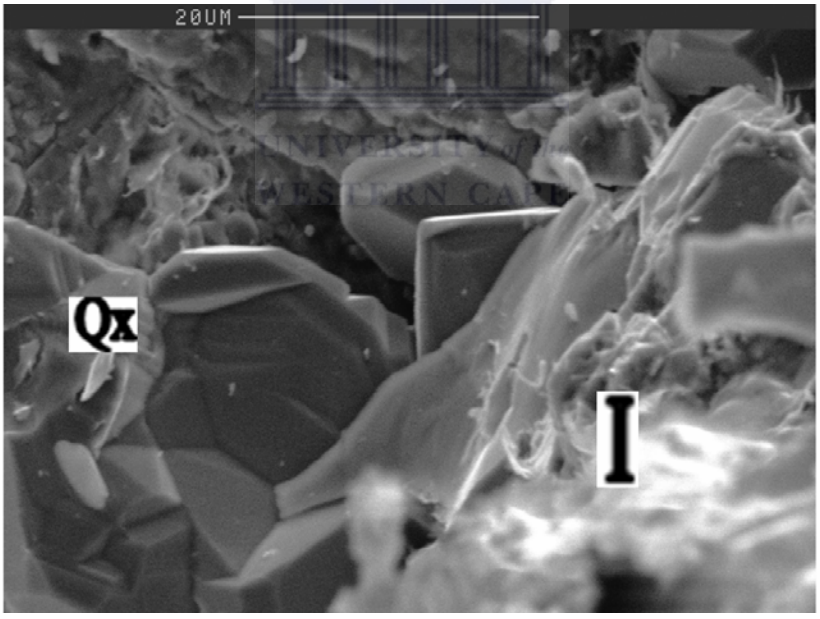

Sample 2.1. (a)Quartz grains (Q) and illite (I) fibers coating the grains. (b) Quartz cement (Qx) is present with grain coating illite (I) clays.

SAMPLE 2.2 Depth 2833.89m

(a)

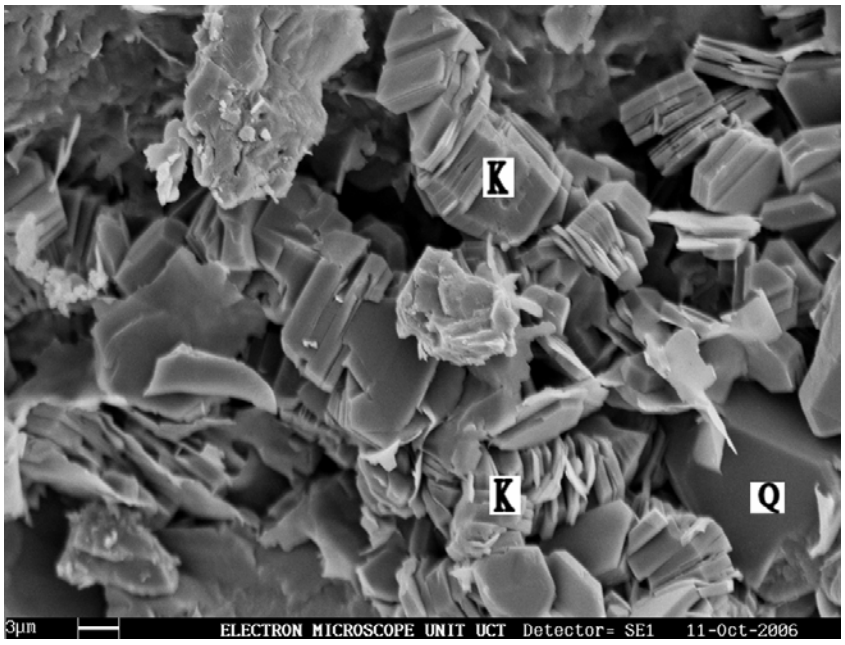

(b)

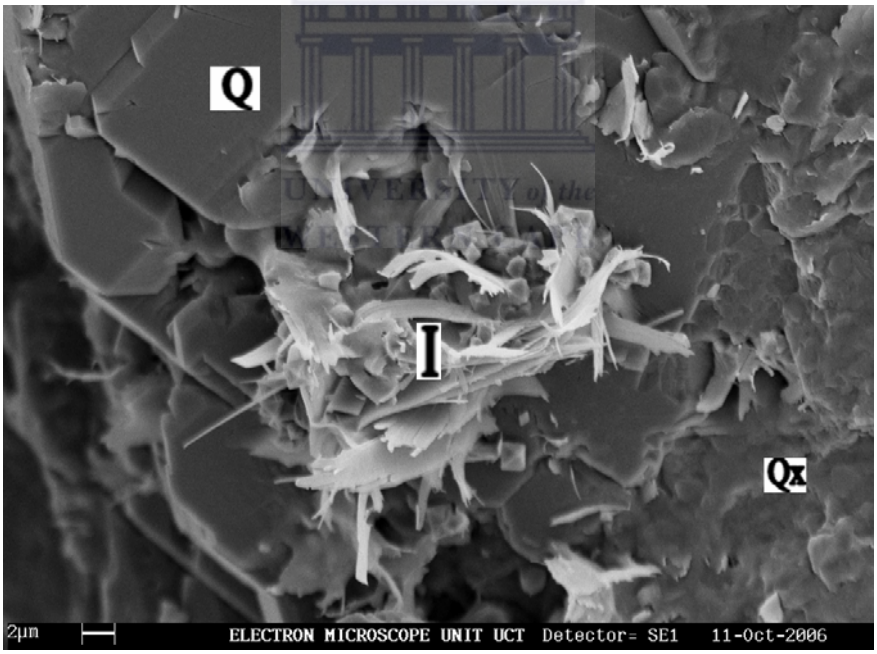

Sample 2.2. (a) Quartz occurs as detrital (Q) grains with kaolinite (K) filling the pores. (b) Quartz (Q) and Quartz overgrowths (Qx) occur with grain coating fibrous illite (I).

SAMPLE 2.3 Depth 2834.05m

(a)

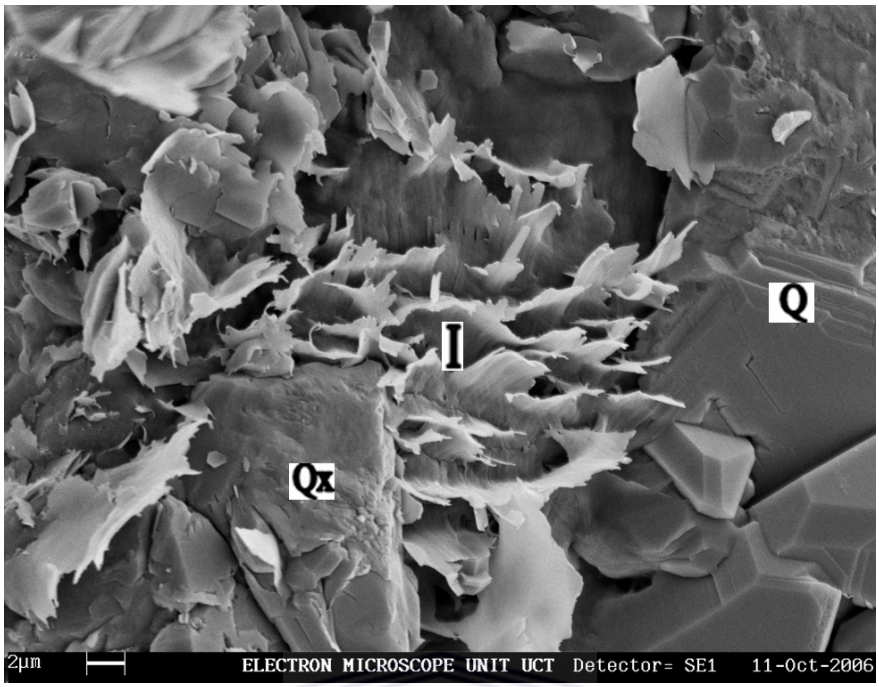

(b)

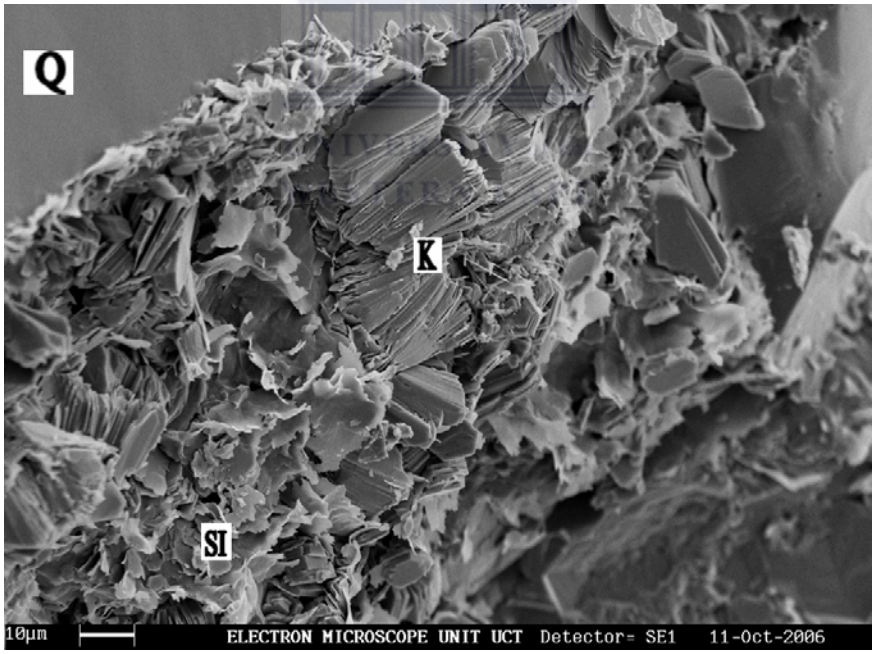

Sample 2.3. (a) Quartz (Q) grains and fibrous illites (I) and quartz overgrowths (Qx). (b) Quartz grains (Q) coated with Smectite-illite (SI) mixed layer clays with kaolinite (K) filling voids.

SAMPLE 2.4 Depth 2835.96m

(a)

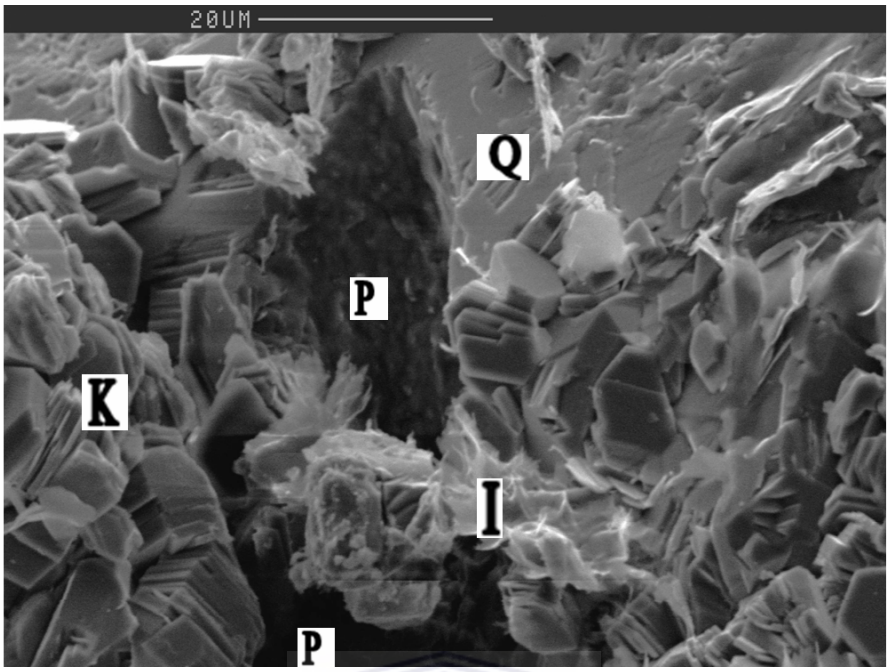

(b)

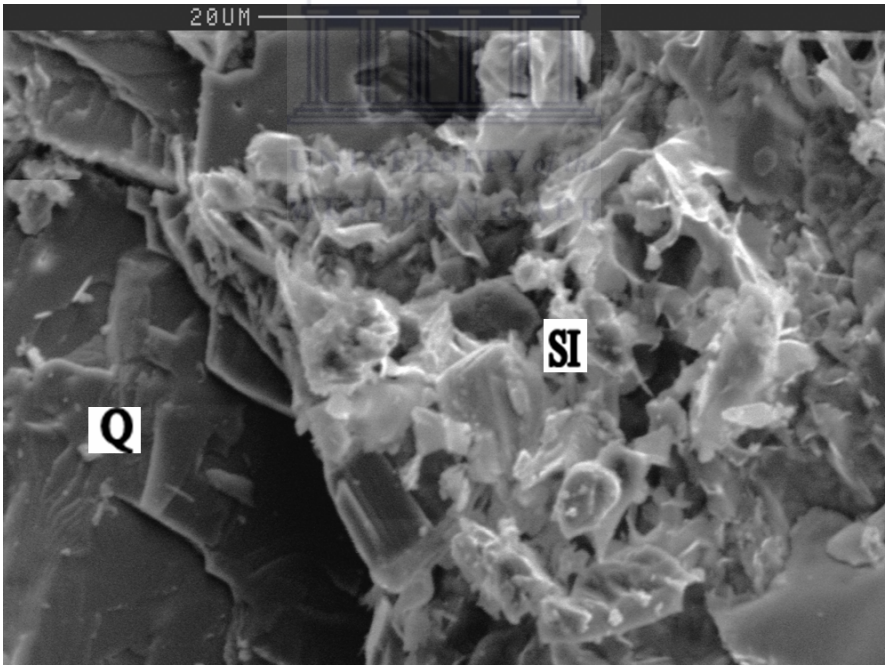

Sample 2.4. (a) Quartz (Q) grains with kaolinite (K) filling the pores (P). Illite (I) can be found blocking a pore throat. (b) quartz grains (Q) with smectite-illite (SI) mixed layer coatings.

SAMPLE 2.5 Depth 2837.94m

(a)

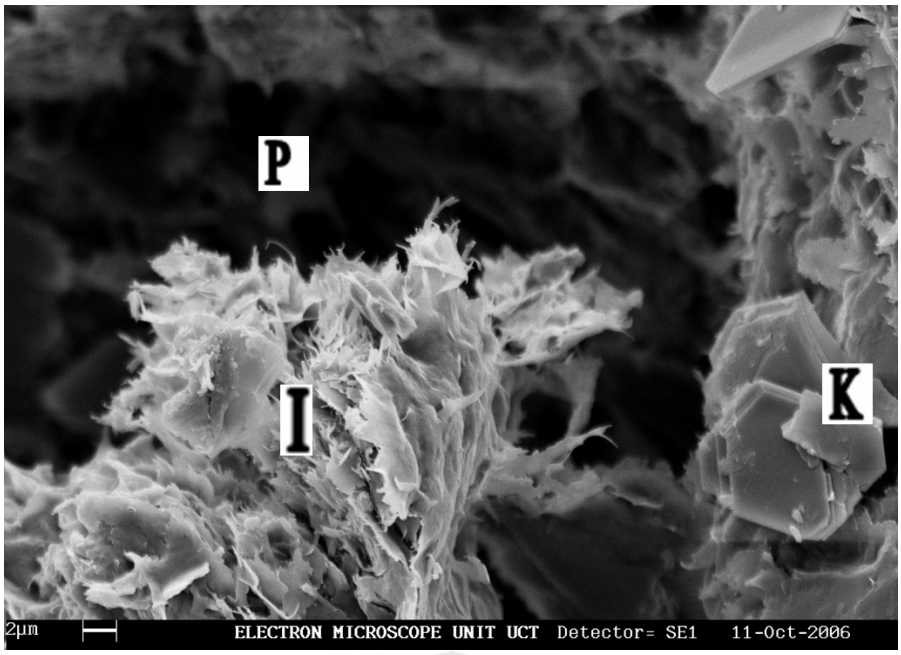

(b)

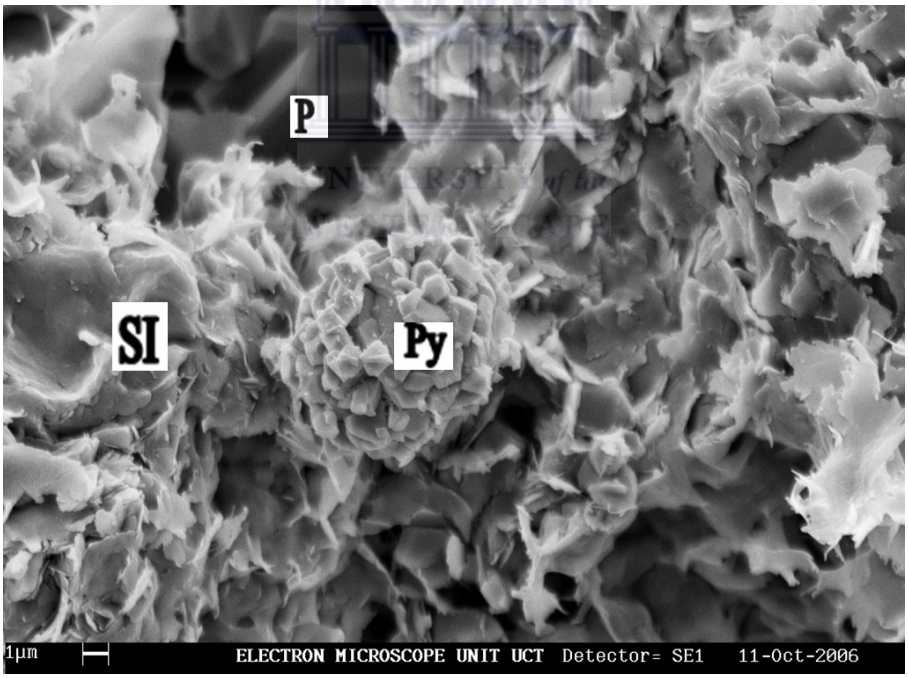

Sample 2.5. (a) Illite (I) and kaolinite (K) fills a pore (P). (b) Smectite-illite (SI) mixed layer clays fills the pore (P) with trace pyrite (Py) precipitated in the pore.

SAMPLE 2.6 Depth 2838.82m

(a)

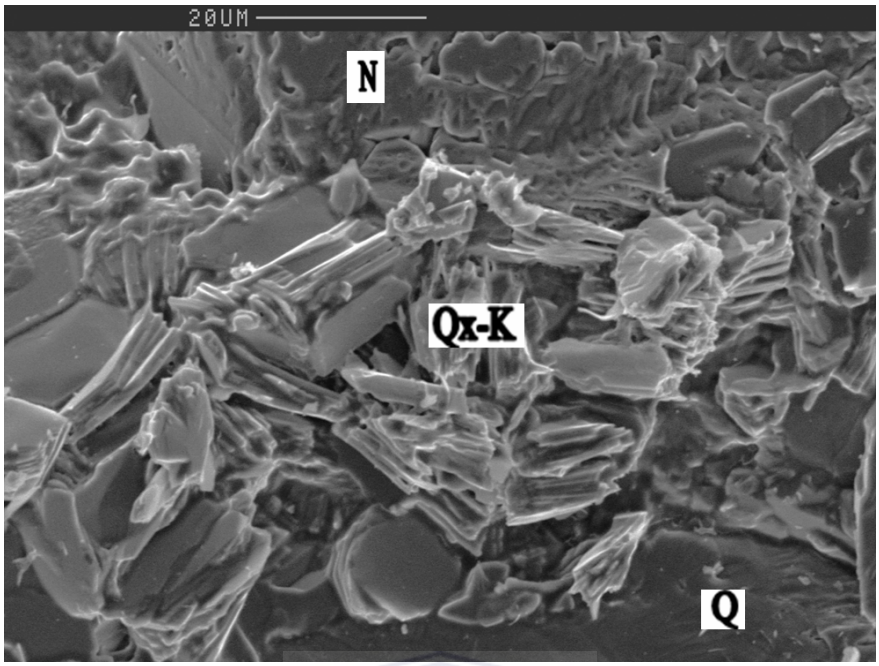

(b)

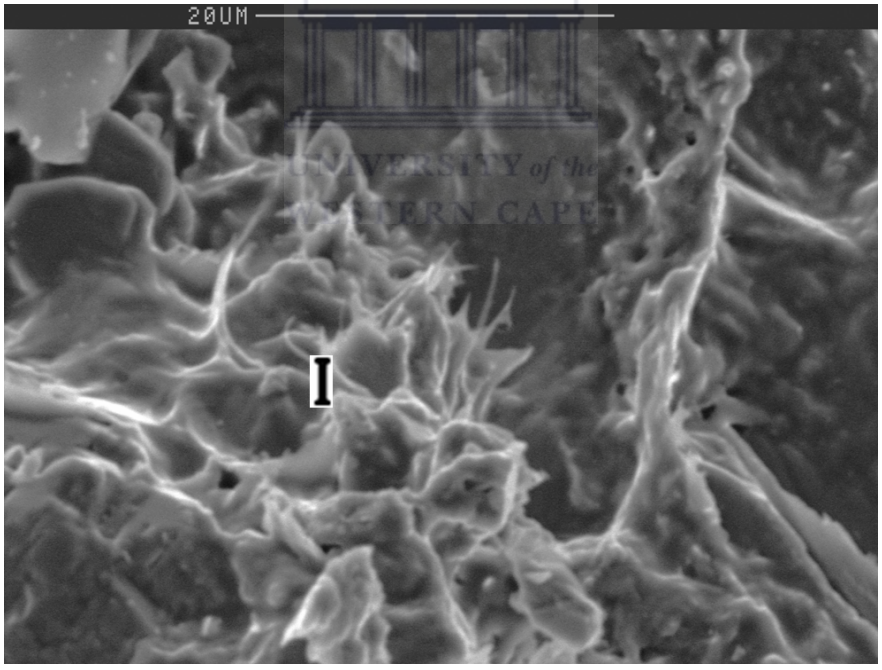

Sample 2.6 (a) Quartz (Q) grains are present with quartz cement (Qx) and kaolinite (K) occurring together along grain contacts. (b) Illite (I) fibers are prominent which coats the grains.

SAMPLE 2.7 Depth 2840.55m

(a)

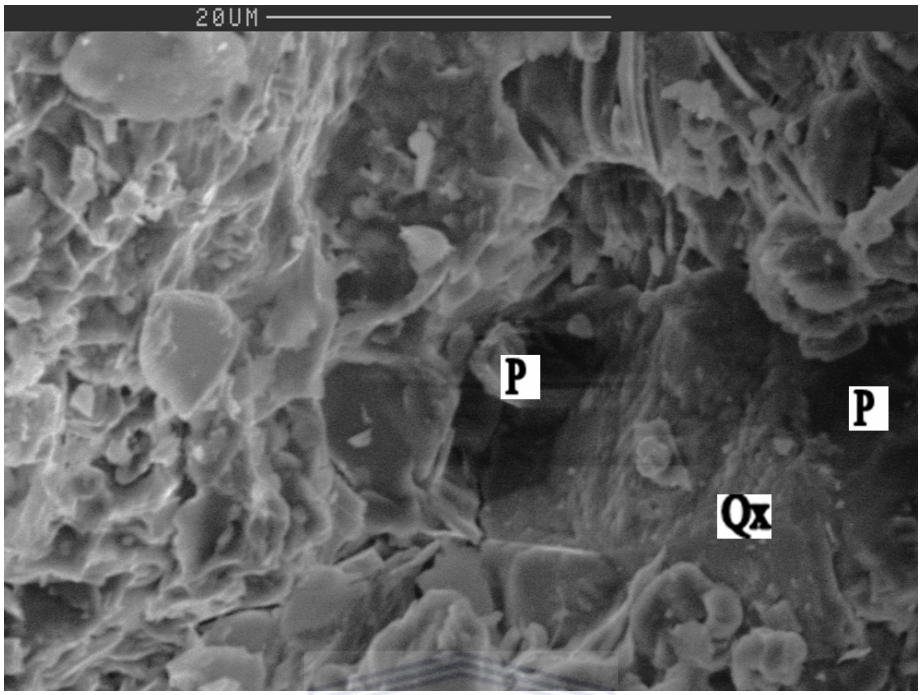

(b)

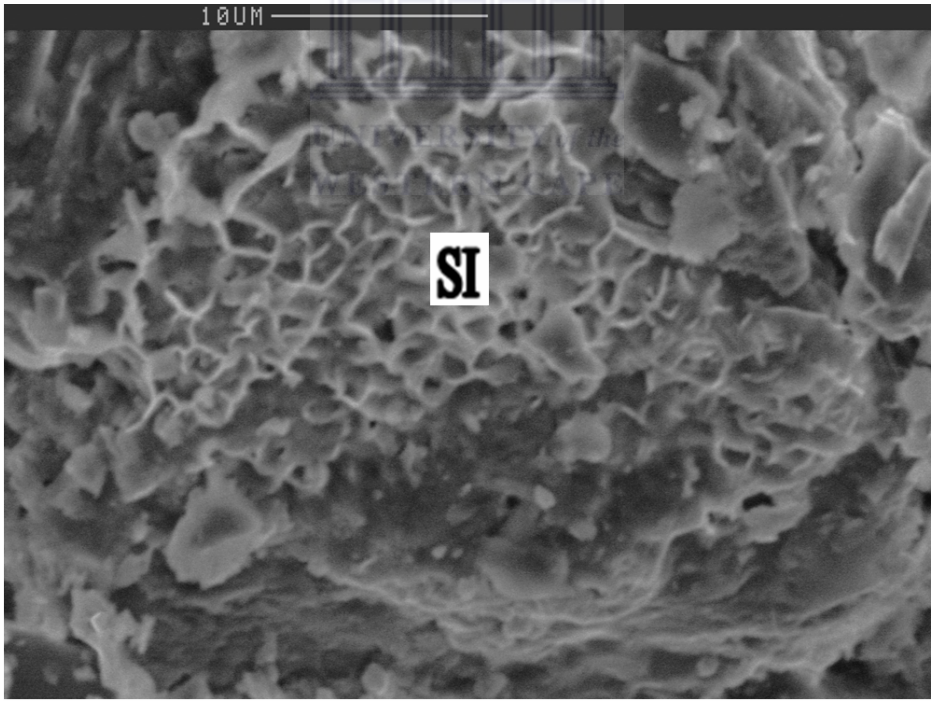

Sample 2.7. (a) Quartz cement (Qx) clearly fill the pores (P). (b) Smectite-illite (SI) mixed layer clays occur as grain coatings

SAMPLE 2.8 Depth 2842.95m

(a)

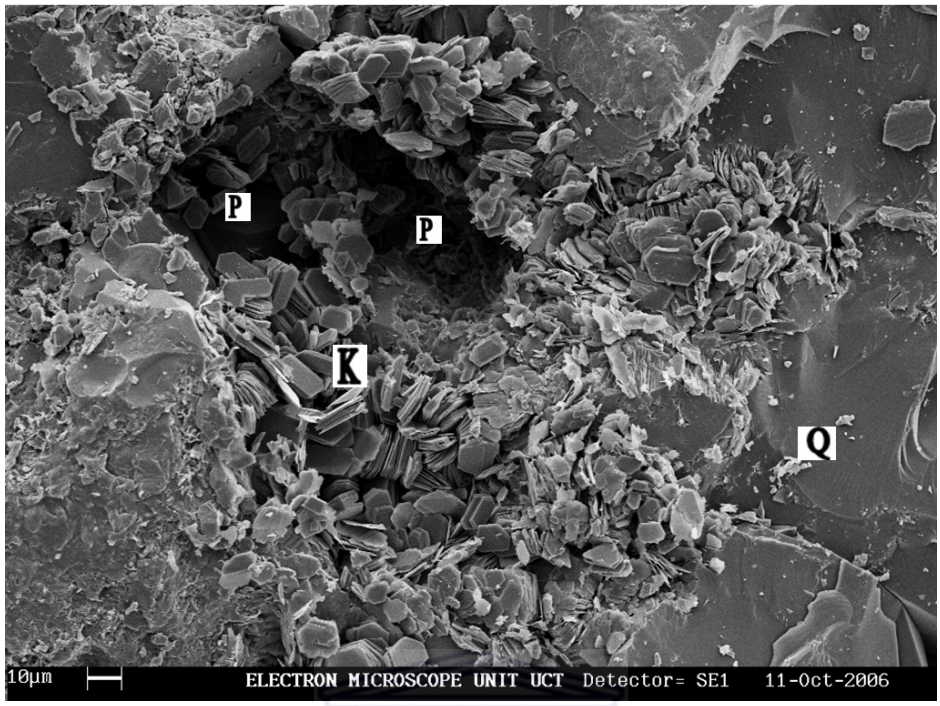

(b)

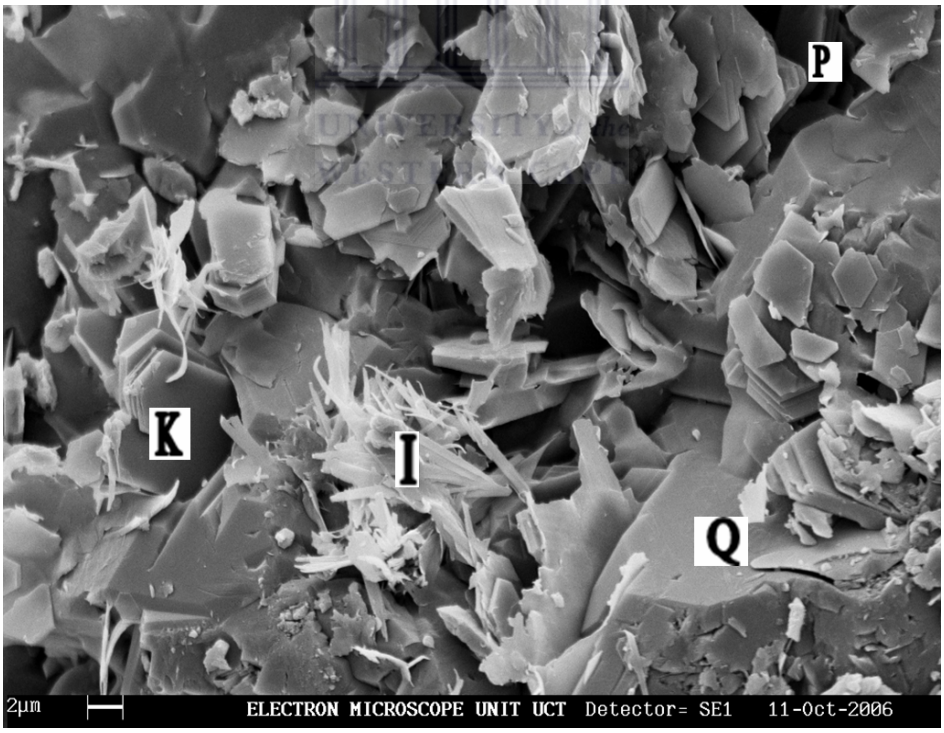

Sample 2.8. (a) Quartz (Q) occur as detrital grains with kaolinite (K) coating it. Kaolinite fills pores (P) and clogs the pore throats. (b) Quartz (Q) is detrital and is coated by illite fibres (I) and kaolinite booklets (k).

4.5 Discussion

4.5.1 Interpretation of the analyses

Quartz and feldspar grains are fractured which is evidence of mechanical compaction. Stylolites and sutured contacts are evidence of chemical compaction causing pressure dissolution. Suturing is mainly intergranular with jagged and concavo-convex contacts. Compaction and cementation is the main cause of reduced porosity in the sandstones. Secondary porosity is mainly formed by the dissolution of feldspars and carbonates forming vugs within the sandstones. Feldspar dissolution is often coupled with kaolinite precipitation perhaps caused by meteoric flushing.

Quartz overgrowths formed after burial and compaction, which is shown by intergrown relationships of quartz crystals and fibrous illite. Sources of silica for quartz overgrowths may have come from several sources, viz. pressure dissolution of detrital quartz grains, the alteration of feldspars, illitization of detrital and authigenic kaolinite and smectite, and the entering of hot fluids by magmatism from hotspots as in the paper by Lima and De Ros (2002).
The expulsion of water from the Southern Outeniqua into the Bredasdorp Basin could have released Si-K-Al.

4.5.2. Diagenetic History

Diagenesis of this sandstone was divided into early middle and late diagenetic stages.

Eodiagenesis:
This stage involves the processes after the deposition of sediments and early cementation. Sedimentation of detrital grains (quartz, feldspar, lithic fragments, clay, mica and glauconite) occurred. Minor compaction occurred as more sediment was being deposited. Thus water started migrating out of the rock (dewatering). The circulating fluids precipitated cementing material such as clays and carbonate

cements between the grains these cements aided in lithifying the rock [McConnell, 1998]. This was observed in the thin sections by matrix forming clays and carbonate cements between grains.

The result of this water movement caused detrital grains (feldspar) [McIlreath and Morrow, 1990] to dissolve. Dissolution of orthoclase feldspar usually occurs between depths of 1.5 to 4.5 km [Wilkinson et al. 2001]. K-feldspar dissolution is usually coupled with the precipitation of kaolinite. The initial compaction and cementation phases forced grains closer together.

Mesodiagenesis:

Increased compaction, due to loading, caused detrital clays and micas to bend between the grains, and grain contacts became sutured due to partial dissolution of pressure solution. Grain-rimming clays are observed in the thin sections which were precipitated onto grains from solution. Pressure by increased burial caused fluids to accumulate in pore spaces. These pore fluids act on grains and start to dissolve the grains. This process causes pressure dissolution [Kearey, 1996]. Fluid in the grain is diffused out of the grain and leaves behind a residue which forms a rim around the grains. The residue is the re-deposition of cement [Kearey, 1996]. This was observed in the thin sections mostly on quartz grains as it is more resistant than feldspar, which is more likely to dissolve with the pressures applied.

Minerals which were precipitated out of solution (rock fluid) are mostly authigenic pore-filling clays (kaolinite, chlorite vermiculite), grain-coating clays (illite, smectite-illite mixed layers, nontronite) and minor calcite and carbonate cements. The pore-filling clays were precipitated into secondary pore structures which may have been formed by dissolution of feldspars. These clays and other cements formed at this stage thus reducing secondary porosity.

Telodiagenesis:

The uplift of the basin caused a decrease in pressure and temperature and this resulted in micro-fracturing and the development of granulation seams for accommodation [Kearey, 1996]. Fracturing increases porosity and permeability and generates migration pathways which facilitates fluid flow in rocks. It also caused activity inside the fracture pore area by dolomite replacement cement. The dolomite cement began replacing carbonate cement which formed before fracturing. This dolomite cement appears as cubic crystals which pierce into the pore indicating that it formed after the fracture parted. The fractures viewed in the thin sections at depths 2827.5m and 2828m were, on average, 0.1mm in width.

Granulation seams are accommodation structures under conditions of high stress, low confining pressures and low temperature [Mitra, S., 1988]. This is characterized by the reduction in grain size and granulation within the seam area caused by cataclasis [Kearey (1996), Mitra, (1988)]. The particles in the granulation seam are reduced in size by rolling and sliding against each other [Kearey (1996)]. The presence of this finer-grained material inside the seam causes a decrease in porosity and permeability because the material blocks fluid flowing through it. The granulation seams viewed in the thin sections were on a scale of 0.05mm in width. This is an indication of tectonic activity (normal faulting) occurring in the Bredasdorp Basin.

The final diagenetic phase, in the late diagenetic stage, is characterized by recrystallization and replacement of carbonate cement by dolomite cement. This type of cement has a distinct crystal lattice form (cubic) and forms with temperatures in the range 90°C to 180°C [Mountjoy, 1999].

The presence of clays and cements which fill the pores (both primary and secondary) and coat the framework grains have impacts on the reservoir quality. The presence of these authigenic minerals reduces porosity and permeability. This is an indication of numerous diagenetic processes of compaction, pressure solution/dissolution,

precipitation and replacement which these sandstones were subjected to during various levels of burial and uplift.

A basic paragenetic history is proposed which illustrates all diagenetic processes which took place in this sandstone.

Table 4 General Paragenetic History

Paragenetic History						
Authegenic Minerals	**Early Diagenesis**		**Middle Diagenesis**		**Late Diagenesis**	
Matrix Clays						
Carbonate Cement						
Feldspar Dissolution						
Pore-Filling Clays						
Calcite Cement						
Quartz Cement						
Dolomite Cement						
Oil						
	TIME →					

4.5.3 The texture of the rock and what it reveals

The average porosity of sandstone ranges 5-30% and is determined by the size of the grains as well as its arrangement (packing) in rock. Fine grains tend to have much less porosity than coarser grains. Permeability (connectivity) tends to be higher in coarser grained material than in fine grained material. The following figure describes the permeability determined by the grain size.

Figure 5 Permeability determined by grain sizes

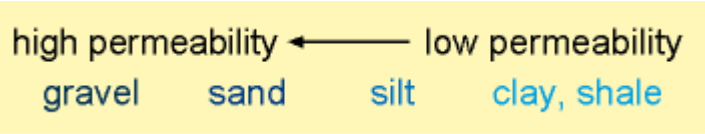

Source: McConnell, 2000

Sorting of grains are based on the "uniformity of grain sizes" [Nelson, 2005]. The density of the particles and the energy of the transporting medium determine the sorting. High energy flow may carry large grains over large distances. A decrease in energy will thus cause the larger, denser grains to be deposited [Nelson, 2005] with the lighter, smaller grains still suspended in the transport medium. In the case of the thin sections observed the general sorting of the grains are moderate to poor. The type of sorting can thus determine the origin of the deposits. The poorly sorted thin section samples are thus characterized by a rapid deposition type [Nelson, 2005]. The grain shape is a tool in determining the residence time of the grains in the transporting medium. This is also known as roundness of grains and ranges from round to angular. The grain shapes of the thin sections are mostly sub angular which indicated a fairly moderate residence time of transportation.

Thus the overall textural aspects of the rocks in well E-BA1 are fine- to medium-grained, moderately- to poorly-sorted and sub angular grain shapes which is an indication of a rapidly moving, high-energy transportation over a large distance [Nelson, 2005]. The location of the well indicates the high energy flow due to turbidity currents. Turbidity flow was in the form of a large mass of sediments caused by gravity flow which is an indication of a moderately to poorly sorted grain type [Nelson, 2005]. The mass flow was as a result of the formation of the basin. The initial deposition was by palaeostreams and rivers which produced channel fills and lobes. Once rifting commenced the increase in subsidence rate caused sediment flows from the continental shelf towards the basin.

4.5.4 Porosity and Permeability

Many tests performed on the sandstones drilled in this borehole revealed that it has the potential to be commercially viable. The cores (#1 & #2) drilled revealed porosities ranging from trace values to 11% and permeabilities from 0.041mD to 43mD (PetroSa unpublished data). The relationship between porosity and permeability can be seen in the Porosity versus Permeability graph.

Figure 6 Porosity versus Permeability Graph

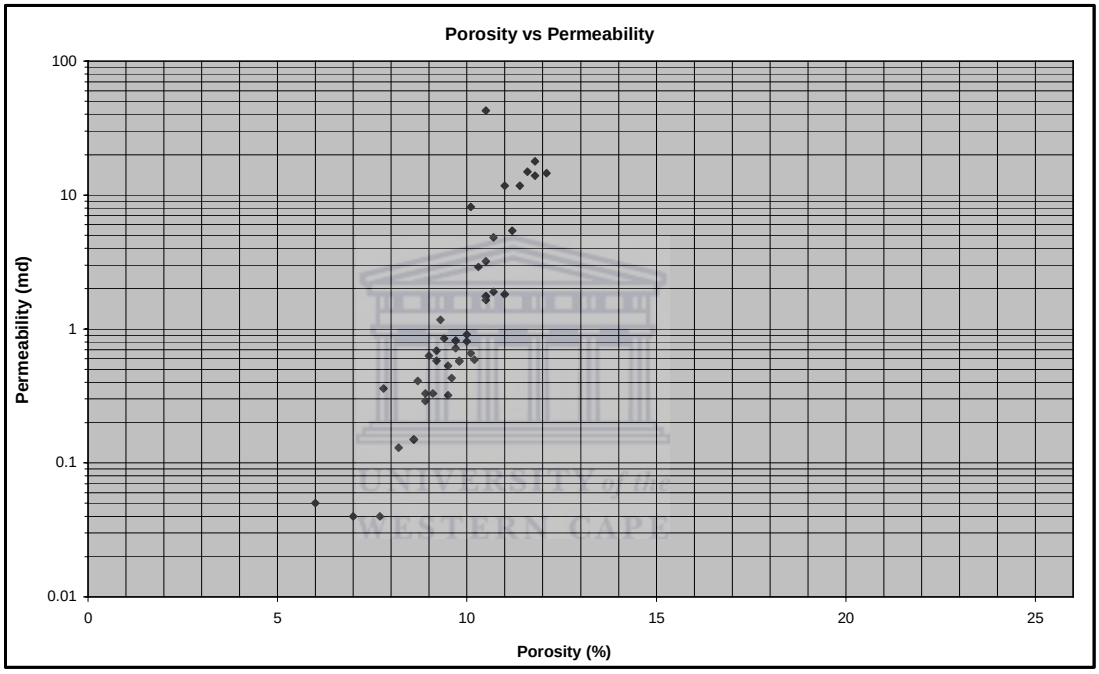

The above graph displays the relationship between porosity and permeability and how one affects the other. The graph was formulated by porosity and permeability data taken from tests within the well. The trend of the data shows a “clean” sandstone with minor influences of cementation and authigenesis governing the above relationship.

Repeat Formation Testing (RFT) (PetroSa unpublished data) revealed a gas gradient of 0.13psi/ft in sandstones above the 9At1 horizon. Thin gas-charged sandstones were detected below 9At1 but lacked prospect due to limited vertical extent. The 14A sequence also presents poor reservoirs, with negligible gas shows. Drill Stem Tests (DST) (PetroSa unpublished data) reveals a maximum gas-condensate flow rate of

482.5m^3/day and a maximum gas flow rate of 577 600m^3/day obtained from a perforated interval from 2805 to 2829m.

Even though, the claystone source rocks showed strong oil sources, most reservoirs in the sandstones between 2805m and 2829m are potentially gas and gas-condensate reservoirs in the higher permeable zones. Potential reservoir properties are evident in the hydrocarbon-bearing sandstones above 9At1. These are, however, interbedded with claystones, having variable porosity and permeability. This could be problematic when attempting to calculate reserve potentials, due to the claystones acting as possible permeability barriers on a local scale. This is illustrated in the permeability versus Depth and Porosity versus Depths graphs below.

The graphs that follow display the changes in permeability and porosity with respect to depth showing clear levels of significant permeability and porosity decreases characterized by the presence of claystone mineralogy also noted in the thin sections. The increase in permeability between these barriers displays a “jump” effect on these zones by overpressures. The trend of porosity is all over the place moving from low to high but still showing marked decreases in the claystone zones. The irregular pattern of the porosity is as a result of the effects of clays and cements.

Figure 7 Permeability versus depth Graph

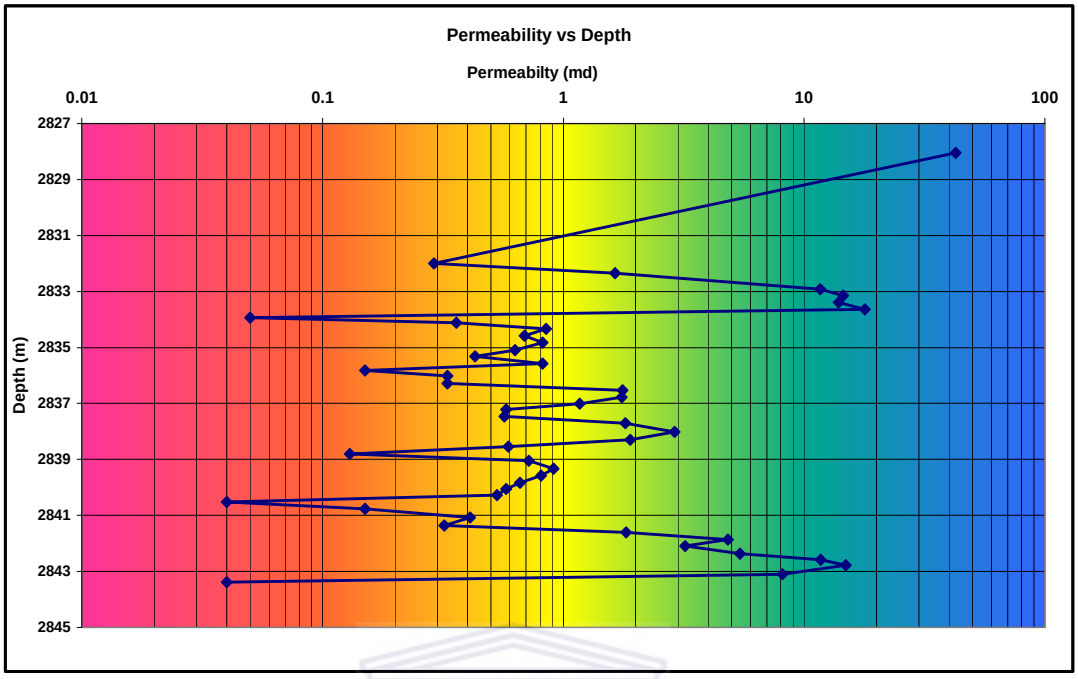

Figure 8 Porosity versus Depth Graph

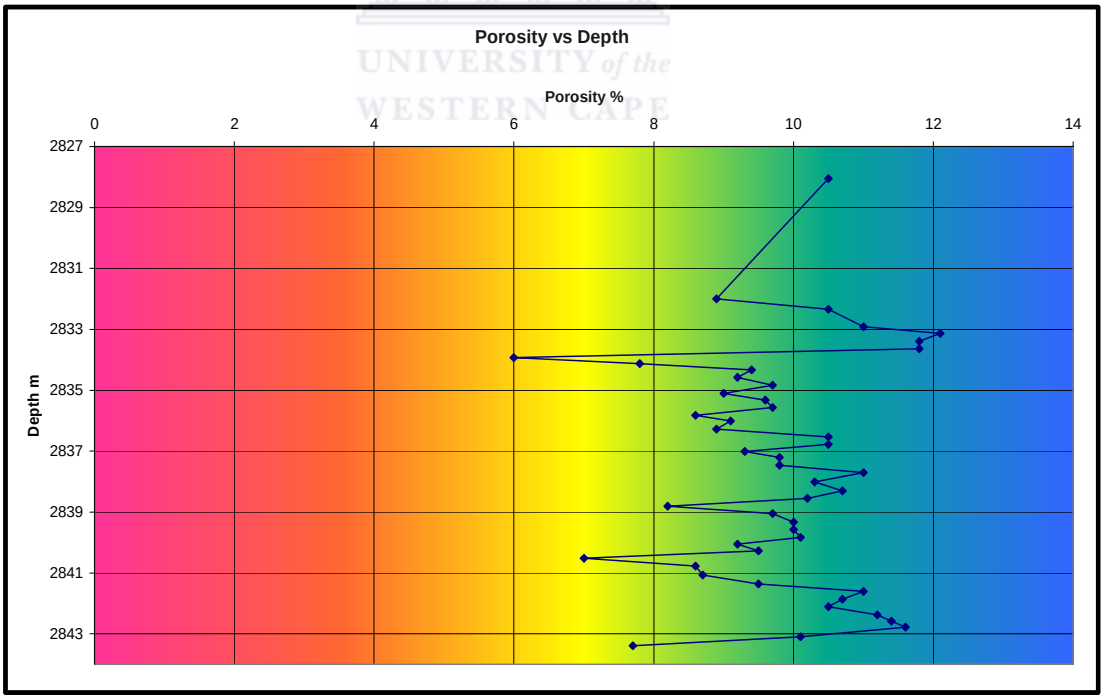

It is clear that the reservoir displays zones of heterogeneity with respect to porosity and permeability. If the claystone barriers are local then a single, compartmentalized reservoir is considered yet, if the claystone barriers are regional (laterally extensive) then more than one reservoir may exist.

The presence of a change in grain size from sandstone to claystone was observed at depths 2828.64m and 2829.67m. This could cause flow problems during recovery if it is laterally extensive. The rise in permeability above and below the claystone zones is due to compartmentalization with the impact of pressure on the sandstone zones. The connectivity can be enhanced by secondary recover methods which will be discussed in the recommendations to further improve the flow rate of gas and gas-condensate.

CONCLUSIONS

The current research conducted within the thesis has indicated that well E-BA1 is one of moderate to good quality having a gas to gas-condensate component. The outcome of hydrocarbon type is partly a result of the unusual thermal history. The introduction of increased temperatures followed by decreased temperatures has affected the diagenesis of the basin. The introduction of hot fluids from neighboring basins has also caused an increase in chemical and physical reactions which have shaped the Bredasdorp Basin to what it is today. These reactions have also affected the nature of the hydrocarbons which is more gas than oil. The thermal history along with the formation of the basin by rifting and drifting with varied levels of sedimentation have formed a heterogeneous reservoir which could prove beneficial for recovery but may lack viability without secondary recovery methods.

The overall porosity and permeability show variability with zones of heterogeneity in terms of fluid flow (conductivity). Permeability barriers and baffles which could be either laterally extensive (barrier) or local (baffle) tend to decrease the permeability of the reservoir at certain depths. Overpressure by claystones drives fluid flow in reservoir zones. Due to low permeabilities of claystones the sandstones between these layers could be under pressure and causes heterogeneity in terms of permeability. This is a likely result of the channel fill structure of a reservoir characterized by lobes and channels. Thus the sandstones found in this reservoir are from turbidity flows over ancient channels of palaeostreams and rivers.

These palaeostreams and rivers produced channel fill and lobe structures. Submarine canyons, formed by the palaeostreams and rivers, acted as ‘triggers’ for turbidity flow into the deeper regions of the basin. This mass flow content was as a result of the formation of the Bredasdorp Basin by rifting which caused progressive subsidence rates and the ‘detachment’ of shelf deposits and the transport by mass sediments.

RECOMMENDATIONS

SKIN EFFECT

Skin is the indication of altered permeability in the wellbore and near wellbore zones [Chen and Chang, 2006]. The permeability of this zone is less than that of the formation. It is formed when mud (from drilling or acidization) penetrates or invades the formation near the wellbore [Chen and Chang, 2006]. In borehole E-BA1, the calculated final skin was 26, attributed to "blockage' [Steyn, 1990] of the pore throats in the near wellbore area. These blockages were caused by condensate drop-out due to flow below dew point as well as mud which was dropped on perforations [PetroSA unpublished data]

PROPOSED SOLUTIONS FOR ENHANCED RECOVERY

Well testing techniques are essential in determining the lifespan of a well [Penuela and Civan, 2000]. Gas-condensate reservoirs fall risk of diminishing at a rapid rate as a result of the drop of flowing bottom-hole pressure below saturation pressure of fluid at reservoir conditions [Penuela and Civan, 2000]. Wells should be routinely stimulated for enhanced recovery and productivity. Many treatments conducted in the Ghawar field [Rahim and Al-Qahtani, 2003] have revealed that for high skin factors (E-BA1=26), a matrix treatment would be more sufficient than fracturing. Most matrix acidization treatments can be performed in two phases, firstly a preflush phase of hydrochloric acid followed by a main flush of mud-based acid [Lievaart and Davies, 1987].

The sandstones from borehole E-BA1 displays influential amounts of clays and cements which affect the porosity and permeability. These factors play a key role in selecting a suitable enhanced recovery method, along with the heterogeneous nature of the reservoir zone in relation to porosity and permeability. Thus a secondary method can be applied, for instance matrix acidization injection coupled with Hydraulic/acid fracturing. Fracturing is performed first by high pressure viscous

injection [Mumallah, 1996] followed by an acid injection into the formed fracture. Heterogeneity within the reservoir zone could cause a problem whereby acid will be more proned to enter higher permeability zones. A solution for this problem is the introduction of foam [Siddiqui et al., 2002] which would divert the acid towards lower permeability zones. This is favourable as the foam is clean, which minimizes damage to the formation and can be removed after the acidizing treatment. The redirected acid treatment moves along the fracture towards the lower permeable zones and etches the walls, dissolving and breaking up the clays and cements [Mumallah, 1996]. The pressure is released and the fracture closes yet a pathway, formed by the etched surfaces, remains and acts as a conductive network from the formation into the wellbore. The aspect of Fines migration [Lievaart and Davies, 1987] poses a risk of clogging pore throats with dislodged clay particles. To alleviate this problem a suitable acid should be selected which would dissolve most of the clay particles.

In the case of wellbore E-BA1, the lower section of the reservoir zone has been perforated leaving a 5m upper section unperforated. This 5m section is hydraulically linked to the lower section. Further improvement to the recovery will be obtained by perforating the remaining 5m section of the reservoir. The low permeability barriers can by fractured to enhance connectivity for improved gas and gas-condensate flow. The above methods of treatment can thus be considered.

BIBLIOGRAPHY

Amy, L.A., Talling, P.J., Peakall, J., Wyn, R.B. and Arzola Thynne, R.G. (2005). Bed Geometry used to test recognition criteria of turbidites and (sandy) debrites. Sedimentary Geology, vol. 179: 163-174.

Barber, Z. (1999). Using the reflection microscope. United Kingdom: University of Cambridge. [Online]. Available http://www.msm.cam.ac.uk/doitpoms/tlplib/CD1/rmicroscope.php

Boggs, Jr., S. (2001). Principles of Sedimentology and Stratigraphy, Third Edition. Prentice-Hall, Inc., New Jersey, pp 162-168.

Brown, L.F., Benson, J.M., Brink, G.J., Doherty, S., Jollands, A., Jungslager, E.H.A., Keenan, J.H.G., Muntingh, A. and Van Wyk, N.J.S. (1995). Sequence stratigraphy in offshore South African divergent basins. In: Am. Ass. Petrol. Geol., Studies in Geology, 41, An Atlas on Exploration for Cretaceous Lowstand traps, by Soekor (Pty) Ltd, pp 83-131.

Chen, C. and Chang, C. (2006). Theoretical evaluation of non-uniform skin effect on aquifer response under constant rate pumping, Journal of Hydrology 317: 190-201.

Davies, C.P.N. (1997). Unusual biomarker maturation ratio changes through the oil window, a consequence of varied thermal history. Organic Geochemistry, vol. 27, no. 7/8: 537-560.

Davis, G.H. and Reynolds, S.J. (1996). Structural Geology of Rocks and Regions. John Wiley & Sons, Inc., Canada, pp 577-578.

De Wit, M.J. and Ransome, I.G.D. (1992). Inversion Tectonics of the Cape Fold Belt, Karoo and Cretaceous Basins of Southern Africa, A.A. Balkema, Nederlands, pg 49.

Gier, S. and Johns, W.D. (2005). Clay mineral diagenesis in interbedded sandstones and shales (Aderklaa-78, Vienna Basin): Comparisons and correlations, Geophysical Research Abstracts, vol. 7, European Geosciences Union 2005.

Hamel, C. and Thom, R. (2001). A petrographic comparison of Sandstones from the Hibernia Formation, Mississauga Sands and the Avalon Formation. In: Rock the Foundation Convention, Canadian Society of Petroleum Geologists, pp18-22.

Haszeldine, R.S., Cavanagh, A.J. and England, G.L. (2003). Effects of oil charge on illite dates and stopping quartz cement: calibration of basin models. Journal of Geochemical Exploration Abstracts 78-79: 373-376.

Hussain, M.; El Hassan, W.M and Abdulraheen, A. (2006). Controls of grain-size distribution on geomechanical properties of reservoir rock- A case study:

Cretaceous Khafji Member, Zuluf Field, offshore Arabian Gulf, Journal of Marine and Petroleum Geology, Vol. 23: 703-713.

Karmakar, R., Manna, S.S. and Dutta, T. (2003). A geometrical model of diagenesis using percolation theory. Physica A 318: 113-120.

Kearey, P. (1996). Dictionary of Geology, Penguin Books Ltd., England, pp 366.

Kuntcheva, B., Kruhl, J.H. and Kunze, K. (2006). Crystallographic orientations of high-angle grain boundaries in dynamically recrystallized quartz: First results. Tectonophysics 421: 331-346.

Lee, Y.I., Sur, K.H. and Hisada, K. (2005). Assymmetric diagenetic changes in a half-graben basin: the Kanmon Group (Lower Cretaceous), SW Japan. Cretaceous Research 26: 73-84.

Lievaart, L. and Davies, D.R. (1987). The role of fines during acidizing treatments, Marine and Petroleum Geology, Vol. 4: 127-131.

Lima, R.D. and De Ros, L.F. (2002). The role of depositional setting and diagenesis on the reservoir quality of Devonian sandstones from the Solimões Basin, Brazilian Amazonia. Marine and Petroleum Geology 19: 1047-1071.

Ludik, H.R. (1990). Borehole: E-BA1, Core: #1, Depth: 2828m-2834m (Core Analysis Report), Soekor (Pty) Ltd., pp 4.

Matthews, G.P. and Ridgway, C.J. (1996). Modelling of simulated clay precipitation within reservoir sandstones. Marine and Petroleum Geology, vol. 13, no. 5: 581-589.

Mc Millan, I.K., Brink, G.J., Broad, D.S. and Maier, J.J. (1997), Late Mesozoic Sedimentary Basins off the South Coast of South Africa, In: African Basins. Sedimentary Basins of the World 3, Edited by R.C. Selley, Series Editor K.J. Hsü, Elsevier Science B.V., Amsterdam, pp. 319-376.

McConnell, (2000). Rock Properties. The Mcgraw-Hill Companies. [Online]. Available http://www.mhhe.com/earthsci/geology/mcconnell/demo/prop.htm

McConnell, D. (1998). Sedimentary and Metamorphic rocks. University of Akron. [Online]. Available http://enterprise.cc.uakron.edu/geology/natscigeo/Lectures/smrocks/sedmeta.htm

McHardy, W.J., Wilson, M.J. and Tait, J.M. (1982). Electron microscope and X-ray diffraction studies of filamentous illitic clay from sandstones of the Magnus Field. Clay Minerals, vol. 17: 23-39.

McIlreath, I.A. and Morrow, D.W. (1990). Diagenesis, Geological Association, Canada, pp165-324.

Mitra, S. (1988). Effects of deformation mechanisms on reservoir potential in Central Appalachian overthrust belt, Bull. Am. Ass. Petrol. Geol. 72: 536-554.

Mountjoy, E. (1999). Burial Dolomitization in the Devonian of Western Canada Sedimentary Basin: What were the Mg-Bearing Fluid and Heat Sources and the Driving Mechanisms? UK: Journal of Conference Abstracts. [Online] Available http://www.the-conference.com/JConfAbs/4/945.html

Mumallah, N.A. (1996). Hydrochloric acid diffusion coefficients at acid-fracturing conditions, Journal of Petroleum Science and Engineering 15: 361-374.

Nelson, S.A., Prof. Sedimentary Rocks. Tulane University. [Online] Available http://www.earthsci.org/teacher/basicgeol/sed/sed.html

Pasquini, C., Lualdi, A. and Vercesi, P. (2004). Depositional dynamics of glaucony-rich deposits in the Lower Cretaceous of the Nice arc, southeast France. Cretaceous Research 25: 179-189.

Penuela, G. and Civan, F. (2000). Prediction of the gas-condensate well productivity, Journal of Petroleum Science and Engineering 28: 95-110.

Petroleum Agency SA (2003). South African Exploration Opportunities, South African Agency for Promotion of Petroleum Exploration and Exploitation, Cape Town, pp 27.

Petroleum Agency SA (2004/5). South African Exploration Opportunities, South African Agency for Promotion of Petroleum Exploration and Exploitation, Cape Town, pp 27.

Press, F., Siever, R., Grotzinger, J. and Jordan, T.H. (2004). Understanding Earth, Fourth Edition, W.H. Freeman and Company, England, pp165-169.

Rahim, Z. and Al-Qahtani, M.Y. (2003). Selecting perforation intervals and stimulation technique in the Khuff reservoir for improved and economic gas recovery, Journal of Petroleum Science and Engineering 37: 113-122.

Ranoszek, M. and Labuschagne, H. (1990). Geological Well- Completion Report of Borehole E-BA1, Soekor (Pty) Ltd., pp10.

Rasmussen, B. (2005). Radiometric dating of sedimentary rocks: the application of diagenetic xenotime geochronology. Earth Science Reviews 68: 197-243.

Renard, F., Ortoleva, P. and Gratier, J.P. (1997). Pressure solution in Sandstones: Influence of clays and dependence on temperature and stress. Tectonophysics 280: 257-266.

Roux, J. (2005). Gas Exploration and Potential in South Africa. South Africa: Spintelligent. [Online]. Available http://www.esi-africa.com/archive/esi_1_2005/18_1.php

Shanmugam, G. and Moiola, R.J. (1985). Submarine Fan Models: Problems and Solutions. In: A.H. Bouma, W.R. Normark and N.E. Barnes (eds.). Submarine Fans and Related turbidite Systems. Springer-Verlag New York, Inc., pp29-33.

Siddiqui, S.; Talabani, S.; Saleh, S.T. and Islam, M.R. (2002). Foam flow in low-permeability Berea Sandstone cores: a laboratory investigation, Journal of Petroleum Science and Engineering 36: 133-148.

Steyn, C. (1990). E-BA1 DST#1 & 1A : Test Analysis Report, Soekor Library, PetroSA unpublished data.

Storvoll, V., Bjørlykke, K., Karlsen, D. and Saigal, G. (2002). Porosity preservation in reservoir sandstones due to grain-coating illite: a study of the Jurassic Garn Formation from the Kristin and Lavrans fields, offshore Mid-Norway. Marine and Petroleum Geology 19: 767-781.

Stow, D.A.V. (1985). Brae Oilfield Turbidite System, North Sea. In: A.H. Bouma, W.R. Normark and N.E. Barnes (eds.). Submarine Fans and Related turbidite Systems. Springer-Verlag New York, Inc., pp231-236.

Stow, D.A.V., Howell, D.G. and Nelson, C.H. (1985). Sedimentary, tectonic, and Sea-Level Controls. In: A.H. Bouma, W.R. Normark and N.E. Barnes (eds.). Submarine Fans and Related turbidite Systems. Springer-Verlag New York, Inc., pp15-22.

Taylor, K.G., Gawthorpe, R.L. and Fannon-Howell, S. (2004). Basin-scale diagenetic alteration of shoreface sandstones in the Upper Cretaceous Spring Canyon and Aberdeen Members, Blackhawk Formation, Book Cliffs, Utah. Sedimentary Geology 172: 99-115.

Thomson, K. (1999). Role of continental break-up, mantle plume development and fault reactivation in the evolution of the Gamtoos Basin, South Africa. Marine and Petroleum Geology 16: 409-429.

Turner, J.R., Grobbler, N. and Sontundu, S. (2000). Geological modeling of the Aptian and Albian sequences within Block 9, Bredasdorp Basin, Offshore South Africa, Journal of African Earth Sciences, Geocongress 2000: A new millennium on ancient crust, 27th Earth Science Congress of the Geological Society of South Africa, edited by Kisters, A.F.M. and Thomas, R.J., pg 80.

Van Der Spuy, D. (2000). Early-Aptian potential source rocks in South African Cretaceous basins, Journal of African Earth Sciences, Geocongress 2000: A new millennium on ancient crust, 27th Earth Science Congress of the Geological Society of South Africa, edited by Kisters, A.F.M. and Thomas, R.J., pg 83.

Weaver, C.E. and Pollard, L.D. (1975). Developments in Sedimentology: Chemistry of Clay Minerals, Elsevier Scientific Publishing, Ltd.

Wilde, P., Normark, W.R., Chase, T.E. and Gutmacher, C.E. (1985). Potential petroleum reservoirs on Deep-Sea Fans off Central California. In: A.H. Bouma,

W.R. Normark and N.E. Barnes (eds.). Submarine Fans and Related turbidite Systems. Springer-Verlag New York, Inc., pp35-41.

Wilkinson, M., Milliken, K.L. and Haszeldine, R.S. (2001). Systematic Destruction of K-feldspar in deeply buried rift and passive margin sandstones, Journal of the Geological Society, London, Vol. 158: 675-683.